Studies on synthesis, structure, and reaction of palladium complexes coordinated by bidentate N[21], N[22]-bridged porphyrins

高尾, 優子

(Degree)
博士（理学）

(Date of Degree)
2003-09-19

(Date of Publication)
2009-06-18

(Resource Type)
doctoral thesis

(Report Number)
乙2711

(URL)
https://hdl.handle.net/20.500.14094/D2002711

博　士　論　文

Studies on Synthesis, Structure, and Reaction of Palladium Complexes Coordinated by Bidentate N^{21},N^{22}-Bridged Porphyrins

（２座配位性ポルフィリンパラジウム錯体の合成、構造、反応に関する研究）

平成１５年８月

神戸大学大学院自然科学研究科

高　尾　優　子

CONTENTS

Chapter 1

General Introduction

1.1 Palladium Complexes Coordinated by Porphyrin Ligand.

Many transition-metal complexes have been prepared and structurally characterized finding the special property and function, while the complexes have been investigated as structural model of enzyme including transition metal and to be responsible for highly efficient and selective reactions. Since in the transition-metal complexes, configuration of central metal ion and oxidation-reduction potential can be controlled by the several structures and kinds of ligands and coordinating atoms, multiple applications have been studied in coordination chemistry. Thus the development of Organometallics chemistry and catalysis involving transition metals has been closely associated with the realization that their formation, stability, and reactivity are governed by the fundamental rules of the coordination chemistry. Some of the complexes are useful reagents in organic reactions, such as oxidations, hydrogenations, carbonylations, addition reactions and polymerizations.[1] For example, Wacker reaction for oxidation of ethylene and Ziegler catalyst for ethylene polymerization have been well-known and Wilkinson complex catalyzed hydrogenation of alkenes. Further acetic acid was synthesized by carbonylation of methanol using Rh catalyst and cycroaddition of a vinylallele with 1,3-diene was achieved by the use of Pd catalyst.[2] Instead of heterogeneous catalyst as Ziegler catalyst the homogeneous metallocene catalysts and further non-metallocene type initiators led to the polymerizations

with specific microstructures and high molecular weight polyolefines in adding to the arousal of the interests in ligand effects on stereoregulation.[3,4] Recently, efforts have been made to study the complexes consisting of a late transition metal to find novel catalysts for the purpose of invention of excellent polymer materials.

Among aforementioned reactions, palladium has made important contributions to organic synthesis chemistry, beginning with Wacker method, extend to recent polymerization catalyst as Pd complex having diimine ligand. Palladium in the fifth periodic metal of platinum group, and is valuable metal presence of which is only about 24 thousands t in the earth , and has been used in also as ornament etc. While initial expense of the palladium compound is high, though comparable to the cost of many organic reagents, the palladium is usually easily recovered, essentially quantitatively, and is reusable. Homogeneous reactions catalyzed by Pd complexes have been developed progressively, for example, synthesis of substituted olefins by cross coupling reactions of aryl halides and olefins (Heck reaction)[5] and of vinylboranes and organohalides (Suzuki coupling reaction).[6] Furthermore recently bulky *t*-butyl phosphine ligand was designed to promote reductive elimination of substrate to arise the activity.[7] Thus the ligand design of Pd complexes have received renaissance and the structure and the behavior have been investigated to elucidate the catalytic function in the intermediate of diverse reactions contributed by Pd catalyst.

Although most of the complexes used for organic synthesis earlier as homogeneous catalysts were with optically active ligands coordinating through phosphorus, more recent developments have highlighted the use of " nitrogen-donors".[8] For examples, optically active cyclometalated compound playing roles of C,N-donors were useful for the separation of racemic

mixtures,[9] and the coupling of secondary Grignard reagents with alkenyl halides was chelating P,N-system.[10] Further for asymmetric allylic alkylation, alkaloid (-)-sparteine and a noble asymmetric bis(pyrazolyl)methane were prepared as bidentate nitrogen base ligand.[11] In general, donor-accepter bonds formed by nitrogen donors are strong in contrast to those formed by phosphorus donors, and their strength shows drastic changes, if the metal center is changed.[8] And the strength of the M-N bonds will be affected much more by steric effects than that of the corresponding M-P bonds. Ligands containing sp^2-hybridized nitrogen atoms, particularly when the N atom is part of an aromatic system, have extensive coordination chemistry.

Porphyrin is presented as one of the compound which can become bidentate or tridentate ligand coordinating through nitrogen atoms sp^2-hybridized to be part of aromatic system. It is known well that porphyrin is vital substance playing pivotal rolls as hemoglobin in blood cell, chlorophyll in plants, cytochrome in enzyme and so on. Many efforts have been made for the elucidation of the important vital functions and for the biomimetic study from the view of fine chemistry. While the study relating the porphyrins seems to have been developed along the interest in vital reactions mimicking the vital reactions, recently porphyrin is tried to apply to several field such as optical functional material, photosensityzer, and solar cells. Porphyrins include a large aromatic π-electron system as a tetrapyrrole structure in which there is a site occupied by several metal ions to afford the diverse complexes. Since normal porphyrin plays a roll of tetradentate ligand, in palladium(II) complex the effective site of Pd are full of a porphyrin ligand to be unreactive for catalytic reactions. But it is considered that modification of porphyrin as N-alkylation will afford different site to metals and enable also palladium to be reactive for some new reactions.

In this study, with purpose of finding potential of modified (porphyrinato)palladium(II) complexes, the Pd(II) complexes coordinated by *N*,*N*'-etheno-bridged porphyrins are synthesized and applied to some reactions.

In Chapter 2, stable complexization and structure of Pd(II) porphyrins with a two-carbon (etheno) bridge were studied compared with those include a one-carbon bridge.

In Chapter 3, the ligand substitution reaction of palladium porphyrins with amines is attempted in order to see how strong their bent Pd-N bondings are. Furthermore, dynamic behaviors of the palladium porphyrins ligated by ethylenediamine are discussed on the basis of their spectroscopic properties.

In Chapter 4, the synthesis and isomerization behavior of derivatives with N^{21},N^{22}-bridged porphyrin ligands, and the roles of porphyrin ligands in controlling cis-trans isomerization and also in the spectroscopic characterization of (π-allyl)palladium complexes will be discussed detail.

In Chapter 5, the synthesis of μ-(dihydroxo)-bridged complexes of dimeric palladium(II) porphyrins, the geometry of μ-(dihydroxo)dipalladium(II) core, and isomerization behavior are studied. And the reactions of μ-(dihydroxo)dipalladium(II) bisporphyrin with active methylene compounds to afford new organopalladium(II) porphyrins are proposed, including that with allyl compounds as the third method to prepare (π-allyl)Pd^{II}(porphyrin)s.

In Chapter 6, the insertion of isocyanides into (π-allyl)palladium(II) complexes of N^{21},N^{22}-etheno-bridged porphyrin ligands is attempted. And the reactivity is studied.

1.2 References

1. (a) Rausch, M. D.; Siegel, A.; Klemann, L. P. *J. Org. Chem.*, **1966**, *31*, 2703. (b) McKnight, A. L.; Waymouth, L.; Atwood, J. L.; Zhang, H. *J. Am. Chem. Soc.* **1998**, *98*, 2587.
2. Murakami, M.; Itami, K.; Ubukata, M.; Tsuji, I.; Ito, Y. *J. Synth. Org. Chem. Jpn.*, **1998**, *56*, 406.
3. Even, J. A.; Haspeslagh, L.; Atwood, J. L.; Zhang, H. *J. Am. Chem. Soc.* **1987**, *109*, 6544.
4. Yasuda, G *J. Synth. Org. Chem. Jpn.*, **1998**, *56*, 54.
5. Jean, M; Craig, E.; Mossman, J. *J. Org. Chem.*, **2000**, *65*, 7792.
6. Hobbs, P. D.; Upender, V. *Chem. Comm.* **1996**, 923.
7. Nishiyama, M.; Yamamoto, T.; *Tetrahedron Lett.* **1998**, *39*, 617.
8. Togni, A.; Venanzi, L. M. *Angew. Chem., Int. Ed. Engl.* **1994**, *17*, 497.
9. (a) Bruce, M. I. *Angew. Chem.* **1977**, *89*, 75. (b) Roberts, N. K.; Wild, S. B. *J. Am. Chem. Soc.* **1979**, *101*, 6254.
10. (a) Hayashi, T.; Konishi, M.; Okamoto, Y.; Kabeta, K.; Kumada, M. *J. Org. Chem.*, **1986**, *51*, 3772. (b) Hayashi, T.; Hagihara, T.; Katsuro, Y.; Kumada, M. *Bull. Chem. Soc. Jpn.* **1983**, *56*, 363.
11. (a) Togni, A.; Rihs, G.; Pregosin, P. S.; Ammann, C. *Helv. Chim. Acta* **1990**, *73*, 723. (b) Bovents, M.; Togni, A.; Venanzi, L. M. *J. Organomet. Chem.* **1993**, *451*, C28.

Chapter 2

Synthesis and Structure of Palladium(II) Complexes with N^{21},N^{22}-Bridged Porphyrin Ligands

2.1 Introduction

Palladium complexes with a bidentate nitrogen base ligand have recently been applied to a number of organic transformations as catalysts as well as conventional Pd complexes with phosphine ligands.[1] On the other hand, ordinary palladium(II) porphyrins are coordinatively saturated by the four pyrrole nitrogens of a porphyrin ligand, and thus Pd(II) porphyrins have been studied so far only in the fields of photo and redox chemistry.[2] There have been reported metalloporphyrins in which metals are coordinated by porphyrins as bidentate or tridentate ligands and positioned out of the plane of porphyrin rings.[3,4] Those structures are, however, unstable and readily converted to usual metalloporphyrins coordinated by four pyrrole nitrogens. In this context, N^{21},N^{22}-bridged porphyrins are of interest in the sense that they can act as bidentate nitrogen base ligands, like 2,2'-bipyridine, because two alkylated pyrrole nitrogens are not used for coordination to metals. Two unsubstituted pyrrole nitrogens are basic and canted towards the opposite side of the N^{21},N^{22}-bridge, which is appropriate to the coordination to metals.[5] It has been shown that the reactions of N^{21},N^{22}-vinylideno-bridged porphyrin and metal carbonyls result in the formation of metalloporphyrins with the elimination of the N^{21},N^{22}-bridge.[6] There have been two reports of palladium complexes of N^{21},N^{22}-bridged porphyrins,[7,8] and ones in which two adjacent

nitrogens of porphyrin core are bridged by a one-carbon (methano) bridge were isolated only by Callot and co-workers.[7]. They showed that two imine-type nitrogens and two bromine atoms of N^{21},N^{22}-[CH(OBn)](TPP)·PdBr (**4c**) (CH(OBn) = (benzyloxy)-methylene, TPP = 5,10,15,20-tetraphenylporphyrin dianion) occupy square-planar coordination sites. (Chart 1). Those Pd(II) complexes also tend to lose the bridge moiety, yielding ordinary Pd(II) porphyrins upon standing, even as crystals. This type of square- planar Pd(II) complex is of great interest not only in view of the stereochemical influence of the porphyrin ligand moiety on the coordination chemistry of Pd(II), but also in view of the unique photochemical and redox activity of N^{21},N^{22}-bridged porphyrins.[9,10] Hence it seems worthy to develop stable Pd complexes of N^{21},N^{22}-bridged porphyrins. This chapter is concerned with the synthesis and structure of stable Pd(II) porphyrins with a two-carbon (etheno) bridge.[11]

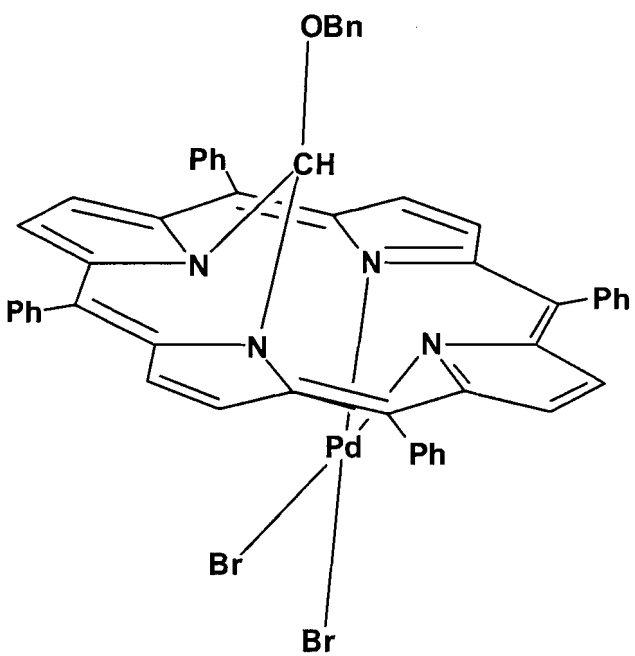

(**4c**)

Chart 1.

2.2 Results and Discussion

2.2.1 **Synthesis of Palladium(II) Complexes with N^{21},N^{22}-Bridged Porphyrin Ligands.**

Although the free base forms are suitable for the metallation reaction of N-substituted porphyrins, N^{21},N^{22}-bridged porphyrins exist as the monoprotonated forms due to their basic nature. Of a few examples of the metallation reaction of N^{21},N^{22}-bridged porphyrins previously reported,[6,7,8,12] Balch and co-workers successfully used a monoprotonated form as well as a free base form of the N^{21},N^{22}-(1,1-diarylvinylideno)-bridged porphyrin in a metallation reaction with $[Ru3(CO)_{12}]$.[12] However, the monoprotonated forms of N^{21},N^{22}-etheno-bridged porphyrins, N^{21},N^{22}-(RC=CR)(TPP)$HClO_4$ (**1a** : R = ethyl, **1a'** : R = phenyl) and N^{21},N^{22}-(RC=CR)(OEP)$HClO_4$ (**1b** : R = ethyl, **1b'** : R = phenyl) (OEP = 2,3,7,8,12,13,17,18-octaethylporphyrin dianion), did not react with $[PdCl_2(MeCN)_2]$ in MeCN at room temperature. Then, the corresponding TPP free base forms, N^{21},N^{22}-(RC=CR)(TPP) (**2a**, **2a'**), were prepared at first by the treatment of a CH_2Cl_2 solution of the monoprotonated form **1a** and **1a'** with a 10% KOH solution.[13] When **2a** was allowed to react with $[PdCl_2(MeCN)_2]$ (3 - 4 molar amounts) in acetonitrile, the brown color of the free base porphyrin changed to reddish green in 30 min at room temperature to form an initial product (**Ia**), whose UV-vis spectrum is substantially the same as that of the monoprotonated porphyrin **1a**. After evaporation of acetonitrile and extraction of the initial product with $CHCl_3$ under aerobic conditions, porphyrin residue was allowed to stand in a $CHCl_3$ solution. This initial product gradually changed to a green Pd complex (**3a**) in $CHCl_3$ in 3 d to give a 79% yield based on **2a**. The complex **3a'** was obtained in 87% yield within 17 h through the initial product (**Ia'**).[14] The Pd complexes, **3a** and **3a'**, include

two $PdCl_2$ units per porphyrin on the basis of a CHN elemental analysis. Vigorous stirring of a two-phase mixture of a THF-CH_2Cl_2 solution of **3a** or **3a'** and a saturated aqueous NaCl solution resulted in the formation of the mononuclear Pd complexes (**4a**, **4a'**) in quantitative yields.

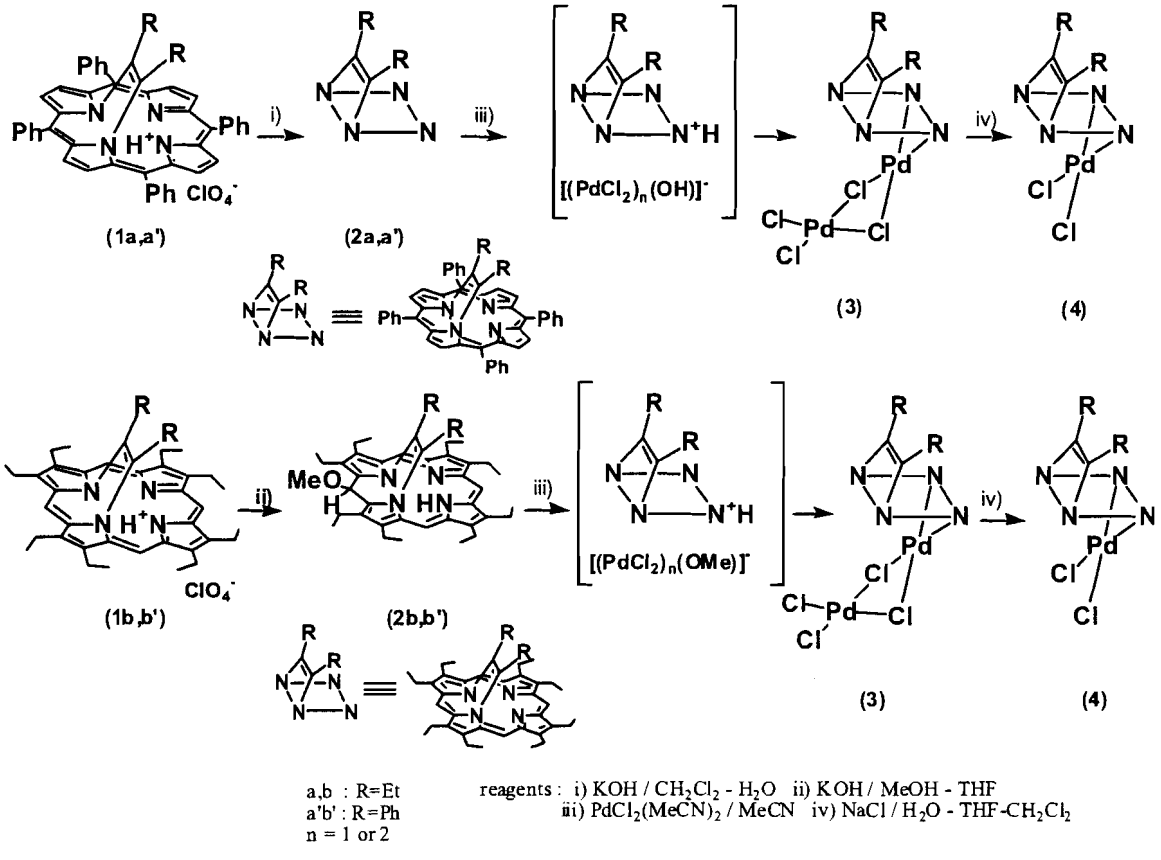

Scheme 1

Since the basicity of OEP pyrrole nitrogens is higher than that of TPP pyrrole nitrogens, the monoprotonated OEP analogues, **1b** and **1b'**, could not be deprotonated. A methoxide ion attacked on the 5-meso position of **1b** and **1b'** gave 5-methoxy-5,22-dihydroporphyrins (**2b**, **2b'**) when **1b** and **1b'** were treated with KOH in methanol.[9] The addition of $[PdCl_2(MeCN)_2]$ (3 - 4 molar amounts) to blue solution of **2b** and **2b'** in MeCN resulted in the formation of red initial products; these were converted into green dinuclear Pd complexes

(**3b**, **3b'**). The mononuclear Pd complexes (**4b**, **4b'**) were obtained by the same procedure as in the case of the TPP analogues. The reaction of equimolar amounts of **2a** and $[PdCl_2(MeCN)_2]$ resulted in the formation of a mixture of **3a** and **4a** with a ratio of 3 : 2. In the case of **2b**, the product ratio of **3b** and **4b** was 5 : 2. This is indicative of the relatively higher stability of the dinuclear complexes than the mononuclear complexes.

2.2.2 **UV-visible Spectroscopic Characteristics.**

A series of reactions described above were monitored by UV-vis spectroscopy. The spectral changes in the reactions from **1b** to **4b** are shown in Figures. 1 and 2. The UV-vis spectra of the initial products generated from **2** and $PdCl_2(MeCN)_2$ were virtually the same as those of **1** and they were characteristic of monoprotonated N^{21},N^{22}-bridged porphyrins. This suggests that the initial products are monoprotonated porphyrin compounds, which do not have strong coordination of pyrrole nitrogens to Pd(II). In the reaction of OEP analogues, $PdCl_2$ as a Lewis acid seems to abstract a methoxide anion from the basic dihydroporphyrins, **2b** and **2b'**, to give monoprotonated porphyrins probably with $[(PdCl_2)_n(OMe)]^-$ (n = 1 or 2) as a counter anion as shown in Scheme 1. The UV-vis spectra of the obtained Pd complexes of N^{21},N^{22}-bridged porphyrins show that the Soret bands are split into two absorptions in the 400 - 480 nm region. As shown in Figure. 3, the Soret bands of the Pd complexes of N^{21},N^{22}-bridged TPP (**3a**, **3a'**, **4a**, and **4a'**) are also split into two bands, the longer wavelength absorptions of which have a higher intensity. This UV-vis spectral pattern is similar to that of N^{21},N^{22}-[CH(OBn)](TPP)$PdBr_2$ (**4c**).[7] Each Soret band moved to longer wavelength regions upon going from the dinuclear Pd complexes to the mononuclear ones.

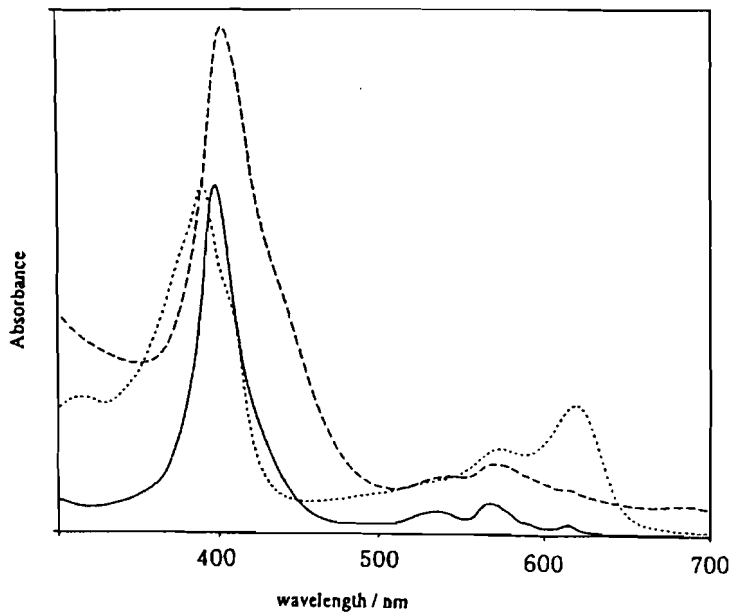

Figure 1. UV-Vis spectra of **1b** in CH_2Cl_2 (solid line), **2b** in hexane (dotted line), and initial product in CH_3CN (dashed line). The ordinate for the absorbance is arbitrarily.

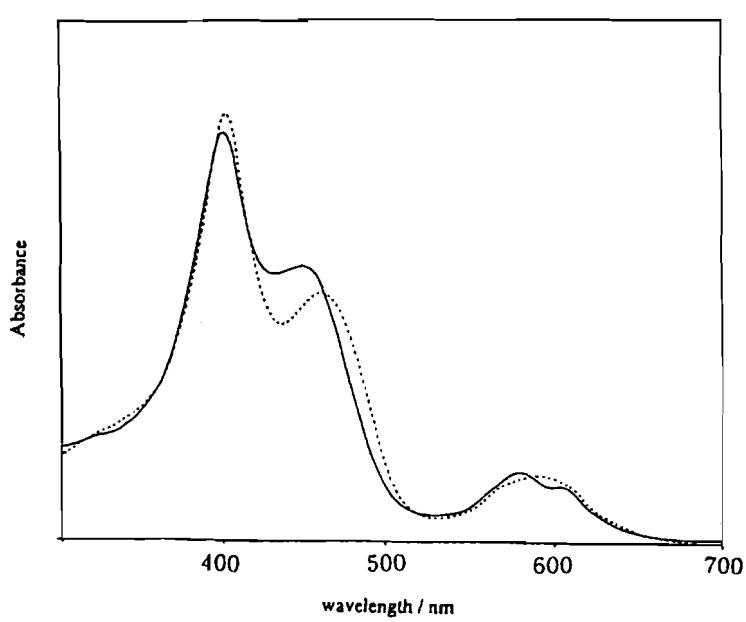

Figure 2. UV-Vis spectra of **3b** (solid line) and **4b** (dotted line) in CH_2Cl_2. The ordinate for the absorbance is arbitrarily.

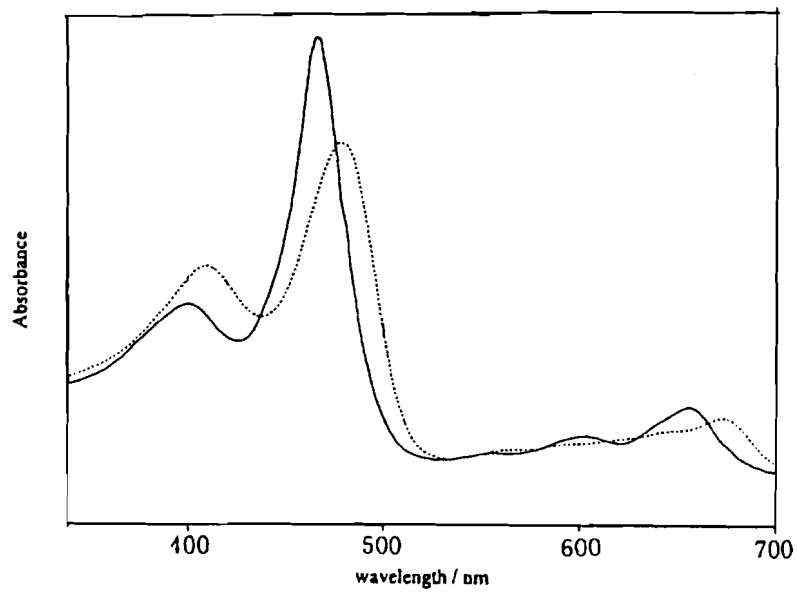

Figure 3. UV-Vis spectra of **3a** (solid line) and **4a** (dotted line) in CH_2Cl_2. The ordinate for the absorbance is arbitrarily.

2.2.3 Structure of Di-μ-chlorodipalladium Complex with N^{21},N^{22}-Bridged TPP : Pd Coordination structure.

Although the crystal of **3a** contains two independent molecules, A and B, in an asymmetric unit, there are no significant differences in the structural parameters for these two chemically equivalent molecules. The selected interatomic distances and angles are given in Table 1 and an ORTEP drawing of the molecule A is illustrated in Figure. 4. Two CH_2Cl_2 and two H_2O molecules are present in the vicinity of molecule B. The structure of **3a** has C_s symmetry and contains a folded di-μ-chlorodipalladium core. The atom-numbering scheme for **3a** is shown in Figure. 5. Pd(1) is coordinated by

two adjacent imine nitrogens, N(3) and N(4), of the porphyrin as the terminal ligand. Pd(1) is placed out of the porphyrin 4N mean plane, PL(4N), by 1.32 Å towards the opposite side to the etheno bridge. The dihedral angle (A) is 69.3° between the 4N mean plane of the porphyrin and the square plane of the Pd(1) coordination sphere. The distal Pd(2) is placed at a distance of 3.78 Å from the 4N mean plane and two square planes of Pd coordination, PL(Pd1) and PL(Pd2), are folded along the axis passing through Cl(1) and Cl(2) with a dihedral angle (B) of 139.8° (see Figure. 6).

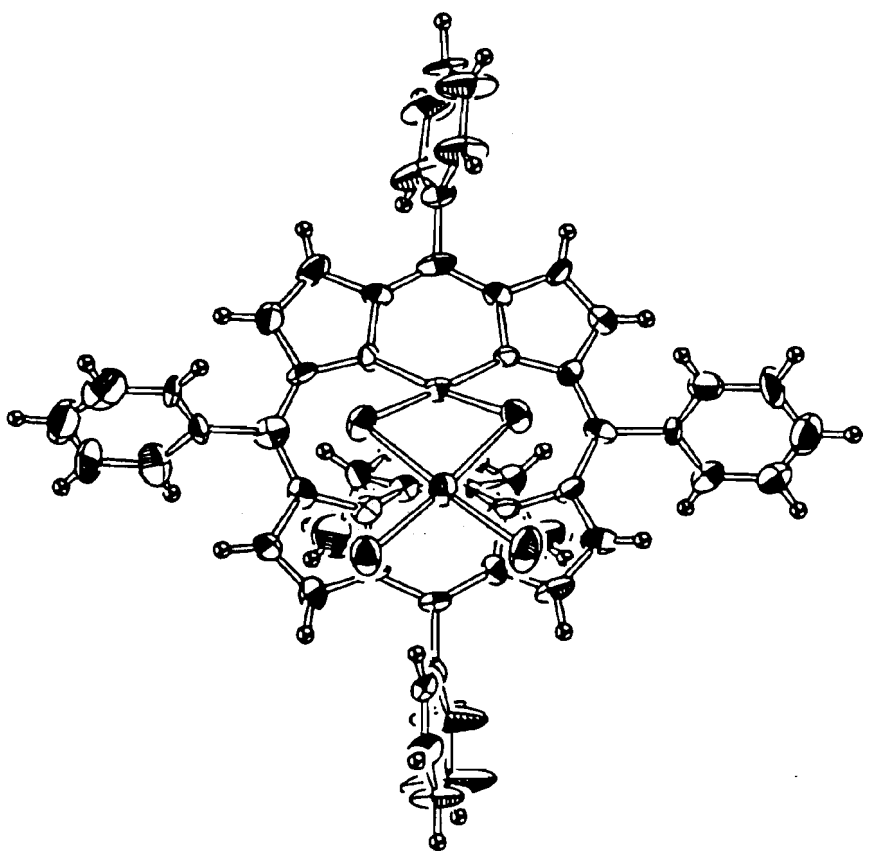

Figure 4. An ORTEP drawing of **3a**.

Table 1. Selected Bond Distances (Å) and Angles (deg) of **3a** with Their Estimated Standard Deviations[a)]

	molecule A	molecule B
Pd(1)-Cl(1)	2.324(4)	2.334(5)
Pd(1)-Cl(2)	2.333(4)	2.332(5)
Pd(1)-N(3)	2.02(1)	2.03(1)
Pd(1)-N(4)	2.01(1)	2.03(1)
Pd(2)-Cl(1)	2.353(5)	2.359(5)
Pd(2)-Cl(2)	2.325(4)	2.228(5)
Pd(2)-Cl(3)	2.265(5)	2.259(5)
Pd(2)-Cl(4)	2.251(5)	2.264(5)
C(45)-N(1)	1.43(2)	1.44(2)
C(46)-N(2)	1.43(2)	1.45(2)
C(45)-C(46)	1.34(2)	1.32(2)
Cl(1)-Pd(1)-Cl(2)	84.6(2)	84.7(2)
N(23)-Pd(1)-N(24)	87.0(5)	86.4(5)
Cl(1)-Pd(1)-N(3)	175.0(4)	176.1(4)
Cl(1)-Pd(1)-N(4)	93.6(4)	95.1(4)
Cl(2)-Pd(1)-N(3)	94.4(4)	93.5(4)
Cl(2)-Pd(1)-N(4)	175.9(4)	173.4(4)
Pd(1)-Cl(1)-Pd(2)	87.7(2)	89.2(2)
Pd(1)-Cl(2)-Pd(2)	88.2(2)	89.7(2)
Cl(1)-Pd(2)-Cl(2)	84.2(2)	84.0(2)
Cl(3)-Pd(2)-Cl(4)	92.1(2)	91.0(2)
Cl(1)-Pd(2)-Cl(3)	92.2(2)	93.0(2)
Cl(2)-Pd(2)-Cl(4)	91.5(2)	92.0(2)
Cl(1)-Pd(2)-Cl(4)	175.3(2)	175.9(2)
Cl(2)-Pd(2)-Cl(3)	175.5(2)	176.3(2)
C(16)-N(4)-Pd(1)	117(1)	116(1)
C(19)-N(4)-Pd(1)	130(1)	130(1)
C(16)-N(4)-C(19)	108(1)	107(1)
C(11)-N(3)-Pd(1)	129(1)	130(1)
C(14)-N(3)-Pd(1)	116(1)	117(1)
C(11)-N(3)-C(14)	108(1)	108(1)
N(1)-C(45)-C(46)	120(1)	121(1)
N(1)-C(45)-C(47)	115(1)	113(1)
C(46)-C(45)-C(47)	123(1)	125(1)
N(2)-C(46)-C(45)	121(1)	119(1)
N(2)-C(45)-C(49)	115(1)	116(1)
C(45)-C(46)-C(49)	122(1)	122(1)

[a)]Atoms related by symmetry operations. Atom numberings are shown in Figure 5.

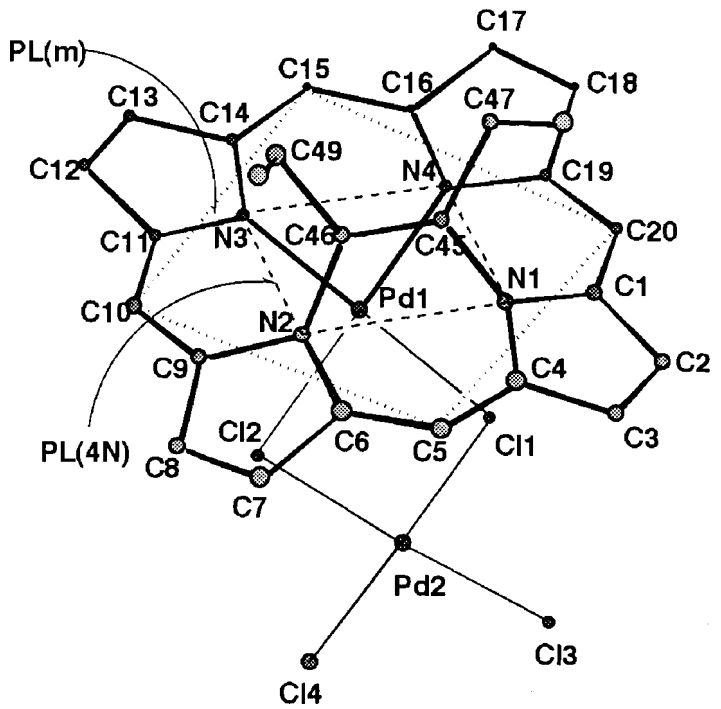

Figure 5. Diagram of a porphyrin mean plane (PL(m)) containing four meso carbons, a 4N mean plane (PL(4N)), and two square planes of Pd coordination of **3a** with showing the atom numbering scheme. *meso*-phenyl groups are omitted for clarity.

Although the Pd-Cl distances and the Cl-Pd-Cl angles are similar to those found in other di-μ-chlorodipalladium complexes, the Pd(1)-Cl-Pd(2) bond angles of **3a** are smaller and the Pd(1)–Pd(2) distance is relatively shorter due to the folding of the two Pd square planes (see Table 2).[15] This folding of Pd_2Cl_4 core toward the porphyrin plane may arise from an electronic repulsion between the lone-pair electrons of two bridging chlorides and the porphyrin π-electrons, because the distances between the bridging chlorides (Cl1 and Cl2) and some of porphyrin atoms (N1, C1, C20, C19, N2, C9, C10, C11) in the X-ray structure of **3a** are within van der Waals contacts (see Table 3). Since the distance between the terminal $PdCl_2$ unit and the porphyrin plane is longer than 3.5 Å the interaction between these two moieties is not

important. Therefore, the terminal $PdCl_2$ prefers the folded conformation, where the lone-pair electrons of the bridging chlorides get away from the porphyrin plane. Indeed, the heat of formation of this folded conformation (PL(Pd1)/PL(Pd2) = 139.8°, calculated by a semi-empirical molecular orbital method (PM3), is lower by 19 kcal mol^{-1} than that for a reversed conformation of the terminal $PdCl_2$, in which the dihedral angle between PL(Pd1) and PL(Pd2) is set to −140° with other structural parameters being unchanged. This result may support the idea that the original molecular structure in which Pd(2) is coming close to the porphyrin ring relieves electronic repulsion between the bridging chlorides and the porphyrin ring. This *endo*-type conformation seems to be retained also in solution as suggested by the NMR spectra (See Table 4). One of four β-pyrrolic-H signals of **3a** (9.20 ppm) is specifically shifted to a higher frequency chemical shift by 0.34 ppm upon going from the mononuclear complex to the dinuclear complex, whereas the chemical shift changes for the other β-pyrrole protons are less than 0.2 ppm (See Figure 7). Furthermore, one of three *meso*-H signals (10.92 ppm with 1H integral) and one of three *meso*-C signals (103.00 ppm) of **3b** are shifted to higher frequency region by 0.66 ppm and 4.27 ppm, respectively, relative to the corresponding signals of **4b**, though the chemical-shift differences for the other *meso* protons and *meso* carbons are less than 0.1 ppm and 1.6 ppm, respectively (See Figure 8 and 9). And one methylene-H signal of **3b** (4.37 ppm with a 2H integral) is also shifted to a higher frequency chemical shift. The other peripheral methylene proton signals of **3b** appear in a similar magnetic field (4.13 - 3.78 ppm) to those of **4b**. Similar shifts are observed in the NMR data of **3a'** and **3b'** as shown in Table 4. These high frequency shifts are ascribable to the magnetic deshielding effect of the distal Pd(2) on the 3(pyrrole-β)-, 5(*meso*)-, and 7(pyrrole-β)-positions of the porphyrin ring.

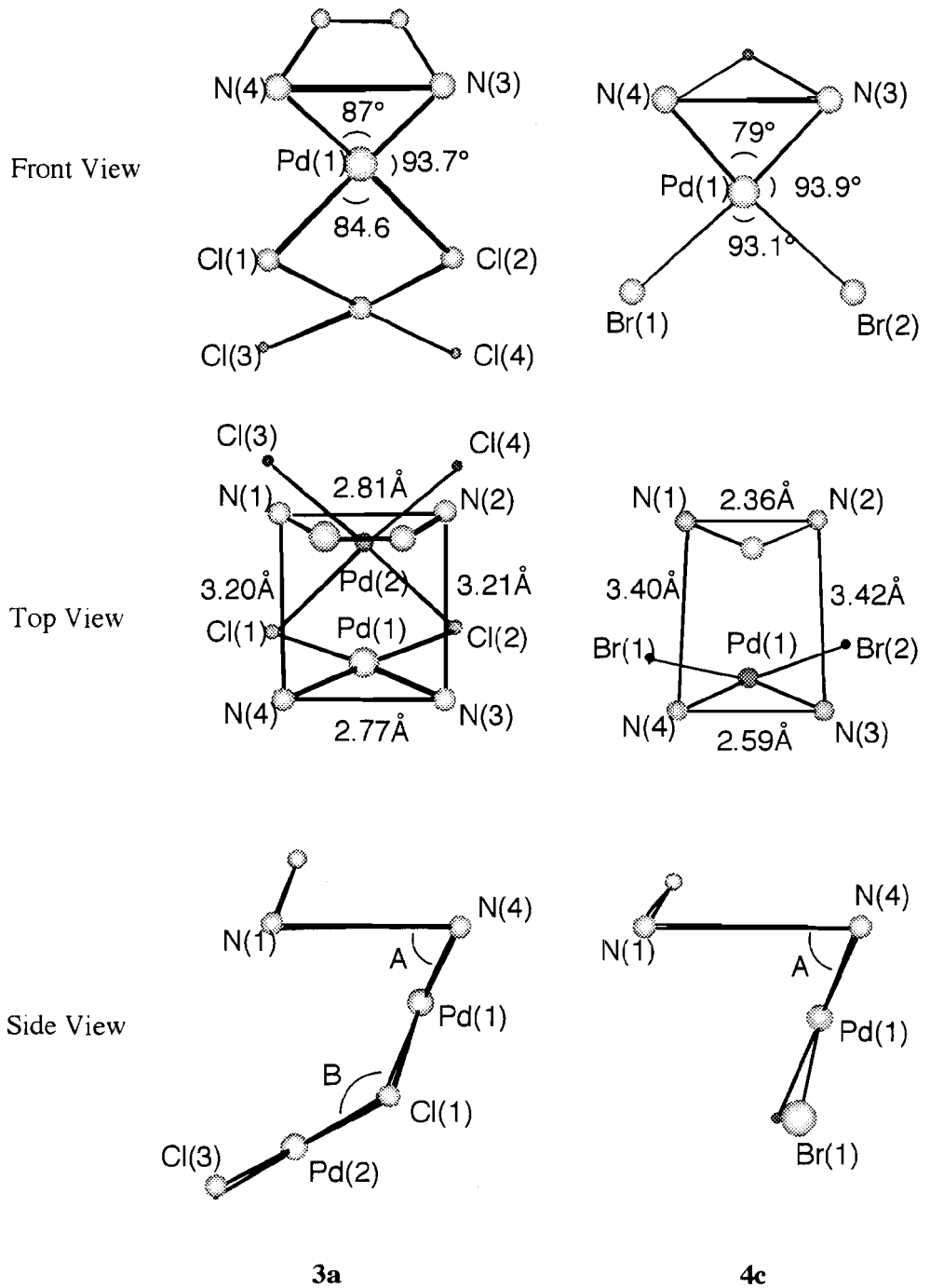

3a **4c**

Figure 6. Comparison of the coordination structures for **3a** and **4c**.

Table 2. The Structural Parameters of Some Di-μ-chlorodipalladium(II) Complexes

Complex	Pd-Cl (Å)[a]	Cl-Pd-Cl (degree)[b]	Pd-Cl-Pd (degree)[c]	Pd-Pd (Å)	Ref.
3a	2.31	84.4	88.0	3.24	
$[PdCl\{CH_2CMe_2CMe{=}N(OH)\}]_2$	2.44			2.99	23(a)[d]
$[PdCl\{C_6H_3(OMe)NMe_2\}]_2$	2.41	85.5	94.5	3.54 3.51 3.50	23(b)
$[PdCl\{CH(CHO)CMe_2CH_2NMe_2\}]_2$	2.41	87.7	92.3		23(c)
$[PdCl\{P(mesityl)_2C_6H_2Me_2CH_2\}]_2$	2.44	85.7	94.4		23(d)

[a]Averaged distances of the four Pd-Cl distances. [b]Averaged angles of two Cl-Pd-Cl angles. [c]Averaged angles of two Pd-Cl-Pd angles. [d]$(PdCl)_2$ core is folded.

Table 3. Selected Distances between the Pd_2Cl_4 Unit and Porphyrin Atoms

atoms	distances (Å)	atoms	distances (Å)
Cl(1)-N(1)	3.50(2)	Cl(2)-N(2)	3.46(1)
Cl(1)-C(1)	3.23(2)	Cl(2)-C(9)	3.25(2)
Cl(1)-C(20)	3.31(2)	Cl(2)-C(10)	3.36(2)
Cl(1)-C(19)	3.41(2)	Cl(2)-C(11)	3.45(2)
Cl(3)-C(22)	4.18(2)	Cl(4)-C(22)	3.83(2)
Cl(3)-C(3)	3.69(2)	Cl(4)-C(7)	4.00(2)
Pd(2)-C(4)	3.85(2)	Pd(2)-C(6)	4.08(2)
Pd(2)-C(5)	4.02(2)		

Table 4. ^{1}H and ^{13}C NMR Chemical Shifts (δ) for Dinuclear Pd Complexes (**3**) and Mononuclear Pd Complexes (**4**) of *N,N'*-Etheno-bridged Porphyrins

compd	pyrrole β-H					
3a	9.20	8.75	8.69	8.53		
4a	8.86	8.66	8.49	8.37		
3a'	9.41	8.83	8.66	8.17		
4a'	9.07	8.67	8.58	8.04		
	meso H		methylene H		meso C	
3b	10.92	10.51[a)]	4.37		109.29	103.59[a)]
	10.23		4.09 - 3.89		103.00	
4b	10.51[a)]	10.26			110.49	105.16[a)]
	10.15		4.13 - 3.78		98.73	
3b'	11.35	10.52	4.56		109.71	103.88[a)]
	10.06[a)]		4.18 - 3.51		103.03	
4b'	10.71	10.49			110.21	105.27[a)]
	10.07[a)]		4.30 - 3.44		99.49	

[a)]Signals of two meso protons or carbons assigned to 10- and 20-positions.

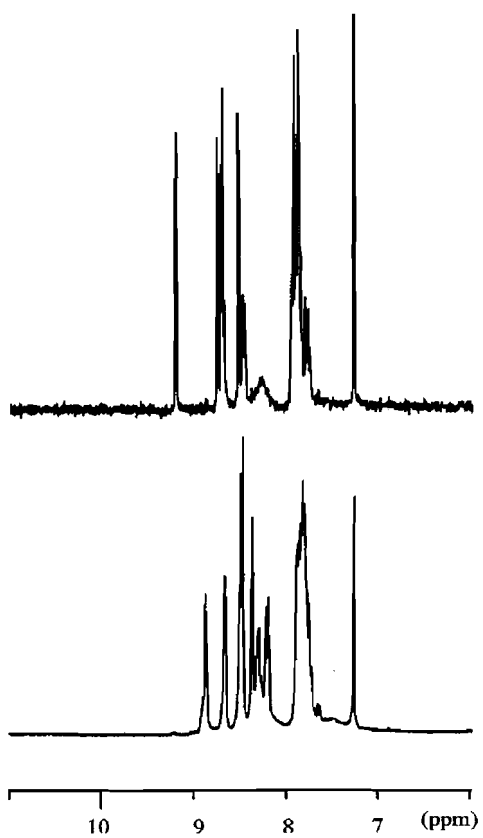

Figure 7. ^{1}H NMR signals of the porphyrin periphery of **3a** (top) and **4a** (bottom) in $CDCl_3$.

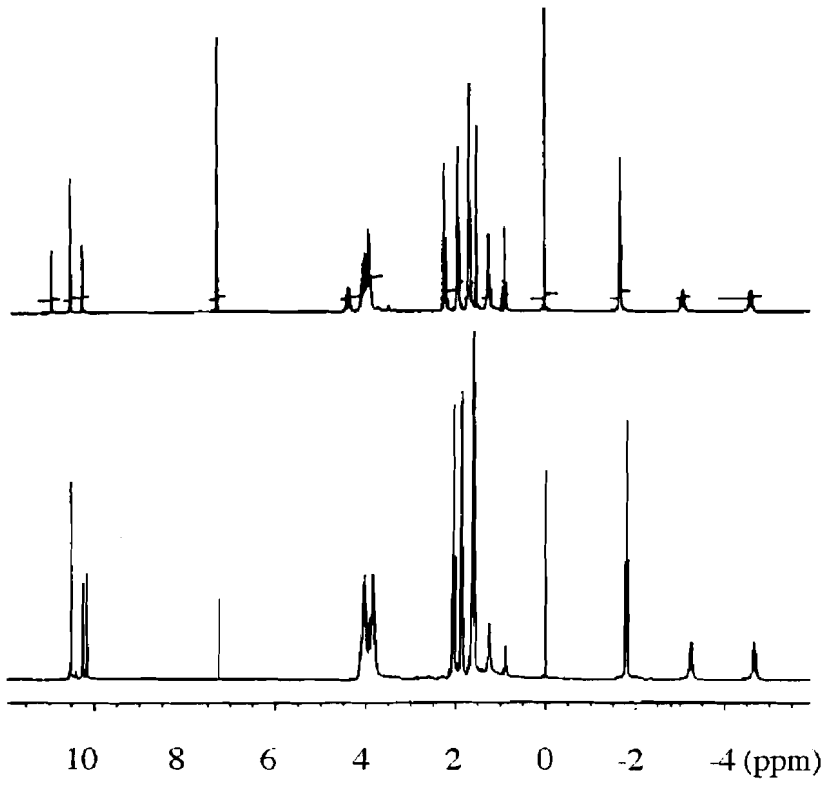

Figure 8. ^{1}H NMR spectra of **3b** (top) and **4b** (bottom) in $CDCl_3$.

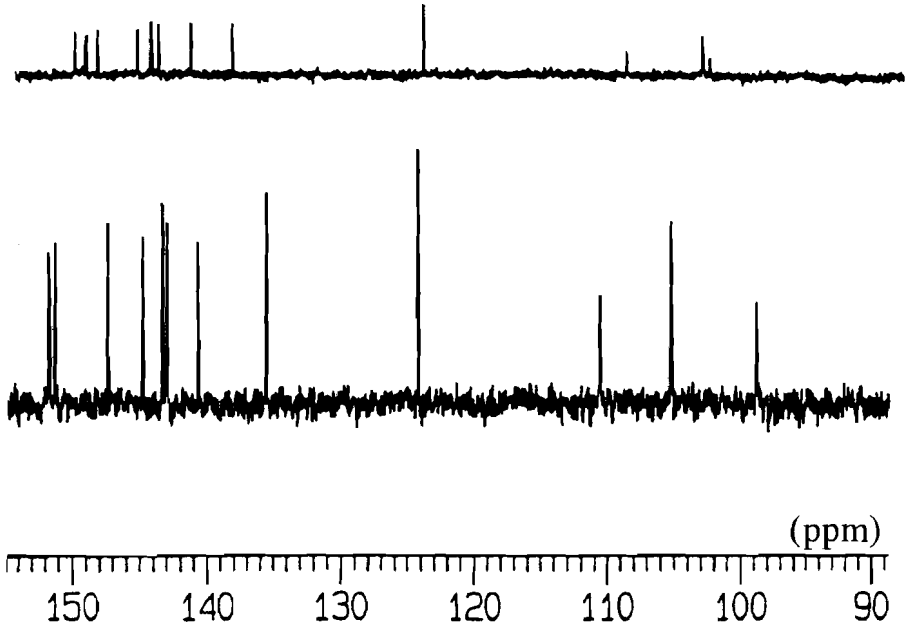

Figure 9. ^{13}C NMR signals of porphyrin periphery of **3b** (top) and **4b** (bottom) in $CDCl_3$.

2.2.4 Structure of Palladium(II) Complex with N^{21},N^{22}-Bridged TPP : Steric Constraint of Etheno-bridged Porphyrin Ligand.

Although the bond lengths of the etheno moiety have normal values, the seven-membered ring, including the etheno bridge, is folded along the axis passing through N(1) and N(2) due to repulsion between the etheno bridge and the porphyrin plane. The angle between the mean plane, PL(C5), containing N(1), C(4), C(5), C(6), and N(2) and the mean plane, PL(B), containing N(1), C(45), C(46), and N(2) is 49.5°. The C(47) and C(49) atoms attached to the bridge olefin carbons are not contained in the plane of the bridge and the dihedral angle between PL(B) and PL(Et) containing C(45), C(46), C(47), and C(49) is 169.5°. This structural feature is indicative of steric constraints between the bridge moiety and the N-unsubstituted pyrrole rings. The distances between the bridge moiety and N(3) or N(4), (N(3)–C(46), N(4)–C(45), N(3)–C(49), and N(4)–C(47)), are 3.09(2), 3.09(2), 3.49(2), and 3.54(2) Å, respectively. Some of them are within van der Waals contacts.

The structure of **3a** is compared with those of N^{21},N^{22}-(etheno)-bridged (TPP)$HClO_4$ (**1d**) and the Pd complex (**4c**) of N^{21},N^{22}-(methano)-bridged TPP in Table 5.[5,7] The methano bridge of **4c** makes the porphyrin 4N core to distort from a square to a rectangle more seriously than the etheno bridges of **3a** and **1d**. Figure 6 shows the structure of a 4N core with bridge carbons and a Pd coordination sphere. The methano bridge shortens the distance between two pyrrole nitrogens and makes an angle strain on the pyrrole rings. This is seen by a larger difference (18.9°) in the angles between C1-N1-C45 and C4-N1-C45 in the case of **4c** than in **3a** (6°) and **1d** (5.8°). The very short distance (2.59 Å) between N(3) and N(4) of **4c** induces the distorted geometry (N(3)-Pd(1)-N(4) = 79.0°) in the Pd coordination sphere, while the etheno

bridge of **3a** does not deform the porphyrin 4N core (N(3)-N(4) distance = 2.77 Å so extraordinarily, and therefore allows Pd to take undistorted geometry (N(3)-Pd(1)-N(4) = 87.0°). Since the N^{21},N^{22}-bridge is forced to get out of the porphyrin plane, the N-substituted pyrrole ring is required to rotate around the axis passing through C1 and C4 or the axis passing through C6 and C9. This is shown by the dihedral angles between PL(N1) and PL(m) (22.9°) and between PL(N2) and PL(m) (18.6°) for **3a**. (PL(N1), PL(N2), PL(N3), and PL(N4) are the pyrrole mean planes containing each pyrrole nitrogen, N(1), N(2), N(3), and N(4), respectively. PL(m) is the mean plane containing four meso carbons.) On the other hand, the N-unsubstituted pyrroles are rotated in the opposite direction to relieve the steric constraint from the N^{21},N^{22}-bridge, as is seen in the dihedral angles between PL(N3) and PL(m) (16.7°) and between PL(N4) and PL(m) (14.7°) for **3a**. Since N-substituted pyrroles bridged by one carbon in **4c** are not allowed to rotate so much as the pyrroles in **3a**, due to an increase in the angle strain on N1-C(bridge)- N2, the cant of N-substituted pyrroles (dihedral angles are 12.7° for PL(N1)/PL(m) and 8.2° for PL(N2)/PL(m)) in **4c** is smaller than that in **3a**. Thus, the porphyrin ring of **3a** is distorted more greatly than **4c** (dihedral angles between PL(4N) and PL(m) are 10.5° for **3a** and 6.4° for **4c**). The distance between methylene proton of the methano bridge moiety and Pd is no longer than 2.58 Å. The close proximity of the Pd atom to the bridge moiety may induce strained bondings of the methano bridge to be cleaved, leading to decomposition into PdTPP. Thus, the unstrained geometries in the porphyrin 4N core, bridged nitrogen, the bridges and the square planar Pd coordination sphere of **3a** seem to be responsible for its more stable nature than **4c**.

Table 5. Selected Distances (Å) and Angles (deg) for **3a**, **4c**, and **1d**

	3a	**4c**	**1d**
bridge	EtC=CEt	CH(OBn)	PhC=CPh
porphyrin	$(TPP)Pd_2Cl_4$	$(TPP)PdBr_2$	$(TPP)HClO_4$
N(1)-N(2)	2.81(2)	2.36(1)	2.797(5)
N(1)-N(4)	3.21(2)	3.40(1)	3.131(7)
N(2)-N(3)	3.20(2)	3.42(1)	3.114(6)
N(3)-N(4)	2.77(2)	2.59(1)	2.776(6)
N(3)-Pd-N(4)	87.0(5)	79.0(2)	-
C(1)-N(1)-C(45)	125(1)	134.5(6)	123.9(4)
C(4)-N(1)-C(45)	119(1)	115.6(6)	118.1(3)
C(6)-N(2)-C(46)	120(1)	117.1(6)	118.2(5)
C(9)-N(2)-C(46)	124(1)	130.3(6)	122.0(4)
PL(4N)/PL(m)[a)]	10.5	6.4	-
PL(N1)/PL(m)	22.9	12.7	18.83
PL(N2)/PL(m)	18.6	8.2	15.15
PL(N3)/PL(m)	16.7	21.3	13.40
PL(N4)/PL(m)	14.7	17.4	4.44
PL(Pd1)/PL(4N)[b)]	69.3	67	-

[a)]PL is the least-squares mean plane: PL(4N) contains four pyrrole nitrogens. PL(m) contains four meso carbons. PL(N1-N4) are the pyrrole planes. [b)]Designated as in Figure. 6.

2.3 Experimental Section

General. N^{21},N^{22}-etheno-bridged porphyrins (**1**) were prepared by a method from the literature.[16] $[PdCl_2(MeCN)_2]$ was prepared by a modification of a literature method.[17] Dichloromethane, methanol, n-hexane, and acetonitrile were dried over calcium chloride. Diethyl ether was dried over benzophenoneketyl. Acetone was dried over drielite and THF was passed through basic Al_2O_3. They were then distilled before use. Other chemicals were of reagent grade. Wakogel C-200 silica gel (Wako Junyaku) was used for column chromatography. The UV-visible spectra were measured on a Hitachi U-3210 spectrophotometer. ^1H NMR and ^{13}C NMR were recorded on a JEOL EX-270 spectrometer in $CDCl_3$. ^1H and ^{13}C chemical shifts are referenced with respect to $(CH_3)_4Si$ (0 ppm) and $CDCl_3$ (77.00 ppm), respectively, as internal standards. Elemental analyses of C, H, and N were made with a Yanaco MT-3 CHN corder.

*Preparation of N^{21},N^{22}-(RC=CR)TPP Free Bases (**2a**, **2a'**).* **2a'** was prepared according to a literature method,[13] and **2a** was synthesized analogously.

N^{21},N^{22}-(EtC=CEt)TPP (**2a**). Yield 55 %. ^1H NMR (δ, $CDCl_3$) 8.45, 8.17, 8.04, 7.91 (d × 4, 2H × 4, pyrrole-β-H); 8.5 - 7.3 (m, 20H, *meso*-phenyl-H); −1.38 (t, 6H, bridge CH_3); −2.45, −3.57 (dq × 2, 2H × 2, bridge CH_2, J_{gem} = 15 Hz). UV/Vis (diethyl ether): λ_{max} 430, 540, 572, 618, 673 nm.

*Preparation of N^{21},N^{22}-etheno-bridged Octaethyl-5-methoxy-5,22-dihydroporphyrins (**2b**, **2b'**).* **2b** and **2b'** were prepared by a modified method from the literature.[9] 20 mL of a 10% KOH solution in methanol was added dropwise to a solution of N^{21},N^{22}-etheno-bridged $OEPHClO_4$ (75 mg) in a mixture of THF (5 mL) and methanol (20 mL). The solution was stirred for

30 min, and the organic solvents were evaporated after the addition of 50 mL of water. Formed purple precipitates were collected by a filter and washed with water. The dried precipitates were extracted with hexane and the solution was evaporated to afford crude N^{21},N^{22}-bridged octaethyl-5-methoxy-5,22-dihydroporphyrin. Further purification was not attempted due to its labile nature.

N^{21},N^{22}-(EtC=CEt)-Octaethyl-5-methoxy-5,22-dihydroporphyrin (**2b**). Yield 81 %. ^{1}H NMR (δ, $CDCl_3$) 7.01, 6.86 (s × 2, 1H × 2, *meso*-H); 7.73 (s, 2H, *meso*-H); 6.41 (s, 1H, NH); 3.26 (s, 3H, OCH_3); 3.2 - 2.9 (m, 16H, CH_2); 1.42 (t, 12H, CH_3); 1.24, 1.12 (t × 2, 6H × 2, CH_3); 0.48, 0.28 (dq × 2, 2H × 2, bridge-CH_2, J_{gem} = 16 Hz); -0.14 (t, 6H, bridge-CH_3). UV/Vis (hexane) λ_{max} 388, 572, 617 nm.

N^{21},N^{22}-(PhC=CPh)-Octaethyl-5-methoxy-5,22-dihydroporphyrin (**2b'**). Yield 97 %. ^{1}H NMR (δ, C_6D_6) 7.37, 7.31 (s × 2, 1H × 2, *meso*-H); 7.47 (s, 2H, *meso*-H); 3.2 - 2.8 (m, 16H, CH_2); 1.50, 1.42, 1.18, 1.05 (t × 4, 6H × 4, CH_3); 6.44 (t, 2H, bridge phenyl-*p*-H); 5.92 (t, 4H, bridge phenyl-*m*-H); 5.01 (br, 4H, bridge phenyl-*o*-H); 3.51 (s, 3H, OCH_3). UV/Vis (hexane) λ_{max} 388, 565, 608 nm.

*Synthesis of Dinuclear Pd (II) Complexes of N^{21},N^{22}-Etheno-bridged Porphyrins (**3a**, **3a'**, **3b**, **3b'**).* A mixture of [$PdCl_2(MeCN)_2$] (80 mg) and **2** (70 mg) in acetonitrile (10 mL) were stirred at room temperature under aerobic conditions. After the UV/Vis spectrum was changed to that of typical monocationic porphyrins **1**, the solution was evaporated and the residue was extracted with $CHCl_3$. The solution was allowed to stand at room temperature under aerobic conditions in the dark for 3 d. After the color of the solution turned green, the solvent was removed. Column chromatography of the residue on silica gel with CH_2Cl_2 - acetone (10:1 - 5:1), followed by

recrystallization of the main fraction from CH_2Cl_2 - hexane, gave a crystalline material.

N^{21},N^{22}-(EtC=CEt)(TPP)$(PdCl_2)_2$ (**3a**). Yield 79 % based on **2a**. Anal. Calcd for $C_{50}H_{38}N_4$ $(PdCl_2)_2 \cdot H_2Cl_2 \cdot H_2O$: C, 53.15; H, 3.67; N, 4.86 %. Found: C, 53.29; H, 3.60; N, 4.59 %. ^{1}H NMR (δ, $CDCl_3$) 9.20, 8.75, 8.70, 8.52 (d × 4, 2H × 4, pyrrole-β-H); 8.67 - 7.66 (m, 20H, phenyl-H); −1.27 (t, 6H, CH_3); −2.71, −4.14 (dq × 2, 2H × 2, CH_2, J_{gem} = 15 Hz). UV/Vis (CH_2Cl_2) λ_{max}(log ε) 400 (4.76), 466 (5.15), 561 (3.86) (sh), 603 (4.11), 656 (4.36) nm.

N^{21},N^{22}-(PhC=CPh)(TPP)$(PdCl_2)_2$ (**3a'**). Yield 87 % based on **2a'**. Anal. Calcd for $C_{58}H_{38}N_4(PdCl_2)_2$: C, 60.81; H, 3.34; N, 4.89 %. Found: C, 61.13; H, 3.51; N, 4.89 %. ^{1}H NMR (δ, $CDCl_3$) 9.41, 8.83, 8.66, 8.17 (d × 4, 2H × 4, pyrrole-β-H); 9.0 - 7.1 (m, 20H, phenyl-H); 6.22 (t, 2H, bridge phenyl-*p*-H); 5.77 (t, 4H, bridge phenyl-*m*-H); 2.23 (br, 4H, bridge phenyl-*o*-H). UV/Vis (CH_2Cl_2) λ_{max}(log ε) 402 (4.89), 469 (5.30), 555 (sh) (4.15), 603 (4.35), 656 (4.54) nm.

N^{21},N^{22}-(EtC=CEt)(OEP)$(PdCl_2)_2$ (**3b**). Yield 78 % based on **2b**. Anal. Calcd for $C_{42}H_{54}N_4(PdCl_2)_2$: C, 52.03; H, 5.61; N, 5.78 %. Found: C, 52.55; H, 5.73; N, 5.92 %. ^{1}H NMR (δ, $CDCl_3$) 10.92, 10.23 (s × 2, 1H × 2, *meso*-H); 10.51 (s, 2H, *meso*-H); 4.37 (dq, 2H, CH_2); 4.09 - 3.89 (m, 14H, CH_2); 2.24, 1.94, 1.70, 1.70 (t × 4, 6H × 4, CH_3); −1.68 (t, 6H, bridge-CH_3); −3.10, −4.61 (dq × 2, 2H × 2, bridge-CH_2, J_{gem} = 15 Hz). ^{13}C NMR (δ, $CDCl_3$) 150.44, 149.58, 148.66, 145.77, 144.71, 144.13, 141.80, 138.67 (pyrrole-C); 124.42 (bridge vinyl-C); 15.35, 8.43 (bridge ethyl-C); 109.29, 103.59, 103.00 (*meso*-C). UV/Vis (CH_2Cl_2) λ_{max}(log ε) 399 (4.76), 442 (4.63), 565 (sh) (3.90), 579 (4.00), 604 (3.88) nm.

N^{21},N^{22}-(PhC=CPh)(OEP)$(PdCl_2)_2$ (**3b'**). Yield 51 % based on **2b'**. Anal. Calcd for $C_{50}H_{54}N_4(PdCl_2)_2 \cdot 2H_2O$: C, 54.51; H, 5.31; N, 5.09 %.

Found: C, 54.50; H, 4.89; N, 5.50 %. ^{1}H NMR (δ, $CDCl_3$) 11.35, 10.52 (s × 2, 1H × 2, *meso*-H); 10.06 (s, 2H, *meso*-H); 4.56 (dq, 2H, CH_2); 4.18 - 3.51 (m, 14H, CH_2); 2.39, 1.91, 1.58, 1.25 (t × 4, 6H × 4, CH_3); 6.03 (t, 2H, bridge phenyl-*p*-H); 5.56 (t, 4H, bridge phenyl-*m*-H). ^{13}C NMR (δ, $CDCl_3$) 151.45, 149.81, 148.12, 146.67, 145.82, 145.04, 142.60, 140.52 (pyrrole-C); 126.79, 126.37, 125.12, 124.35, 124.32 (bridge-C); 109.71, 103.88, 103.03 (*meso*-C). UV/Vis (CH_2Cl_2) λ_{max} (log ε) 404 (4.80), 444 (4.73), 564 (sh) (3.99), 582 (4.08), 600 (sh) (3.96), 625 (sh) (3.81) nm.

*Conversion to Mononuclear Pd(II) Complexes (**4a**, **4a'**, **4b**, **4b'**).* A saturated NaCl aqueous solution (20 mL) was added to a THF - CH_2Cl_2 (1:3) solution (40 mL) of the dinuclear Pd(II) complexes **3** (17 mg); the mixture was then stirred at room temperature for 1 h. After evaporation of the solvent, the product was extracted with CH_2Cl_2, dried over Na_2SO_4, and evaporated to dryness. The residue was then chromatographed on silica gel with CH_2Cl_2 - acetone (10 : 1). The main green fraction was recrystallized from CH_2Cl_2 - hexane to afford mononuclear complexes.

N^{21},N^{22}-(EtC=CEt)(TPP)$PdCl_2$ (**4a**). Yield 80 % based on **3a**. Anal. Calcd for $C_{50}H_{38}Cl_2N_4Pd{\cdot}H_2O$: C, 67.46; H, 4.52; N, 6.29 %. Found: C, 67.82; H, 4.66; N, 6.22 %. ^{1}H NMR (δ, $CDCl_3$) 8.86, 8.66, 8.49, 8.37 (d × 4, 2H × 4, pyrrole-β-H); 8.31 - 7.74 (m, 20H, phenyl-H); −1.41 (t, 6H, CH_3); −2.91, −4.23 (dq × 2, 2H × 2, CH_2, J_{gem} = 15 Hz). UV/Vis (CH_2Cl_2) λ_{max}(log ε) 409 (4.73), 479 (4.92), 555 (sh) (3.79), 673 (4.17) nm.

N^{21},N^{22}-(PhC=CPh)(TPP)$PdCl_2$ (**4a'**). Yield 85 % based on **3a'**. Anal. Calcd for $C_{58}H_{38}Cl_2N_4Pd{\cdot}H_2Cl_2$: C, 67.28; H, 3.83; N, 5.32 %. Found: C, 67.99; H, 3.67; N, 5.11 %. ^{1}H NMR (δ, $CDCl_3$) 9.06, 8.67, 8.56, 8.04 (d × 4, 2H × 4, pyrrole-β-H); 8.6 - 7.3 (m, 20H, phenyl-H); 6.17 (t, 2H, bridge phenyl-*p*-H); 5.75 (t, 4H, bridge phenyl-*m*-H); 2.20 (br, 4H, bridge phenyl-*o*-H).

UV/Vis (CH_2Cl_2) λ_{max}(log ε) 411 (4.73), 485 (4.89), 555 (sh) (3.74), 595 (sh) (3.85), 646 (4.04), 673 (4.09) nm.

N^{21},N^{22}-(EtC=CEt)(OEP)$PdCl_2$ (**4b**). Yield 40 % based on **3b**. Anal. Calcd for $C_{42}H_{54}Cl_2N_4Pd{\cdot}5H_2O$: C, 62.96; H, 6.92; N, 6.99 %. Found: C, 62.99; H, 6.89; N, 6.95 %. ^{1}H NMR (δ, $CDCl_3$) 10.26, 10.15 (s × 2, 1H × 2, *meso*-H); 10.51 (s, 2H, *meso*-H); 4.13 - 3.79 (m, 16H, CH_2); 2.05, 1.88, 1.63, 1.60 (t × 4, 6H × 4, CH_3); –1.79 (t, 6H, bridge-CH_3); –3.24, –4.66 (dq × 2, 2H × 2, bridge-CH_2, J_{gem} = 15 Hz). ^{13}C NMR (δ, $CDCl_3$) 151.73, 141.23, 147.33, 144.71, 143.22, 142.91, 140.63, 135.49 (pyrrole-C); 124.19 (bridge vinyl-C); 14.97, 8.47 (bridge ethyl-C); 110.49, 105.16, 98.73 (*meso*-C). UV/Vis (CH_2Cl_2) λ_{max}(log ε) 403 (4.61), 463 (4.37), 566 (sh) (3.69), 592 (3.80), 610 (sh) (3.73) nm.

N^{21},N^{22}-(PhC=CPh)(OEP)$PdCl_2$ (**4b'**). Yield 44 % based on **3b'**. Anal. Calcd for $C_{50}H_{54}Cl_2N_4Pd{\cdot}5H_2O$: C, 66.93; H, 6.18; N, 6.24 %. Found: C, 67.08; H, 6.37; N, 6.28 %. ^{1}H NMR (δ, $CDCl_3$) 10.71, 10.49 (s × 2, 1H × 2, *meso*-H); 10.07 (s, 2H, *meso*-H); 4.30 - 3.44 (m, 16H, CH_2); 2.17, 1.86, 1.54, 1.14 (t × 4, 6H × 4, CH_3); 6.00 (t, 2H, bridge phenyl-*p*-H); 5.53 (t, 4H, bridge phenyl-*m*-H). ^{13}C NMR (δ, $CDCl_3$) 152.81, 141.70, 146.65, 146.00, 144.71, 144.03, 141.31, 137.02 (pyrrole-C); 127.51, 126.25, 124.82, 124.51, 124.26 (bridge-C); 110.21, 105.27, 99.49 (*meso*-C). UV/Vis (CH_2Cl_2) λ_{max}(log ε) 406 (4.68), 463 (4.43), 571 (sh) (3.81), 594 (3.85), 635 (sh) (3.45) nm.

X-Ray Analysis of 3a. A black prismatic crystal of **3a**·(CH_2Cl_2)(H_2O) was obtained by recrystallization through the slow diffusion of diethyl ether into a CH_2Cl_2 solution of **3a** in a refrigerator. It was mounted on a Rigaku AFC5R diffractometer with graphite-monochromated Mo *Ka* radiation. The crystallographic data are listed in Table 6. The cell constants and orientation matrix, obtained from a least-squares refinement using the setting angles of 25

reflections ($22.04 < 2\theta < 25.72°$), corresponded to a triclinic cell. The space group P1 was determined based on a successful solution and refinement of the structure. The data were collected using the w-2θ scan technique. Scans of $(1.37 + 0.35 \tan \theta)°$ were made at a speed of $16.0° \text{ min}^{-1}$ (in omega).

The intensities of three standard reflections were measured after every 100 reflections, and no decay was observed. An absorption correction based on azimuthal scans was applied. The data were corrected for Lorentz and polarization effects. The structure was solved by heavy-atom Patterson methods and expanded using Fourier techniques.[18] The non-hydrogen atoms were refined anisotropically. Hydrogen atoms were included at standard positions (C-H = 0.95 Å), but not refined. The final cycle of a full-matrix least-squares refinement converged to values of R and R_w of 0.071 and 0.069, respectively. The standard deviation of the unit weight was 2.23. Neutral atom-scattering factors were taken from Cromer and Waber.[19] The values for $\Delta f'$ and $\Delta f''$ were those of Creagh and McAuley.[20] The values for the mass attenuation coefficients are those of Creagh and Hubbel.[21] All of the calculations were performed using the teXsan crystallographic software package of Molecular Structure Corporation.[22]

Tables of atomic coordinates, thermal parameters and least-squares planes are deposited.

Semiempirical MO Calculation. Theoretical calculations were performed with the SPARTAN package version 4.0 (Wavefunction, Inc., Irvine, CA). The MNDO/d MO calculation using a PM3(tm) MO method[23] afforded a heat of formation (567 kcal mol^{-1}) for **3a** on the basis of the atomic coordinates for the x-ray structure. Starting from the original X-ray structure, the Pd(2) square plane was rotated around an axis passing through the bridging chlorine atoms, Cl(1) and Cl(2), in the opposite direction to the N^{21},N^{22}-bridge

until the dihedral angle between PL(Pd1) and PL(Pd2) was set to −140°. A single point energy (heat of formation) for this hypothetical structure, calculated in the same manner as noted above, is 586 kcal mol^{-1}. A further structure optimization for this hypothetical structure was performed by allowing three atoms (Pd(2), Cl(3), and Cl(4)) to move with the rest of the molecule being locked. The energy minimum (576 kcal) was reached without a significant changes in the structural parameters.

Table 6. Crystallographic Data

Formula	$C_{51}H_{42}C_{l6}N_4OPd_2$
Fw	1152.44
Space group	P1
a/Å	19.941(8)
b/Å	20.251(6)
c/Å	13.103(4)
α/deg	96.03(3)
β/deg	105.01(3)
γ/deg	79.32(4)
V/$Å^3$	5013(2)
Z	4
D_{calcd}/g cm^{-3}	1.527
D_{obsd}/g cm^{-3}	1.543[a]
Crystal system	Triclinic
Crystal dimensions	0.20 × 0.10 × 0.50 mm
Diffractometer	Rigaku AFC5R
μ(Mo $K\alpha$)/cm^{-1}	10.78
Scan type	ω–2θ
t/°C	23.0
Scan width/deg	1.37 + 0.35 tan θ
$2\theta_{max}$/deg	55.0
No. of collcd data	18686
No. of unique data	18145
No. of data, $I > 3.00\sigma(I)$	7555
No. of refined	1153
Refln/param ratio	6.6
R[b]	0.070
R_w[c]	0.068

[a]Flotation in a mixed solution of carbon tetrachloride and hexane. [b]$R = \Sigma||F_o| - |F_c||/\Sigma|F_o|$. [c]$R_w = [\Sigma w(|F_o| - |F_c|)^2/\Sigma w|F_o|^2]^{1/2}$.

2.4 References and Notes

1. Togni and L. M. Venanzi, *Angew. Chem., Int. Ed. Engl.*, **33**, 497 (1994).
2. (a) J. A. Mercer-Smith, C, R. Sutcliffe, R. H. Schmehl, and D. G. Whitten, *J. Am. Chem. Soc.*, **101**, 3995 (1979). (b) J. L. Karas, C. M. Lieber, and H. B. Gray, *J. Am. Chem. Soc.*, **110**, 599 (1988). (c) E. M. McGhee, B. M. Hoffman, and J. A. Ibers, *Inorg. Chem.*, **30**, 2162 (1991). (d) A. M. Stolzenberg and L. L. Schussel, *Inorg. Chem.*, **30**, 3205 (1991).
3. Takenaka, Y. Sasada, T. Omura, H. Ogoshi, and Z. Yoshida, *J. Chem. Soc., Chem. Commun.*, **1973**, 792.
4. M. Tsutsui, D. Ostfeld, and L. M. Hoffman, *J. Am. Chem. Soc.*, **93**, 1820 (1971).
5. H. J. Callot, R. Cromer, A. Louati, B. Metz, and B. Chevrier, *J. Am. Chem. Soc.*, **109**, 2946 (1987).
6. Y. W. Chan, M. W. Renner, and A. L. Balch, *Organometallics*, **2**, 1888 (1983).
7. H. J. Callot, J. Fischer, and R. J. Weiss, *J. Am. Chem. Soc.*, **104**, 1272 (1982).
8. A. W. Johnson, D. Ward, P. Batten, A. L. Hamilton, G. Schelton, and C. M. Elson, *J. Chem. Soc., Perkin Trans. 1*, **1975**, 2076.
9. (a) J. Setsune, M. Ikeda, T. Iida, and T. Kitao, *J. Am. Chem. Soc.*, **110**, 6572 (1988). (b) J. Setsune, H. Yamaji, and T. Kitao, *Tetrahedron Lett.*, **31**, 5057 (1990).
10. J. Setsune, K. Wada, and H. Higashino, *Chem. Lett.*, **1994**, 213.
11. (a) Y. Takao, T. Takeda, K. Miyashita, and J. Setsune, *Chem. Lett.*, **1996**, 761. (b) Y. Takao, T. Takeda, K. Miyashita, and J. Setsune, *Bull. Chem.*

Soc. Jpn., **71**, 1327 (1998).

12. L. Balch, Y. W. Chan, M. M. Olmstead, M. W. Renner, and F. E. Wood, *J. Am. Chem. Soc.*, **110**, 3897 (1988).
13. J. Setsune, Y. Ishimaru, and T. Kitao, *Chem. Lett.*, **1990**, 1351.
14. There was a suggestion that this initial product Ia' may not be related to the formation of **3** and **4**. Since addition of $PdCl_2(MeCN)_2$ to the acetonitrile solution of **2a'** containing triethylamine (10 equivalents) also gave **Ia'**, a direct metallation of the free base **2a'** with $PdCl_2$ to give **3a'** or **4a'** is not plausible. The initial product **Ia'** was separated by column chromatography on silica gel and recrystallized from CH_2Cl_2-n-hexane. The elemental analysis indicates that **Ia'** is a mixture of monoprotonated porphyrins having different number of the $PdCl_2$ unit (one or two) in the counter anion. The ^1H NMR spectrum of **Ia'** shows only one set of signals due to the porphyrin protons, the chemical shifts of which are substantially the same as those of **1a'**. (NMR data of **Ia'** in $CDCl_3$: δ 9.26, 9.10, 8.85, 8.73 (d × 4, 2H × 4, pyrrole-β-H); 8.49 - 7.08 (m, 20H, phenyl-H); 6.31 (t, 2H, bridge phenyl-*p*-H); 5.91 (t, 4H, bridge phenyl-*m*-H); 2.6 (br, 4H, bridge phenyl-*o*-H); 2.63 (s, 1H, OH)). A ^1H-singlet at 2.63 ppm may be assigned to the coordinated OH proton in the counter anion. The largest mass peak in the FAB MS spectrum of **Ia'** is 791 which corresponds to the porphyrin cation. We have confirmed that the isolated initial product **Ia'** is converted into the dinuclear Pd complex **3a'** and that this transformation does not occur by way of the mononuclear Pd complex **4a'**. Thus, we would like to propose the stepwise pathway for the ligation.
15. (a) A. G. Constable, W. S. McDonald, L. C. Sawkins, and B. L. Shaw, *J. Chem. Soc., Dalton Trans.*, **1980**, 1992. (b) N. Barr, S. F. Dyke, G. Smith, C. H. L. Kennard, and V. J. Mckee, *J. Organomet. Chem.*, **288**, 109 (1985).

(c) E. C. Alyea, S. A. Dias, G. Ferguson, A. J. McAlees, R. McCrindle, and P. J. Roberts, *J. Am. Chem. Soc.*, **99**, 4985 (1977). (d) E. C. Alyea, G. Ferguson, J. Malito, and B. L. Ruhl, *Organometallics*, **8**, 1188 (1989).

16. J. Setsune, M. Ikeda, Y. Kishimoto, Y. Ishimaru, K. Fukuhara, and T. Kitao, *Organometallics*, **10**, 1099 (1991).
17. R. F. Heck, "Palladium Reagents in Organic Syntheses", Academic Press, Inc., New York (1980).
18. P. T. Beurskens, G. Admiraal, G. Beurskens, W. P. Bosman, S. Garcia-Granda, R. O. Gould, L. M. M. Smits, and C. Smykalla, "The DIRDIF program system, Technical Report of the Crystallography Laboratory", University of Nijmen, The Netherlands (1992).
19. D. T. Cromer and J. T. Waber, "International Tables for X-ray Crystallography", The Kynoch Press, Birmingham, England (1974), Vol. IV, Table 2.2A.
20. D. C. Creagh and W. J. McAuley, "International Tables for Crystallography", ed by A. J. C. Wilson, Kluwer Academic Publishers, Boston (1992), Vol C, pp. 219 - 222, Table 4.2.6.8.
21. D. C. Creab and J. H. Hubbell, "International Tables for Crystallography", ed by A. J. C. Wilson, Kluwer Academic Publishers, Boston (1992), Vol C, pp. 200 - 206, Table 4.2.4.3.
22. "TeXsan: Crystal Structure Analysis Package", Molecular Structure Corporation, (1985, 1992). J. J. P. Stewart, *J. Comput. Chem.*, **10**, 209 (1989).

Chapter 3

Coordination of Amines to Palladium(II) Complexes of N^{21},N^{22}-Bridged Porphyrins

3.1 Introduction

As shown in chapter 1, N^{21},N^{22}-etheno-bridged porphyrin serves as a bidentate nitrogen base ligand for stable coordination to palladium. This bidentate porphyrin ligand is not only interesting in view of its stereochemical, electrochemical, and photochemical properties but also valuable as an NMR shift reagent. The X-ray crystal structures of these porphyrinatopalladium(II) complexes indicate that two Pd-N bonds are tilted by 21.8 and 23.7 degree from the corresponding pyrrole planes. In spite of their bent Pd-N bondings, these porphyrinatopalladium(II) complexes seem to be quite stable.

There are many reports on Pd complexes of bidentate nitrogen base ligands, such as bipyridine (bpy) and 1,10-phenanthroline (phen), where inter-ligand steric hindrance causes distortion on the coordination geometry and the ligand structure.[1-4] In the case of $[Pd^{II}(bpy)_2]$ complexes, two bidentate ligands can not assume a coplanar arrangement due to a steric repulsion between the hydrogen atoms. Thus, the coordination geometry of Pd is tetrahedrally distorted from square planarity with two bpy ligands in a twisted orientation. A different way to alleviate the steric hindrance between two bpy ligands is to put them in a step-like conformation with some dihedral angle between the Pd square plane and the mean bpy plane. This step-like conformation is accompanied by a bowing of two pyridine rings within one

chelating bpy ligand.[5,6] A similar bowing of two pyrrole rings within a chelating dipyrrylmethene unit is observed in the structure of Pd complexes of N^{21},N^{22}-etheno-bridged porphyrin.[7]

It is known that heteroaromatic bidentate ligands, such as bpy and phen, are readily replaced by ethylenediamine in mixed-ligand Pd complexes with ethylenediamine and heteroaromatic bidentate ligand.[8-10] In this chapter is described the ligand substitution reaction of porphyrinatopalladium(II) complexes with amines in order to see how strong their bent Pd-N bondings are. Furthermore, the dynamic behaviors of the porphyrinatopalladium(II) complexes ligated by ethylenediamine are discussed based on their spectroscopic properties.

3.2 Results and Discussion

3.2.1 **Reaction of Palladium (II) Complexes of N^{21},N^{22}-Bridged Porphyrins with Amines.**

Dichloropalladium(II) complex (**1a**), (μ-dichloro)dipalladium(II) complexes (**2a**, **2b**), and bis(aqua)palladium(II) complexes (**3a**, **3c**) of N^{21},N^{22}-etheno-bridged porphyrin were used as starting materials.[7] The μ-dichloro complexes and bis(aqua) complexes have perchlorate ions as counter anions. Amine adducts (**4a-10a**, **5b**, **6c**) of these starting complexes were prepared in good yields (70 - 100%) as shown in Scheme 1. The reaction of **1a** with excess pyridine (4 equiv) in CH_2Cl_2 at room temperature caused replacement of only one chloride to give **4a**. Similar mono(pyridine) adducts (**5a**, **5b**) were obtained from **2a** and **2b**, and bis(pyridine) adducts (**6a**, **6c**) were readily obtained from **3a** and **3c**. It took 11.2h for half amounts of **1a** to be

converted to **4a** by the addition of pyridine (0.040 mol dm^{-3}) to **1a** (0.010 mol dm^{-3}) in $CDCl_3$ at room temperature, while the formation of **5a** and **6a** occurred almost instantly. The addition of excess ethylenediamine (1.2 - 2.5 equiv) to **1a**, **2a**, and **3a** resulted in the formation of ethylenediamine chelate complexes, (**7a-9a**), respectively, without any dissociation of the porphyrin ligand. The time required for the conversion of half amounts of **1a** by ethylenediamine (0.040 mol dm^{-3}) to **1a** (0.010 mol dm^{-3}) was much shorter (23 min) than that by pyridine under the same conditions as indicated above. ESI MS spectra of **4a**, **5a**, and **5b** showed molecular monocationic peaks and those of **6a** – **9a** and **6c** showed molecular dicationic peaks to suggest that one chloride anion coordinate strongly in **4a**, **5a**, and **5b**. ESI MS spectrum of **7a** is given as one example in Figure 1.

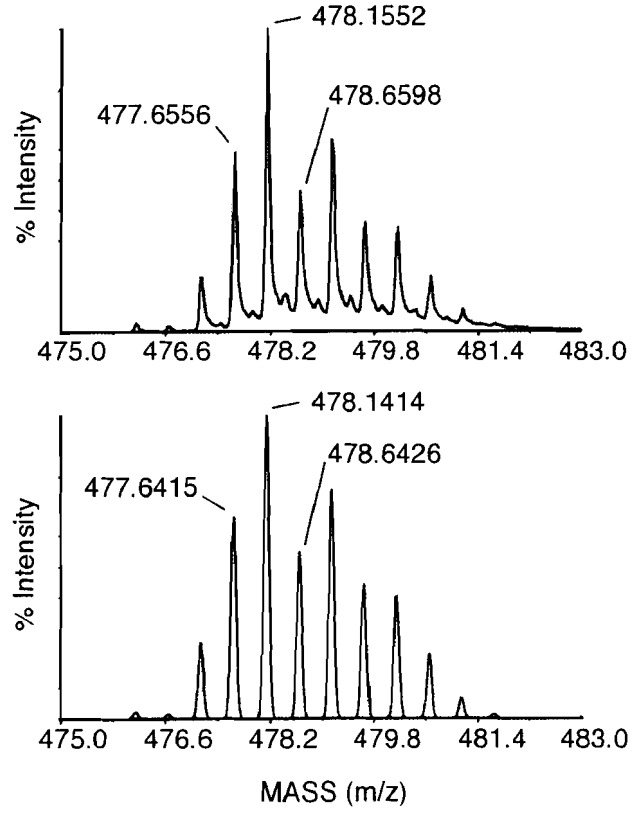

Figure 1. ESI-MASS spectrum of **7a** (top) and simulation for $[\mathbf{7a}\text{-}2(ClO_4^-)]^{2+}$ (bottom).

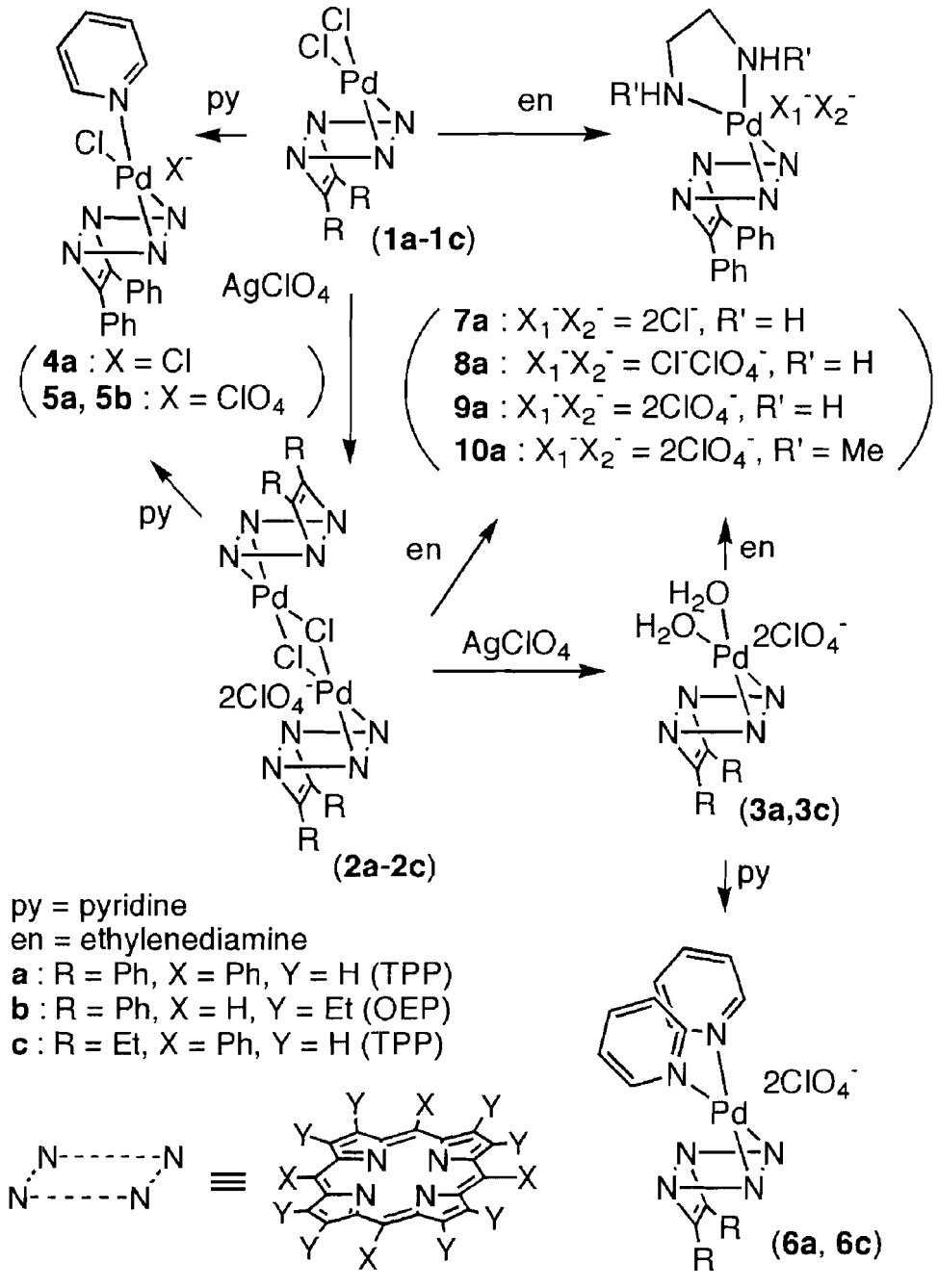
py
en
AgClO4
(1a-1c)
(4a : X = Cl
5a, 5b : X = ClO4)
(7a : X1-X2- = 2Cl-, R' = H
8a : X1-X2- = Cl-ClO4-, R' = H
9a : X1-X2- = 2ClO4-, R' = H
10a : X1-X2- = 2ClO4-, R' = Me)
(2a-2c)
(3a,3c)
(6a, 6c)
py = pyridine
en = ethylenediamine
a : R = Ph, X = Ph, Y = H (TPP)
b : R = Ph, X = H, Y = Et (OEP)
c : R = Et, X = Ph, Y = H (TPP)

Scheme 1

3.2.2 **Spectroscopic Characteristics.**

UV-Vis spectra of Pd complexes of N^{21},N^{22}-bridged porphyrin show split Soret bands of porphyrin chromophore at around 410 nm and 440 nm. The intensity ratio of the latter band relative to the former band is much greater for the bis(pyridine) adduct (**6a**) than for the mono(pyridine) adducts (**4a**, **5a**) (see Figure. 2; middle). This Soret band splitting may be diagnostic of whether porphyrinatopalladium(II) is ligated by at least one anionic ligand. In fact, the shape of the Soret band of **6a** is very similar to that of bis(perchlorate) (**3a**), while the Soret bands of **4a** and **5a** look like that of dichloride (**1a**) (see Figure. 2; top). The C_s symmetric chelating molecular structure is indicated for all of the ethylenediamine complexes, (**7a-9a**), by their ^{1}H NMR spectra. However, their UV-Vis spectra indicate that the structure of bis(perchlorate) (**9a**) is very similar to that of **6a**, but different from those of **7a** and **8a**. (See Figure. 2; bottom). The splitting pattern of the Soret bands of **7a** and **8a** are similar to that of mono(pyridine) adducts (**4a**) and (**5a**). This observation suggests that coordination of chloride anion is occurring in the complexes of **7a** and **8a**.

The ^{1}H NMR spectra of **7a**, **8a**, and **9a** show four broad 2H-signals due to the chelated ethylenediamine protons in the chemical shift range between 0.4 and -2.6 ppm as shown in Figure 3. One of the amino proton signals (-1.50, -2.48, and -2.53 ppm for **7a**, **8a**, and **9a**, respectively) is greatly shifted to a lower frequency region than TMS due to the porphyrin ring current effect, and thus associated with the proton very close (syn) to the porphyrin plane, as depicted in Scheme 2. The chemical shift of H_{syn} moves toward the higher frequency region upon going from **9a** to **8a** and **7a** and also upon going from -15 °C to 5 °C and then 25 °C, as summarized in Table 1. Since the amino protons at the apical site would experience a smaller ring-current effect of the porphyrin than at the basal site, these chemical shift changes of H_{syn} may be induced

through the ligation of chloride to Pd followed by transposition of the amino ligand from the basal site (structure **A**) to the apical site (structure **B**). It is reasonable to assume that such a change in the coordination geometry is promoted by the presence of greater amount of chloride anion and at a higher temperature. As a matter of fact, the addition of $Me_4N^+Cl^-$ (3 molar eq.) to a $CDCl_3$ solution of **9a** caused a change in the ^1H NMR chemical shift of H_{syn} from –2.53 to –1.50 ppm. Signals due to ethylenediamine protons of **7a**, **8a**, and **9a** are broad with half-height line widths in the range of 22.15 ~ 24.80 Hz. The flipping motion of the five-membered metallacycle may be responsible for this line broadening. However, the line widths of signals due to β-pyrrole protons are more sensitive to the counter anion and temperature. The half-height line widths of the β-pyrrole protons at around 9.4 ppm of **7a**, **8a**, and **9a** are 12.83, 8.60, and 2.45 Hz, respectively, in $CDCl_3$, as can be seen in Figure 3 and that of **7a** at 9.37 ppm becomes smaller from 12.83 to 9.69, and then to 3.44 Hz with decreasing temperature from 25 °C to 5 °C and then to –15 °C. These phenomena may also be explained in terms of the coordination - dissociation equilibrium of chloride and transposition of the coordinated chloride between the apical site and the basal site as shown in Scheme 2. Although the bis(perchlorate) (**9a**) shows sharp NMR signals in $CDCl_3$ as noted above, the β-pyrrole proton signal of **9a** become much broader in DMSO where the half-height line width is 12.94 Hz. This is well explained in terms of the coordinating ability of DMSO.

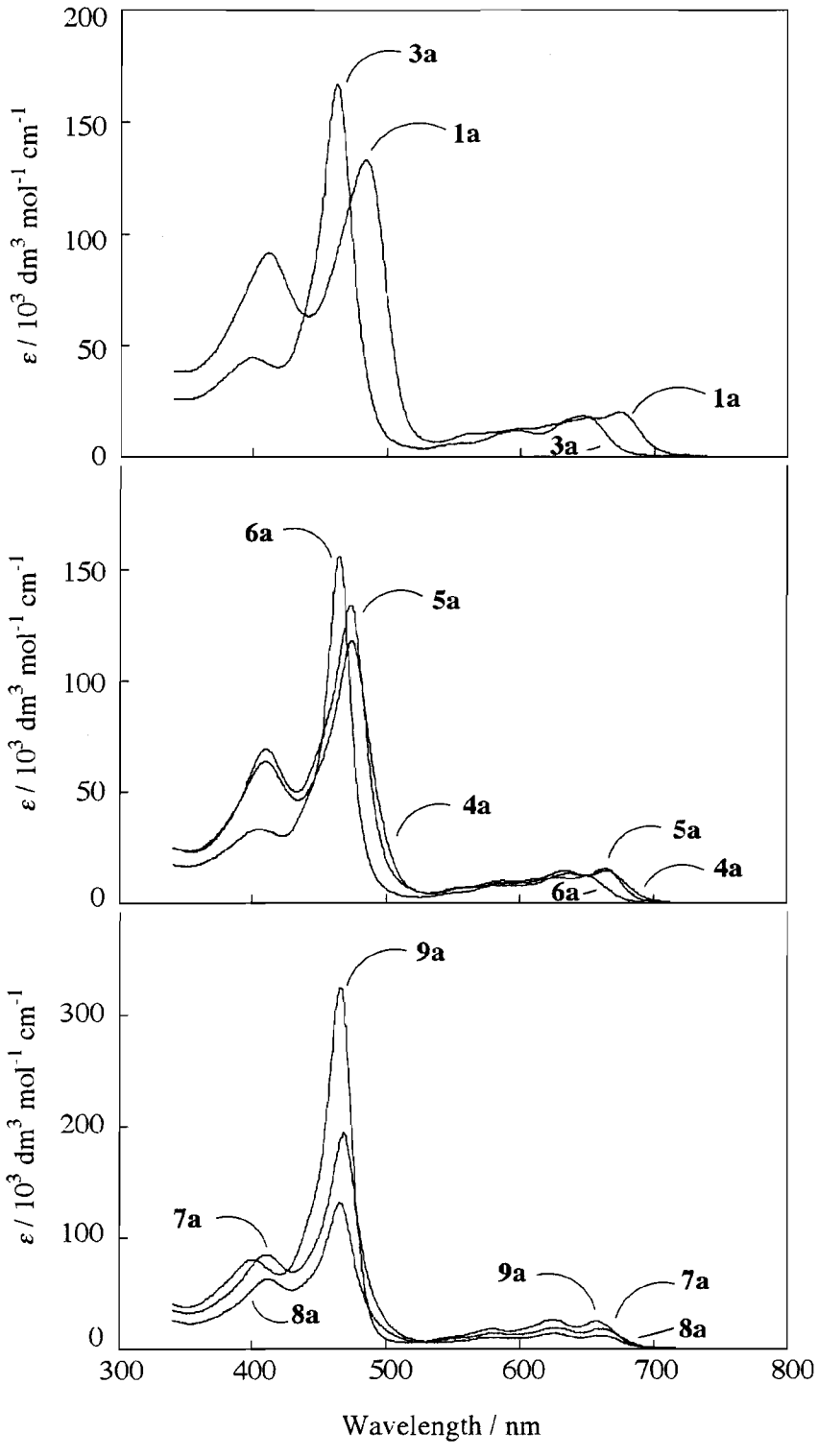

Figure 2. UV-Vis spectra of porphyrinatopalladium(II) complexes (top : **1a** and **3a**), pyridine complexes (middle : **4a-6a**), and ethylenediamine complexes (bottom : **7a-9a**) in CH_2Cl_2.

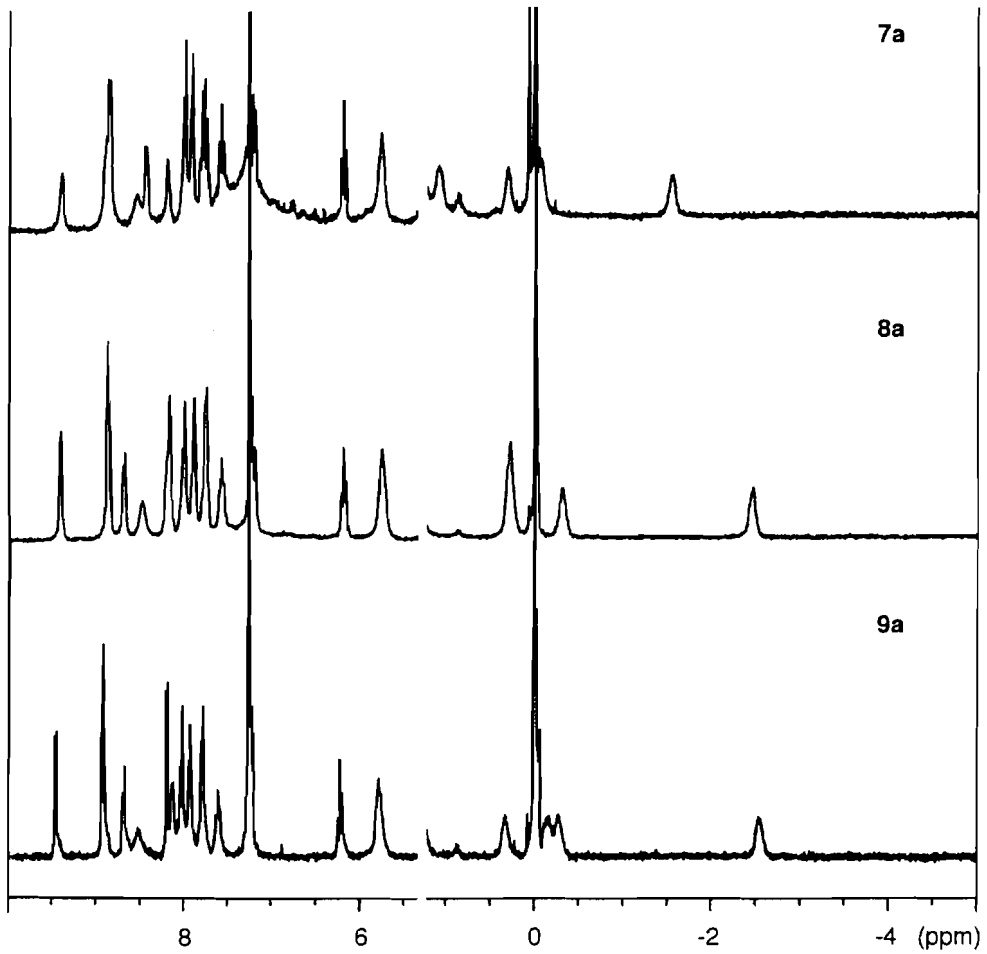

Figure 3. ^{1}H NMR spectra of ethylenediamine complexes (**7a-9a**) in $CDCl_3$ at 25 °C (270 MHz).

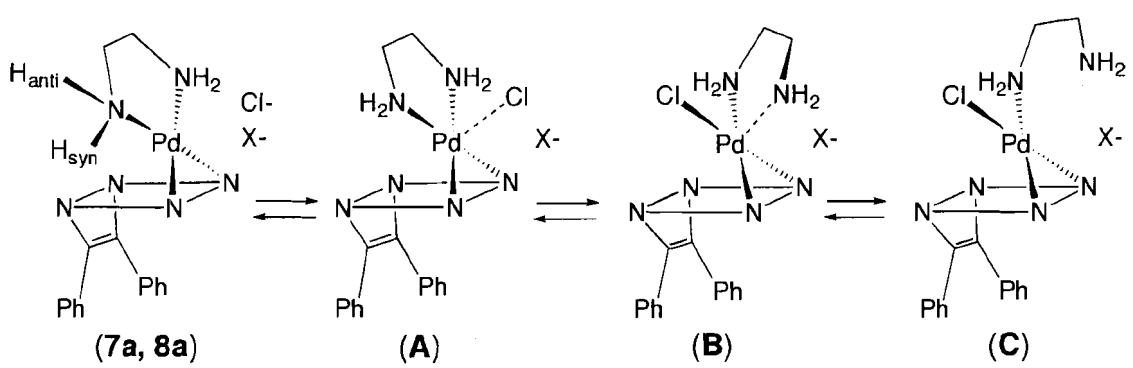

Scheme 2

Table 1. ^{1}H NMR[a] Data of Pd(II) Porphyrins

comp.	temp.	chemical shift (ppm)		
	(°C)	pyridine-α	pyridine-β	pyridine-γ
4a	25	3.62	6.23	7.09
5a	25	3.63	5.80	7.01
5b	25	-[b]	6.03	7.25
6a	25	-[c]	6.34	6.88
6c	25	-[c]	6.32	6.85

comp.	temp.	chemical shift (ppm)		line width (Hz)
	(°C)	en-CH_2	en-NH_2	pyrrole-β[d]
7a	25	0.32, -0.05	1.09 , -1.50	12.83
7a	5	0.28, -0.05	1.06, -1.61	9.69
7a	-15	0.26, -0.14	1.06, -1.74	3.44
8a	25	0.33, -0.22	0.00, -2.48	8.60
9a	25	0.32, -0.27	-0.13, -2.53	2.45
9a[e]	25	-0.13, -0.89	1.35, -2.09	12.94

[a] 270 MHz [b] overlapped [c] not detected [d] half height width
[e] in d_6-DMSO

3.2.3 **Dynamic Behavior.**

The NH_2 signals of ethylenediamine were assigned based on the H-D exchange. Both signals assigned to the amine H_{syn} (-1.50 ppm) and the amine H_{anti} (1.09 ppm) of **7a** disappeared rapidly in $CDCl_3$ upon the addition of D_2O, while the amine H_{syn} (-2.53 ppm) of **9a** exchanged with D_2O much more slowly than the amine H_{anti} (-0.13 ppm), as shown in Figure 4. Since the Pd-ligand bonding is weaker in the five-coordinated complexes than in the four-coordinated complexes, rapid H-D exchange in the complex (**7a**) would take place after dissociation of an amino group from Pd (structure **C**). The difference in the H-D exchange kinetics between H_{syn} and H_{anti} in the case of **9a** is remarkable and this suggests that H-D exchange of the amino protons occurs without dissociation of the amino group. D_2O molecule is not easily accessible to the amino H_{syn} proton of **9a** due to the steric hindrance of the porphyrin ligand.

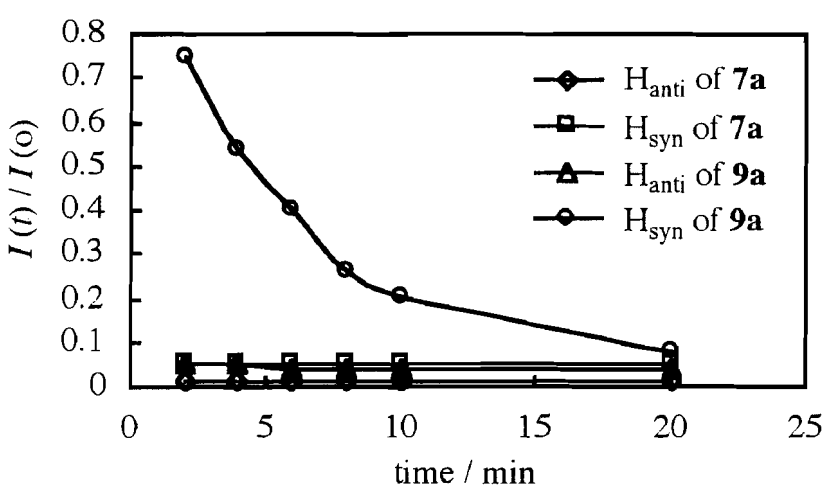

Figure 4. Decay of ^1H NMR signals due to amino protons (H_{syn} and H_{anti}) of **7a** and **9a** with time by exchange to D_2O in $CDCl_3$ at 25 °C. $I(t)$: Signal intensity at the time t.

The dynamic behavior in which bond dissociation between Pd and a nitrogen followed by the rotation around the remaining Pd-N bonding and then remaking of the Pd-N bonding should cause an exchange between the amine H_{syn} and the amine H_{anti} of the ethylenediamine ligand. Since the line widths of the coordinated ethylenediamine protons do not depend on the counter anion and temperature, we think that the bond dissociation between Pd and a porphyrin nitrogen is not occurring in these complexes. This is in agreement with the fact that the half-lives for the substitution of the porphyrin ligand of **7a** and **9a** under pseudo first-order conditions by ethylenediamine (0.5 mol dm^{-3}) in MeOH at 25 °C are 2.90×10^3 s and 2.94×10^3 s, although bpy ligand of $[Pd(en)(bpy)]Cl_2$ is replaced by ethylenediamine under the same conditions within a few seconds.[9] The half-lives are evaluated from the decay curves for absorbance at Soret band in UV-Vis spectra after the addition of ethylenediamine to the MeOH solution of **7a** and **9a** as illustrated in Figure 5 ($k = 4.78 \times 10^{-4}$ L mol^{-1} s^{-1} and 4.72×10^{-4} L mol^{-1} s^{-1} for **7a** and **9a**, respectively).

In this chapter, it was shown that the N^{21},N^{22}-bridged porphyrin ligand strongly coordinates to Pd and influences the dynamic behavior of the coexisting ligand in the same coordination sphere and that the changes in the metal coordination structure are sensitively detected by the spectroscopic properties of the porphyrin ligand.

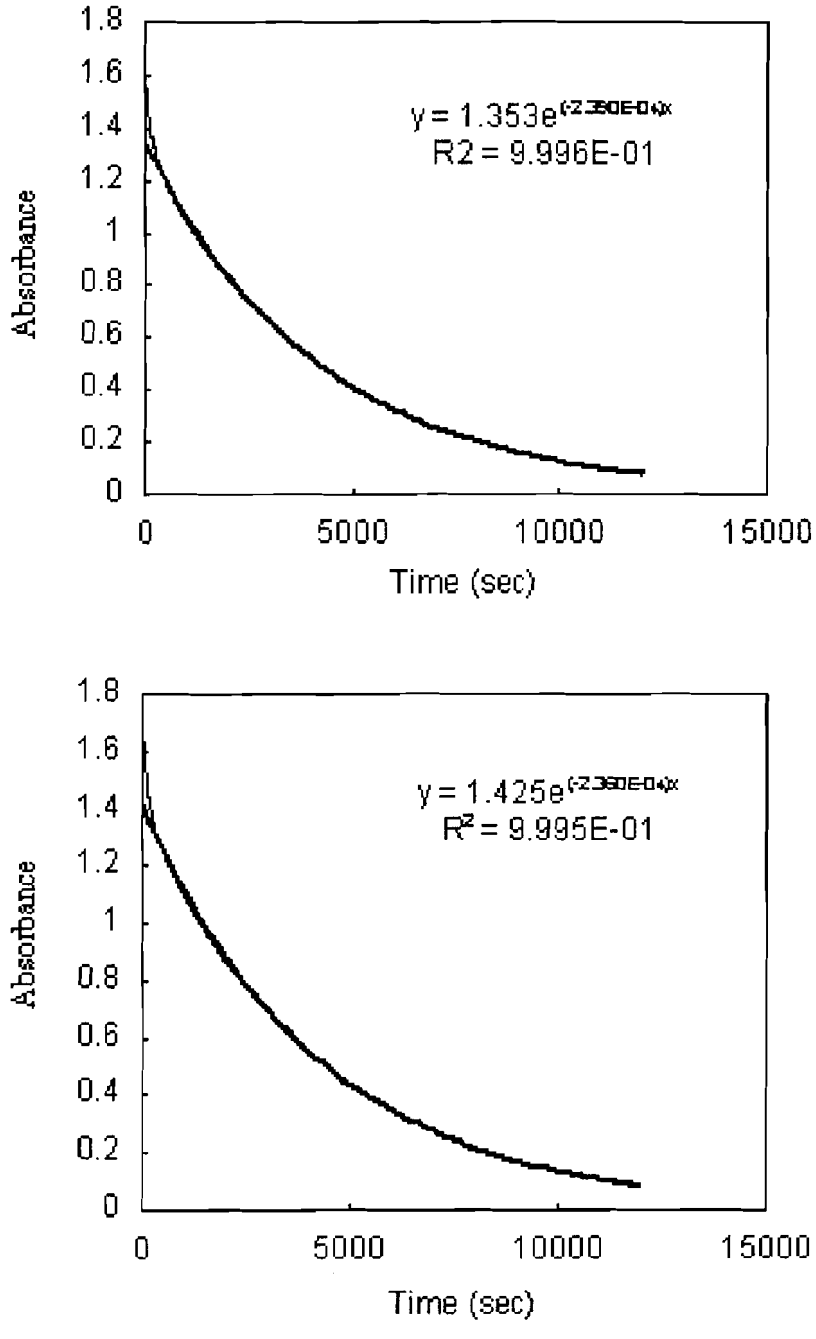

Figure 5. Decay curves of **7a** (top) and **9a** (bottom). Bold lines are fitting curves.

3.3 Experimental Section

General Procedure of Preparation for Mono(perchlorato)Pd(II) Porphyrins (2a-c). A mixture of **1a** (0.05 mmol), $AgClO_4$ (0.05 mmol), and dichloromethane (5 mL) was stirred vigorously at room temperature. The white precipitate of AgCl appeared within 1 h. AgCl was filtered off after stirring for 3 h. The filtrate was evaporated and the product was recrystallized from dichloromethane – hexane.

$[N^{21},N^{22}$-(PhC=CPh)(TPP)PdCl$]_2(ClO_4)_2$ (**2a**). ^{1}H NMR (300 MHz, $CDCl_3$): δ 9.41, 8.49, 8.47, 7.69 (d × 4, 2H × 4, β-Pyrrole-H), 8.39-7.03 (m, 20H, meso-Ph-H), 5.98 (t, 2H, bridge-Ph p-H), 5.49 (br, 4H, bridge-Ph m-H). Anal. Calcd for $C_{58}H_{38}N_4O_4Cl_2Pd{\cdot}H_2O$: C, 66.33; H, 3.84; N, 5.33 %. Found: C, 66.29; H, 3.80; N, 5.31 %. UV/Vis (CH_2Cl_2), nm: 655.0, 603.5, 461.5, 407.5. MS (ESI in MeOH) *m/z* 963.1429 (calcd for ($C_{59}H_{42}N_4OClPd$ ((M – $2ClO_4$)/2]) + CH_3OH): 963.2093).

$[N^{21},N^{22}$-(PhC=CPh)(OEP)PdCl$]_2(ClO_4)_2$ (**2b**). ^{1}H NMR (300 MHz, $CDCl_3$): δ 10.77, 10.20, (s × 2, 1H × 2, meso-H), 9.15 (s, 2H, meso-H), 4.28-3.34 (m, 16H, CH_2), 1.38, 1.15, 0.97, 0.94 (t × 4, 6H × 4, CH_3), 5.73 (t, 2H, bridge-Ph p-H), 5.17 (br, 4H, bridge-Ph m-H). Anal. Calcd for $C_{50}H_{54}N_4O_4Cl_2Pd$: C, 63.06; H, 5.72; N, 5.88 %. Found: C, 62.94; H, 5.83; N, 5.48 %. MS (ESI in MeOH) *m/z* 852.2066 (calcd for $C_{50}H_{54}N_4ClPd$ ((M-$2ClO_4$)/2): 852.3082).

$[N^{21},N^{22}$-(EtC=CEt)(TPP)PdCl$]_2(ClO_4)_2$ (**2c**). ^{1}H NMR (300 MHz, $CDCl_3$): δ 9.06, 8.33, 8.18, 8.06 (d × 4, 2H × 4, β-Pyrrole-H), 8.10-7.08 (m, 20H, meso-Ph-H), −1.87 (t, 6H, bridge-CH_3), −3.52, −5.12 (dq × 2, 2H × 2, bridge-CH_2, J_{gem} = 15Hz). Anal. Calcd for $C_{50}H_{38}N_4O_4Cl_2Pd{\cdot}2H_2O$: C, 61.77; H, 4.35; N, 5.76 %. Found: C, 61.93; H, 4.71; N, 5.24 %. FAB MS *m/z* 1772

(calcd for $C_{100}H_{76}N_8O_4Cl_3Pd_2$ (M-ClO_4): 1772.9) and 836 (calcd for $C_{50}H_{38}N_4ClPd$ ((M – 2ClO_4)/2): 836.3).

General Procedure for Preparation of Bis(perchlorato)Pd(II) Porphyrins (3a-c). A mixture of **1a-c** (0.05 mmol), $AgClO_4$ (0.20 mmol), and dichloromethane (5 mL) was stirred vigorously at room temperature. The white precipitate of AgCl appeared within 1 h. The work-up procedure was the same as for **2a-2c**.

N^{21},N^{22}-(PhC=CPh)(TPP)Pd(ClO_4)$_2$ (**3a**). ^{1}H NMR (300 MHz, $CDCl_3$): δ 9.35, 8.91, 8.68, 8.20 (d × 4, 2H × 4, β-Pyrrole-H), 8.66-7.31 (m, 20H, meso-Ph-H), 6.22 (t, 2H, bridge-Ph *p*-H), 5.77 (br, 4H, bridge-Ph m-H). Anal. Calcd for $C_{58}H_{38}N_4O_8Cl_2Pd{\cdot}2H_2O$: C, 58.72; H, 4.08; N, 4.72 %. Found: C, 58.49; H, 4.00; N, 4.53 %. UV/Vis (CH_2Cl_2), nm: 652.5, 633.0, 589.0, 463.5, 413.0. MS (ESI in MeOH) *m/z* 995.30 (calcd for $C_{58}H_{38}N_4O_4ClPd$ (M – ClO_4): 995.15).

N^{21},N^{22}-(PhC=CPh)(OEP)Pd(ClO_4)$_2$ (**3b**). ^{1}H NMR (300 MHz, $CDCl_3$): δ 11.14, 10.59, (s × 2, 1H × 2, meso-H), 10.12 (s, 2H, meso-H), 4.47-3.63 (m, 16H, CH_2), 2.31, 1.85, 1.39, 1.25 (t × 4, 6H × 4, CH_3), 6.03 (t, 2H, bridge-Ph *p*-H), 5.56 (br, 4H, bridge-Ph m-H). Anal. Calcd for $C_{50}H_{54}N_4O_8Cl_2Pd{\cdot}2H_2O$: C, 55.18; H, 5.74; N, 5.15 %. Found: C, 55.59; H, 5.62; N, 4.59 %.

N^{21},N^{22}-(EtC=CEt)(TPP)Pd(ClO_4)$_2$ (**3c**). ^{1}H NMR (300 MHz, $CDCl_3$): δ 9.17, 8.78, 8.76, 8.55 (d × 4, 2H × 4, β-Pyrrole-H), 8.53-7.85 (m, 20H, meso-Ph-H), −1.36 (t, 6H, bridge-CH_3), −2.85, −4.27 (dq × 2, 2H × 2, bridge-CH_2, J_{gem} = 15Hz). Anal. Calcd for $C_{50}H_{38}N_4O_8Cl_2Pd{\cdot}4H_2O$: C, 54.19; H, 4.55; N, 5.06 %. Found: C, 54.28; H, 4.40; N, 5.05 %. FAB MS *m/z* 899 (calcd for $C_{50}H_{38}N_4O_4PdCl$ (M – ClO_4): 899).

Preparation Procedures and Spectroscopic and Analytical data for

*Compounds, (**4a**, **5a**, **5b**, **6a**, **6c**, and **7a-10a**).* To a CH_2Cl_2 solution containing 0.02 mmol of **1a-3a**, **2b**, and **3c** were added the amines (4 equiv of pyridine for **4a-6a**, **5b**, and **6c**, 1.2 equiv of ethylenediamine for **7a**, 2.5 equiv of ethylenediamine for **8a** and **9a**, and 2.5 equiv of dimethylethylenediamine for **10a**). The mixture was stirred overnight at room temperature, the products were then deposited from CH_2Cl_2-hexane as green solid and washed with ether.

4a: Yield 76 %. ^{1}H NMR (300 MHz, at 25 °C in $CDCl_3$) δ 3.62 (br, 2H, py-α-H), 6.23 (br, 2H, py-β-H), 7.09 (t, 1H, py-γ-H), 9.34, 9.20, 9.04, 9.01, 8.83, 8.73, 8.66, 8.20 (d × 8, 1H × 8, β-pyrrole-H), 8.57-6.83 (m, 20H, meso-Ph-H), 6.17 (m, 2H, bridge-Ph p-H), 5.76 (br, 4H, bridge-Ph m-H), o-H is not detected. Anal. Calcd for $C_{63}H_{43}N_5Cl_2Pd{\cdot}3H_2O$: C, 68.70; H, 4.48; N, 6.36 %. Found: C, 68.30; H, 4.01; N, 5.85 %. UV/Vis (CH_2Cl_2): λ_{max}(log ε) 410 (4.80), 474 (5.07), 591 (3.95), 637 (4.12), 665 (4.16) nm. MS (ESI in MeOH) *m/z* 1010.2351 (calcd for $C_{63}H_{43}N_5ClPd$ (M – Cl): 1010.2254).

5a: Yield 90 %. ^{1}H NMR δ 3.63 (br, 2H, py-α-H), 5.80 (br, 2H, py-β-H), 7.01 (t, 1H, py-γ-H), 9.46, 9.18, 9.02, 8.83, 8.72, 8.26, 8.21 8.17 (d × 8, 1H × 8, β-pyrrole-H), 8.58-6.83 (m, 20H, meso-Ph-H), 6.18 (m, 2H, bridge-Ph p-H), 5.80 (br, 4H, bridge-Ph m-H), o-H is not detected. Anal. Calcd for $C_{63}H_{43}N_5Cl_2O_4Pd{\cdot}H_2O$: C, 67.00; H, 4.02; N, 6.20 %. Found: C, 67.09; H, 4.13; N, 6.28 %. UV/Vis (CH_2Cl_2): λ_{max}(log ε) 410 (4.84) , 473 (5.13), 587 (3.99), 634 (4.16), 665 (4.19) nm. MS (ESI in MeOH) *m/z* 1010.1200 (calcd for $C_{63}H_{43}N_5ClPd$ (M – ClO_4): 1010.2254).

5b: Yield 81 %. ^{1}H NMR δ 6.01 (br, 2H, py-β-H), 7.25 (t, 1H, py-γ-H), α-H is not detected, 11.09, 10.69, 10.28, 9.59 (s × 4, 1H × 4, meso-H), 4.68-3.32 (m, 16H, CH_2), 2.15, 2.03 (t × 2, 3H × 2, CH_3) 1.92, 1.56, 1.22 (t × 3, 6H × 3, CH_3), 6.03 (m, 2H, bridge-Ph p-H), 5.57 (br, 4H, bridge-Ph m-H), o-H is not detected. Anal. Calcd for $C_{55}H_{59}N_5Cl_2O_4Pd$: C, 64.05; H, 5.77; N,

6.79 %. Found: C, 63.79; H, 5.57; N, 6.50 %. MS (ESI in MeOH) *m/z* 930.2750 (calcd for $C_{55}H_{59}N_5ClPd$ (M – ClO_4): 930.3504).

6a: Yield 94 %. ^{1}H NMR δ 6.34 (br, 4H, py-*β*-H), 6.88 (t, 2H, py-*γ*-H), α-H is not detected, 9.73, 9.03, 8.44, 8.05, (d × 4, 2H × 4, β-pyrrole-H), 8.99-6.88 (m, 20H, meso-Ph-H), 6.20 (t, 2H, bridge-Ph p-H), 5.76 (br, 4H, bridge-Ph m-H), o-H is not detected. Anal. Calcd for $C_{68}H_{48}N_6Cl_2O_8Pd{\cdot}H_2O$: C, 64.18; H, 3.96; N, 6.60 %. Found: C, 64.37; H, 3.55; N, 6.36 %. UV/Vis (CH_2Cl_2): λ_{max}(log ε) 406 (4.52) , 465 (5.19), 585 (3.90) , 629 (4.07), 650 (4.09) nm. MS (ESI in MeOH) *m/z* 527.1230 (calcd for $C_{68}H_{48}N_6Pd$ ((M – $2ClO_4$)/2): 527.1493).

6c: Yield 85 %. ^{1}H NMR δ 6.32 (br, 4H, py-*β*-H), 6.85 (t, 2H, py-*γ*-H), α-H is not detected, 9.52, 8.85, 8.53, 8.39, (d×4, 2H×4, β-pyrrole-H), 8.73-7.65 (m, 20H, meso-Ph-H), -1.44 (t, 6H, bridge-CH_3), –2.97, –4.46 (dq × 2, 2H × 2, bridge-CH_2, J_{gem} = 15.0Hz). Anal. Calcd for $C_{60}H_{48}N_6Cl_2O_8Pd{\cdot}2H_2O$: C, 60.33; H, 4.39; N, 7.04 %. Found: C, 60.01; H, 4.50; N, 6.55 %. MS (ESI in MeOH) *m/z* 479.1073 (calcd for $C_{60}H_{48}N_6Pd$ ((M – $2ClO_4$)/2): 479.1492).

7a: Yield 91 %. ^{1}H NMR δ 1.09, –1.50 (br × 2, 2H × 2 en-NH_2), 0.32, –0.05 (br × 2, 2H × 2 en-CH_2), 9.37, 8.87, 8.85, 8.17, (br × 4, 2H × 4, β-pyrrole-H), 8.55-7.19 (m, 20H, meso-Ph-H), 6.18 (t, 2H, bridge-Ph p-H), 5.75 (br, 4H, bridge-Ph m-H), o-H is not detected. Anal. Calcd for $C_{60}H_{46}N_6Cl_2Pd{\cdot}3H_2O$: C, 66.58; H, 4.84; N, 7.76 %. Found: C, 66.18; H, 4.50; N, 8.14 %. UV/Vis (CH_2Cl_2): λ_{max}(log ε) 411 (4.93), 468 (5.29), 582 (4.14), 628 (4.27), 661 (4.25) nm. MS (ESI in MeOH) *m/z* 478.1552 (calcd for $C_{60}H_{46}N_6Pd$ ((M – 2Cl)/2): 478.1414).

8a: Yield 85 %. ^{1}H NMR δ 0.00, –2.48 (br × 2, 2H × 2 en-NH_2), 0.33, –0.22 (br × 2, 2H × 2 en-CH_2), 9.38, 8.86, 8.18 (br × 3, 2H + 4H + 2H, β-pyrrole-H), 8.72-7.21 (m, 20H, meso-Ph-H), 6.20 (t, 2H, bridge-Ph p-H),

5.77 (br, 4H, bridge-Ph m-H), o-H is not detected. Anal. Calcd for $C_{60}H_{46}N_6Cl_2O_4Pd{\cdot}0.5Pd(C_2H_8N_2)Cl(ClO_4)$: C, 58.94; H, 4.05; N, 7.89 %. Found: C, 59.19; H, 3.67; N, 7.85 %. UV/Vis (CH_2Cl_2): λ_{max}(log ε) 412 (4.80), 466 (5.12), 581 (4.00), 626 (4.13), 661 (4.08) nm. MS (ESI in MeOH) *m/z* 478.1044 (calcd for $C_{60}H_{46}N_6Pd$ ((M – Cl – ClO_4)/2): 478.1414).

9a: Yield 100 %. ^{1}H NMR δ –0.13, –2.53 (br × 2, 2H × 2 en-NH_2), 0.32, –0.27 (br × 2, 2H × 2 en-CH_2), 9.44, 8.91, 8.90, 8.18 (d × 4, 2H × 4, β-pyrrole-H), 8.68-7.20 (m, 20H, meso-Ph-H), 5.90 (t, 2H, bridge-Ph p-H), 5.42 (br, 4H, bridge-Ph m-H), o-H is not detected. Anal. Calcd for $C_{60}H_{46}N_6Cl_2O_8Pd{\cdot}H_2O$: C, 60.44; H, 4.23; N, 7.05 %. Found: C, 60.82; H, 4.21; N, 7.04 %. UV/Vis (CH_2Cl_2): λ_{max}(log ε) 400 (4.90), 466 (5.51), 579 (4.24), 625 (4.41), 658 (4.39) nm. MS (ESI in MeOH) *m/z* 478.1136 (calcd for $C_{60}H_{46}N_6Pd$ ((M – 2ClO_4)/2): 478.1414).

10a: Yield 70 %. ^{1}H NMR δ 0.06 (d, 6H, NCH_3), –0.65, –2.05 (br × 2, 2H × 2, en-CH_2), 9.38, 9.03, 8.97, 8.24 (d × 4, 2H × 4, β-pyrrole-H), 8.53-6.87 (m, 20H, meso-Ph-H), 6.18 (t, 2H, bridge-Ph p-H), 5.74 (br, 4H, bridge-Ph m-H), o-H is not detected. Anal. Calcd for $C_{62}H_{50}N_6Cl_2O_8Pd{\cdot}H_2O$: C, 61.93; H, 4.36; N, 6.99 %. Found: C, 61.66; H, 4.57; N, 7.22 %. MS (ESI in CH_3CN) *m/z* 1085.38 (calcd for $C_{62}H_{50}N_6PdClO_4$ (M-ClO_4): 1085.25), 492.44 (calcd for $C_{62}H_{50}N_6Pd$ ((M – 2ClO_4)/2): 492.15).

H-D exchange. The H-D exchanges of the amino protons of ethylenediamine complexes (**7a** and **9a**) were monitored by ^{1}H NMR. After adding 3.5 mm^3 of D_2O to a 0.5 cm^3 $CDCl_3$ solution of **7a** or **9a** (3 μmol) in a NMR tube and shaking the sample tube for 20 s, the tube was transferred to a NMR spectrometer at 25 °C. The progress of the H-D exchange of each amino proton was measured by ^{1}H NMR integrations with time.

Kinetics. The substitution of porphyrin ligand of **7a** and **9a** by

ethylenediamine was studied under pseudo first-order conditions with respect to the Pd complex. To a 3 cm^3 MeOH solution of **7a** or **9a** (2.0×10^{-5} and 8.4×10^{-6} mol dm^{-3}) in a photometric cell was added 100 mm^3 (1.5×10^{-3} mol) of ethylenediamine, just after which the cell was transferred to a UV-Vis spectrophotometer at 25 °C. The absorbance of the Soret band at 463 nm of N^{21},N^{22}-bridged porphyrin ligand of the palladium(II) complex decreased with time. The half life period of this pseudo first-order reaction was estimated based on the decay curve.

3.4 References

1. (a) R. Nesper, P. S .Pregosin, K. Puntener, and M. Worle, *Helv. Chim. Acta,* **76**, 2239 (1993). (b) M. Mathis, W. Harsha, T. W. Hanks, R. D. Bailey, G. L. Schimek, and W. T. Pennington, *Chemistry of Materials,* **10**, 3568 (1998).
2. G. Annibale, L. Cattalini, V. Bertolasi, V. Ferretti, G. Gilli, and M. L. Tobe, *J. Chem. Soc., Dalton Trans.* **1989**, 1265.
3. (a) P. Wehman, G. C. Dol, E. R. Moorman, P. C. J, Kamer, P. W. N. M. van leeuwen, J. Fraanje, and K. Goubitz, *Organometallics,* **13**, 4856 (1994). (b) B. Milani, A. Anzilutti, L. Vicentini, A. Sessanta o Santi, E. Zangrando, S. geremia, and G. Mestroni, *Organometallics,* **16**, 5064 (1997).
4. (a) J. R. Wiesner and E. C. Lingafelter, *Inorg. Chem.*, **5**, 1770 (1966). (b) S. Baggio, L. M. Amzel, and L. N. Becka, *Acta Crystallogr., Sect. B,* **26**, 1698 (1970). (c) A. L. Beauchamp, D. Layek, and T. Theophanides, *Acta Crystallogr., Sect. B,* **38**, 1158 (1982). (d) M. Yamashita, K. Toriumi, and T. Ito, *Acta Crystallogr., Sect. C (Cr. Str. Comm.),* **41**, 876 (1985). (e) M. L. Rodgers and D. S. Martin, *Polyhedron*, **6**, 225 (1987).

5. (a) A. J. Carty and P. C. Chieh, *J. Chem. Soc., Chem. Commun.*, **1972**, 158. (b) M. Hinamoto, S. Ooi, and H. Kuroya, *J. Chem. Soc., Chem. Commun.*, **1972**, 356. (c) P. C. Chieh, *J. Chem. Soc., Dalton Trans.* **1972**, 1643.
6. (a) S. Maeda, Y. Nishida, H. Okawa, and S. Kida, *Bull. Chem. Soc. Jpn.*, **59**, 2013 (1986). (b) S. Geremia, L. Randaccio, G. Mestroni, and B. Milani, *J. Chem. Soc., Dalton Trans.* **1992**, 2117.
7. (a) Y. Takao, T. Takeda, J. Watanabe, and J. Setsune, *Organometallics,* **18**, 2936 (1999). (b) Y. Takao, T. Takeda, J. Watanabe, and J. Setsune, *Organometallics,* **22**, 233 (2003).
8. R-D. Schnebeck, L. Randaccio, E. Zangrando, and B. Lippert, *Angew. Chem. Int. Ed.* **37** 119 (1998).
9. M. Cusumano, G. Guglielmo, and V. Ricevuto, *J. Chem. Soc., Dalton.*, **1981**, 1722.
10. A. Bartolotta, M. Cusumano, A. Giannet, and V. Ricevuto, *J. Chem. Soc., Dalton Trans.*, **1984**, 2785.

Chapter 4

Synthesis of π-(Allyl)palladium(II) Complexes with N^{21},N^{22}-Bridged Porphyrin Ligands and Study of the Isomerization Behavior.

4.1 Introduction

Remarkable progress has been made in the chemistry of organopalladium complexes with various amine and phosphine ligands; those with bidentate nitrogen base ligands have recently been recognized as useful in enantioselective organic transformations and polymerizations.[1,2] A coordination site for an organo ligand, however, is not available for ordinary palladium porphyrins because of the tetradentate nature of porphyrin. Therefore, porphyrin has never been well-known to organopalladium chemists, despite not only its interest in photochemical and electrochemical aspect but also its potential in stereochemical effects and NMR ring current effects.[3] The utility of the latter effects has been recognized for five-coordinated and six-coordinated organometallic porphyrin complexes.[4] Proton NMR signals due to the metal-bound organic ligand undergo low-frequency shifts depending on the distance and direction from the center of the porphyrin ring. For example, ring current effects for the metal-bound methyl protons amount to more than 5 ppm.[4b,c] Callot and co-workers reported Pd complexes of N^{21},N^{22}-methano-bridged porphyrin.[5] However, they have never been used for organopalladium chemistry due to their labile nature. In chapter 1 and 2, it has shown that N^{21},N^{22}-etheno-bridged porphyrin serves as a bidentate nitrogen

base ligand for stable coordination to palladium. This chapter is concerned with the synthesis and isomerization behavior of (π-allyl)palladium derivatives with N^{21},N^{22}-bridged porphyrin ligands, and the roles of porphyrin ligands in controlling cis-trans isomerization and also in the spectroscopic characterization of (π-allyl)palladium complexes will be discussed in detail.[6]

4.2 Results and Discussion

4.2.1 **Synthesis of (π-Allyl)palladium(II) Porphyrins.**

Nucleophilic displacement of the coordinated halide ion by allyl anion is one of the most important methods for synthesizing (π-allyl)palladium(II) complexes. Allylsilanes and allyltins, convenient reagents as masked allyl anions, were treated with (dichloro)palladium(II) complexes of (1,2-di-substituted etheno-N^{21},N^{22})-porphyrins, such as (N^{21},N^{22}-PhC=CPh-TPP)$PdCl_2$ (**1a**),[7] (N^{21},N^{22}-PhC=CPh-OEP)$PdCl_2$ (**1b**),[7] and (N^{21},N^{22}-EtC=CEt-TPP)$PdCl_2$ (**1c**). Since these Pd(II) porphyrins did not react with these reagents in $CHCl_3$ at room temperature, the reactivity of Pd was increased by the addition of over 2-fold molar amounts of $AgClO_4$ to **1a-c**. The displacement of the coordinated chlorides gave bis(perchlorate) compounds **2a-c** quantitatively, as is generally seen in Pd chemistry. A broad 4H signal at 0.35 ppm in the ^1H NMR spectrum of **2a** disappeared by adding D_2O. Therefore, this signal is associated with two water molecules coordinated to Pd^{II}. (π-C_3H_5)Pd(II) complexes **3a,b** were synthesized in 93% and 55% isolated yields, respectively, by the reaction of **2a,b** with (η^1-C_3H_5)$SnBu_3$ (1.1 equiv) for 3 h in CH_2Cl_2. The (π-C_3H_5)Pd^{II} complex as a chloride (**3a'**) was obtained alternatively by the reaction of (N^{21},N^{22}-PhC=CPh-TPP) free base with [Pd(C_3H_5)Cl]$_2$ (1.1 equiv) in

benzene at room temperature overnight in a 90% isolated yield. These (π-allyl)Pd^{II} porphyrins are composed of two conformational isomers with respect to the apparent π-allyl ligand rotation. The ^1H NMR signals of the π-allyl group in **3a**,**b** are observed as two C_s-symmetric sets with a ratio of 3:7 at low-frequency regions. Their chemical shifts are influenced greatly by the ring current effect of porphyrin (Table 1). The major component of **3a** shows the signals due to the allyl terminal methylene protons H_{anti} at –4.55 ppm (J_{anti} = 11.9 Hz) and H_{syn} at –0.28 ppm (J_{syn} = 6.9 Hz) and the signal due to the allyl central methine proton H_{cent} at 2.14 ppm. Thus, it was identified as a cis isomer (*cis*-**3a** in Scheme 1) because the terminal methylene protons H_{anti} are estimated to be very close to the porphyrin plane on the basis of the low-frequency chemical shift. The minor component shows H_{anti} at –1.06 ppm (J_{anti} = 10.9 Hz), H_{syn} at –1.37 ppm (J_{syn} = 5.9 Hz), and H_{cent} at –1.25 ppm. The H_{cent} resonates at a 3.39 ppm lower chemical shift and the H_{anti} appears at a 3.49 ppm higher chemical shift than the corresponding protons of *cis*-**3a**. This minor component was identified as a trans isomer, because H_{cent} comes closer to the porphyrin plane, rather than the H_{anti} and H_{syn}. UV-Vis spectrum of **3a** shows split Soret bands at around 410 nm and 470 nm in which the difference between two bands is not so much great as the spectrum of **2a** as seen in Figure 1, to suggest the coordination of allyl anion ligand to Pd.

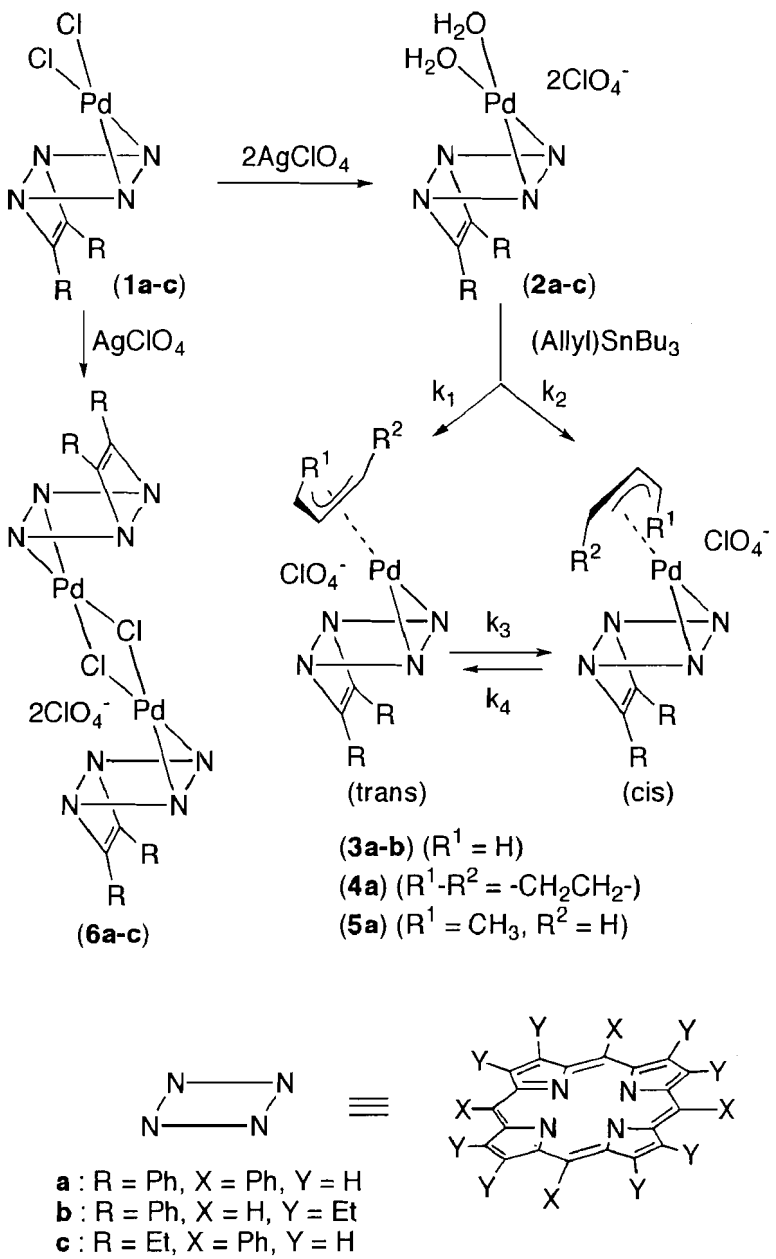
Cl
Cl
Pd
N
N
N
N
R
R
(1a-c)
2AgClO4
H2O
H2O
2ClO4-
(2a-c)
AgClO4
(Allyl)SnBu3
k1
k2
R1
R2
ClO4-
k3
k4
(trans)
(cis)
(6a-c)
(3a-b) (R1 = H)
(4a) (R1-R2 = -CH2CH2-)
(5a) (R1 = CH3, R2 = H)
a : R = Ph, X = Ph, Y = H
b : R = Ph, X = H, Y = Et
c : R = Et, X = Ph, Y = H

Scheme 1

Table 1. ^{1}H NMR Chemical Shifts (δ) for π-Allyl Moieties of π-(Allyl)palladium(II) Porphyrins (**3a-5a**) in $CDCl_3$.

Compound	Central CH	Terminal CH	Other Protons
cis-**3a**	2.14 (m, 1H)	−0.28 (d, 2H, J_{syn} = 6.9 Hz) −4.55 (d, 2H, J_{anti} = 11.9 Hz)	
trans-**3a**	−1.25 (m, 1H)	−1.37 (d, 2H, J_{syn} = 5.9 Hz) −1.06 (d, 2H, J_{anti} = 10.9 Hz)	
cis-**4a**	2.64 (s, 1H)	1.10 (s, 2H)	−1.69, −5.38 (dx2, 2Hx2, J_{gem} = 12.9 Hz, CH_2)
trans-**4a**	−1.68 (s, 1H)	0.27 (s,2H)	−0.91, −1.19 (dx2, 2Hx2, J_{gem} = 13.9 Hz, CH_2)
cis(cis)-**5a**	3.47[b] (m, 1H)	−0.91 (d, 1H, J_{syn} = 6.6 Hz) −3.05 (d, 1H, J_{anti} = 12.7 Hz) 0.96[b] (m, 1H)	−3.77 (d, 3H, CH_3)
cis(trans)-**5a**	2.03 (m, 1H)	−0.50 (d, 1H, J_{syn} = 6.6 Hz) −4.77 (d, 1H, J_{anti} = 12.0 Hz) −3.62 (m, 1H)	−1.10 (d, 3H, CH_3)
trans(cis)-**5a**	−1.43 (m, 1H)	−1.43[a] −0.77[a] −0.77[a]	−1.54 (d, 3H, CH_3)
trans(cis)-**5a**[c]	−1.43 (dt, 1H, J_{syn} = 6.9 Hz, J_{anti} = 12.6 Hz)	−1.54 (d, 1H, J_{syn} = 6.9 Hz) −0.64 (d, 1H, J_{anti} = 12.6 Hz) −0.85 (dq, 1H, J_{syn} = 6.9 Hz)	
trans(trans)-**5a**		−1.90 (d, 1H, J_{syn} = 5.1 Hz) −1.28 (d, 1H, J_{anti} = 12.1 Hz) 0.21[b] (m, 1H)	−1.60 (d, 3H, CH_3)

[a] Signals are overlapped [b] not proved [c] in d_6-DMSO

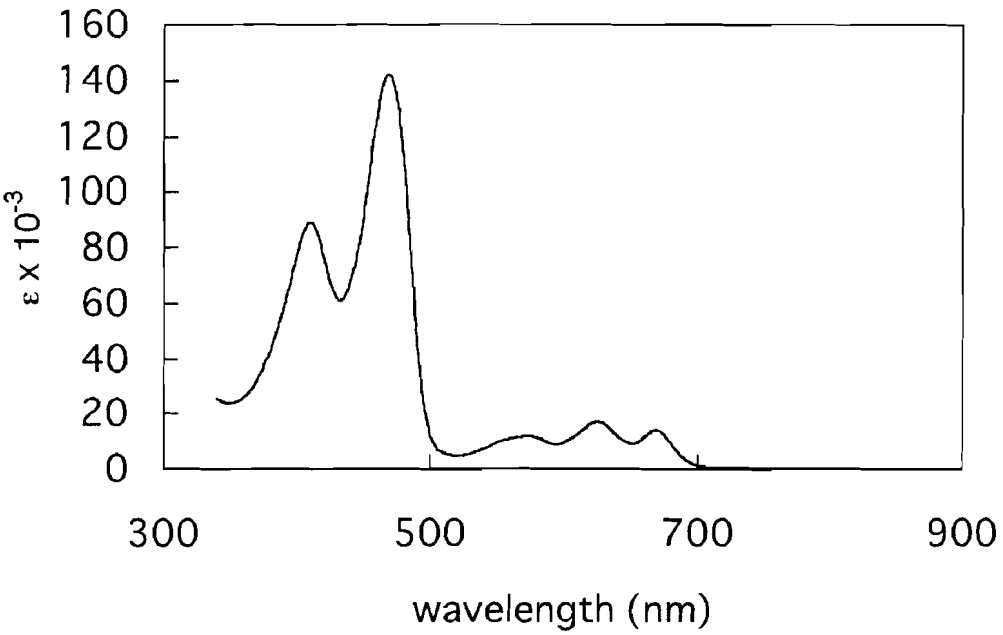

Figure 1. UV-Vis spectrum of a mixture of *cis*- and *trans*-**3a** in CH_2Cl_2.

Reaction of **2a** with (cyclopent-2-enyl)tributyltin afforded the corresponding (π-allyl)Pd^{II} derivative **4a** in 93% yield as a mixture of cis and trans conformational isomers. The ^1H NMR chemical shifts of the allyl central methine proton at 2.64 and –1.68 ppm are very similar to those of *cis*-**3a** and *trans*-**3a**, and therefore, these signals are associated with cis and trans isomers, respectively. The $-CH_2CH_2-$ part of the π-cyclopentenyl ligand of *cis*-**4a** is very close to the porphyrin plane, as judged from the remarkably low frequency signals at –5.38 and –1.69 ppm. The (π-butenyl)Pd^{II} complex **5a** was similarly obtained in 90 % yield when **2a** was allowed to react with (2-butenyl)tributyltin overnight. Since we have used a mixture of *cis*- and *trans*-2-butenyltin reagents, there should arise four stereochemical isomers in this case. In the ^1H NMR spectrum obtained after chromatographic purification, four sets of signals due to the π-butenyl group are observed, including four methyl signals at –1.10,

−1.54, −1.60, and −3.77 ppm with a ratio of 61:29:7:3. Each set of the π-butenyl signals can be associated with one of the four possible isomers of **5a** on the basis of the coupling constants and chemical shifts. The component with the methyl signal at −1.10 ppm shows the allyl central methine proton at 2.03 ppm that is very similar to the corresponding chemical shift of *cis*-**3a**. Furthermore, there are two anti protons of the allyl terminal positions, and their chemical shifts at −4.77 and −3.62 ppm are in the range characteristic of the cis conformation. These NMR features are consistent with the cis isomer of a *trans*-π-butenyl configuration (*cis*(*trans*)-**5a**). In one of the other three components, the extremely high ^{1}H NMR chemical shifts at −3.77 and −3.05 ppm of the methyl group and of the anti protons, respectively, at the allyl terminal positions are indicative of the *cis*-π-butenyl configuration in the cis conformation, which is designated as *cis*(*cis*)-**5a**. The other two components with the methyl signal at -1.54 and -1.60 ppm show signals due to the π-allyl protons in a frequency region similar to that of *trans*-**3a**. The component with the methyl signal at −1.54 ppm shows the allyl central methine proton as a doublet (J_{anti} = 12.6 Hz) of triplets (J_{syn} = 6.9 Hz) in d_6-DMSO. This is indicative of the *cis*-π-butenyl configuration in the trans conformation (*trans*(*cis*)-**5a**). The remaining component with the methyl signal at −1.60 ppm is therefore associated with the *trans*(*trans*)-**5a** isomer.

When **1a-c** was reacted with an equimolar amount of $AgClO_4$, one chloride was displaced to afford the mono(perchlorate) species **6a-c** in quantitative yield. Since the ^{1}H NMR spectra of **6a-c** show a C_s-symmetric signal pattern as well as those for bis(perchlorate) **2a-c**, these mono(perchlorate) compounds are considered to have a (μ-dichloro)dipalladium(II) bis(porphyrin) structure. The ^{1}H chemical shifts of the porphyrin periphery of **6a-c** are remarkably lower than those of the monomeric derivatives due to the shielding

effect of porphyrin. Comparisons of the pyrrole-β protons of **6a** (9.41, 8.49, 8.47, 7.69 ppm) and **2a** (9.35, 8.91, 8.68, 8.20 ppm), of the meso protons of **6b** (10.77, 10.20, 9.15 ppm) and **2b** (11.14, 10.59, 10.12 ppm), and of the methyl protons of **6b** (1.38, 1.15, 0.97, 0.94 ppm) and **2b** (2.31, 1.85, 1.39, 1.25 ppm) nicely illustrate the presence of an additional ring current effect derived from the dimeric structure. Further support for the dimeric structure was obtained by MS spectra of **6b** and **6c**. ESI-MS spectrum of **6a** in methanol showed a principal peak at *m/z* 963.1429 that corresponds to a mononuclear complex with a methanol ligand, $[(N^{21},N^{22}\text{-PhC=CPh-TPP})PdCl(MeOH)]^+$ (963.2093). On the other hand, the dinuclear structure of **6b** was retained under the same ESI-MS conditions in methanol. The observed main peak at *m/z* 852.2066 is in good agreement with the theoretical peak for $\{[(N^{21},N^{22}\text{-PhC=CPh-OEP})PdCl]_2\}^{2+}$ (*m/z* 852.3082) as seen in Figure 2. Although **6c** did not show signals due to the dicationic bis(porphyrin) in the FABMS measurement, a monocationic dinuclear species, $\{[(N^{21},N^{22}\text{-EtC=CEt-TPP})PdCl]_2(ClO_4)\}^+$ (*m/z* 1772), was observed. The monomeric nature of **2c** is indicated by the MS peak at *m/e* = 899 (M – ClO_4) and by the similarity of the ^{1}H NMR chemical shifts to those of **1c**.

A vacant coordination site of Pd is not available in the case of mono(perchlorate) and **6a** did not react with allyltributyltin in CH_2Cl_2 at room temperature.

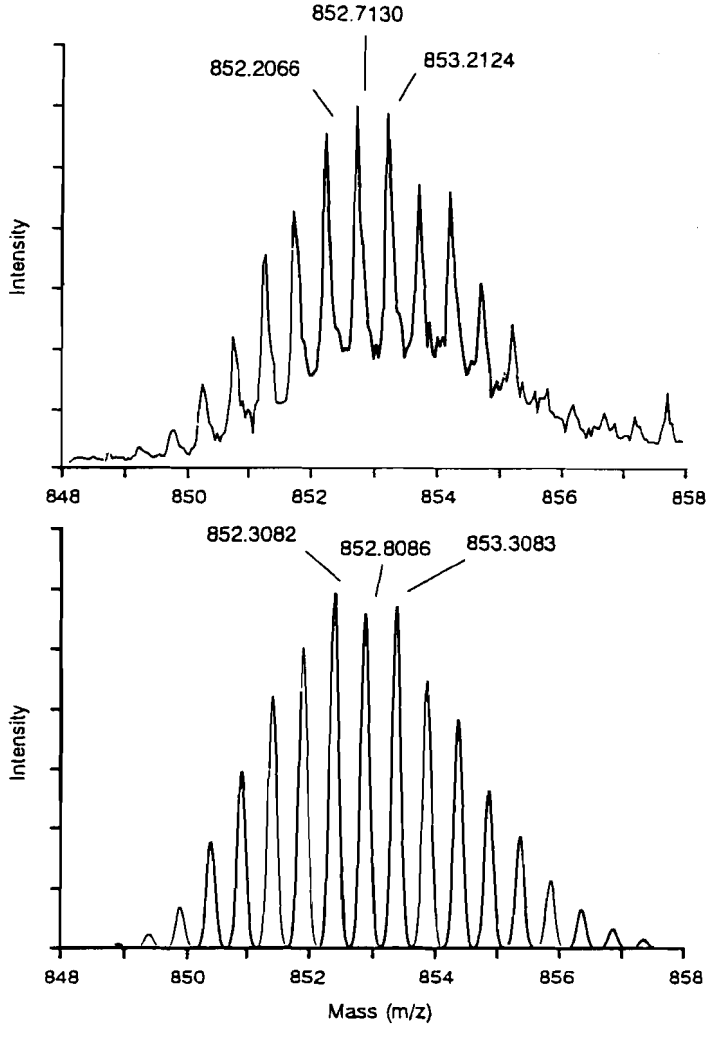

Figure 2. ESI-MS spectrum of **6b**. Isotopic pattern (top) and pattern simulated for $\{[N^{21},N^{22}\text{-(PhC=CPh)(OEP)PdCl}]_2\}^{2+}$

4.2.2 **Structures.**

Recrystallization of a *trans/cis* (3:7) mixture of [(1,2-diphenyletheno-N^{21},N^{22})-*meso*-tetraphenylporphyrinato-N^{23},N^{24}](η^3-allyl)palladium(II) chloride (**3a'**) from CH_2Cl_2 - Et_2O gave crystals of *cis*-**3a'** only. This is probably due to the effect of crystal packing. X-ray molecular structure of *cis*-**3a'** and the crystallographic data are shown in Figure 3 and Table 2. Table 3 exhibits

selected distances, angles, and dihedral angles between least-squares planes for *cis*-**3a'**. The Pd-N (2.106 - 2.118 Å) and Pd-C (2.085 - 2.147 Å) bond lengths as well as the N3-Pd-N4 (83.4°) and C59-Pd-C61 (68.7°) bite angles are similar to those of the π-(allyl)palladium complex of 2,2'-bipyridine.[8-10] The four coordinating atoms (N3, N4, C59, C61) of Pd constitute a square planar coordination plane with deviation of each atom less than 0.06 Å from the mean plane. The allyl central carbon C60 deviates by 0.65 Å from the mean plane, while the Pd atom is displaced by 0.03 Å in the opposite direction.

Table 2. Crystallographic Data for *cis*-**3a'**.

formula	$C_{61}H_{43}N_4ClPd{\cdot}2H_2O$
fw	1009.92
crystal size / mm	0.4 x 0.4 x 0.1
T / K	299
cryst syst	monoclinic
space group	$P2_1/n$
a / Å	16.518(1)
b / Å	16.287(3)
c / Å	18.134(2)
β / deg	92.706(7)
V / Å^3	4873(1)
Z	4
D_{calcd} / g cm^{-3}	1.376
μ (Mo Kα) / cm^{-1}	4.85
no. of collcd data	11988
no. of indep data	11598
no. of rflns above 3s(*I*)	4853
no. of refined params	628
goodness of fit	1.52
R	0.059
R_w	0.041

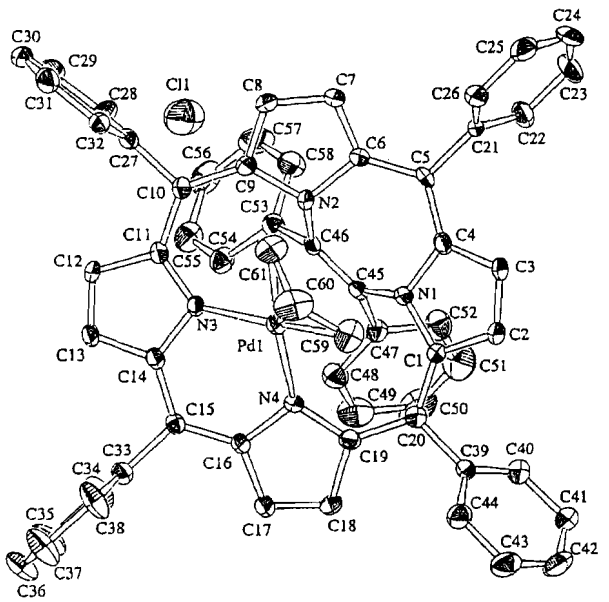

Figure 3. ORTEP drawing of *cis*-**3a'** with 50% thermal ellipsoids.

Table 3. Selected Bond Distances (Å) and Angles (deg) for *cis*-**3a'**

Bond Lengths			
Pd-N3	2.118(5)	Pd-N4	2.106(5)
Pd-C59	2.125(7)	Pd-C61	2.147(7)
Pd-C60	2.085(7)	C59-C60	1.37(1)
C60-C61	1.40(1)		
Bond Angles			
N3-Pd-C59	172.5(3)	N3-Pd-C61	104.8(3)
N4-Pd-C59	103.2(3)	N4-Pd-C61	171.8(3)
N3-Pd-N4	83.4(2)	C59-Pd-C60	68.7(3)
Pd-N3-C14	115.2(5)	Pd-N4-C16	117.5(4)
Pd-N3-C11	131.5(4)	Pd-N4-C19	130.5(4)
C59-C60-C61	121.2(9)		
Dihedral angles between least-squares planes			
N3PdN4/N1N2N3N4			61.82
N3PdN4/C5C10C15C20			53.40
N1C1C2C3C4/C5C10C15C20			22.08
N2C6C7C8C9/C5C10C15C20			16.94
N3C11C12C13C14/C5C10C15C20			12.63
N4C16C17C18C19/C5C10C15C20			15.88
N1C45C46N2/C5C10C15C20			60.89

X-ray crystallography shows that the N3-Pd-N4 plane of cis-**3a** is canted by 53.4° from the porphyrin plane defined by four meso carbons, C5, C10, C15, and C20. The dihedral angle (106.8°) between the π-allyl plane and the N3-Pd-N4 plane is in the range frequently observed for (π-allyl)palladium complexes.[9-12] If this angle is retained in the trans isomer, the π-allyl plane is presumed to tilt by –19.8° with respect to the porphyrin plane in the trans isomer, while the corresponding tilt angle in the cis isomer is 53.5° (Figure 4). This relatively parallel orientation of the (π-allyl) plane with respect to the porphyrin plane in the trans isomer is consistent with the small difference in the ^{1}H NMR chemical shifts between the (π-allyl) protons.

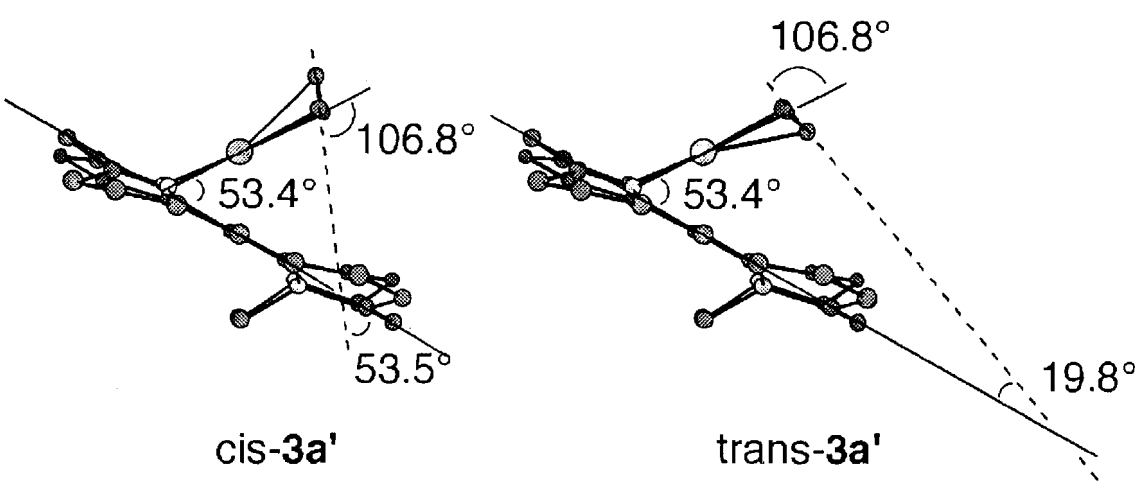

Figure 4. Comparison of the X-ray structure of *cis*-**3a'** and model of *trans*-**3a'**.

4.2.3 **Kinetics.**

The progress of the reactions of **2a,b** (13 mmol L^{-1}) with allyltributyltin (19 mmol L^{-1}) in $CDCl_3$ was monitored by ^1H NMR to show that most of **2a,b** has been consumed in 3 min at 25 °C to give the kinetically favored trans isomers as a major component, that is, a molar ratio of 0.03:0.62:0.35 for **3a**/*trans*-**4**/*cis*-**4**. After this first stage, trans isomers were gradually isomerized to thermodynamically more stable cis isomers until the equilibrium states were reached (vide infra). The amounts of the (π-allyl)Pd^{II} porphyrins were measured with time after allyltributyltin (1.6 equiv) was added to a $CDCl_3$ solution of **2a,b** (12 mmol L^{-1}) at –5 °C, at which temperature the trans-cis isomerization could be neglected for the initial 1 h period (Figure 5). Then the second-order rate constants k_1 and k_2 for the formation of *trans*-**3a** and *cis*-**3a** were estimated as 3.2×10^{-2} and 1.2×10^{-2} L mol^{-1} s^{-1}, and k_1 and k_2 for *trans*-**3b** and *cis*-**3b** were 5.3×10^{-2}, and 4.0×10^{-2} L mol^{-1} s^{-1}, respectively. The difference in the rates of formation between *trans*-**3a** and *cis*-**3a** can be explained in terms of steric hindrance between the tributyltin moiety and the TPP ligand when allyltributyltin approaches Pd. Allyltributyltin in the transition state structure to give (π-allyl)Pd^{II} porphyrins seems to take an orientation where the C-$SnBu_3$ bond undergoes maximum overlap with the C=C π orbitals. Therefore, the $SnBu_3$ group is far from the porphyrin plane when *trans*-**3a** is being formed, whereas it is closer to the porphyrin plane when *cis*-**3a** is being formed, if the transition state structures are deduced from the X-ray structure of *cis*-**3a'** as shown in Figure 3. Since the TPP ligand causes greater steric hindrance than the OEP ligand, it is reasonable that **2b** reacts faster than **2a** and that the selectivity between *trans*-**3b** and *cis*-**3b** is smaller than that between *trans*-**3a** and *cis*-**3a**.

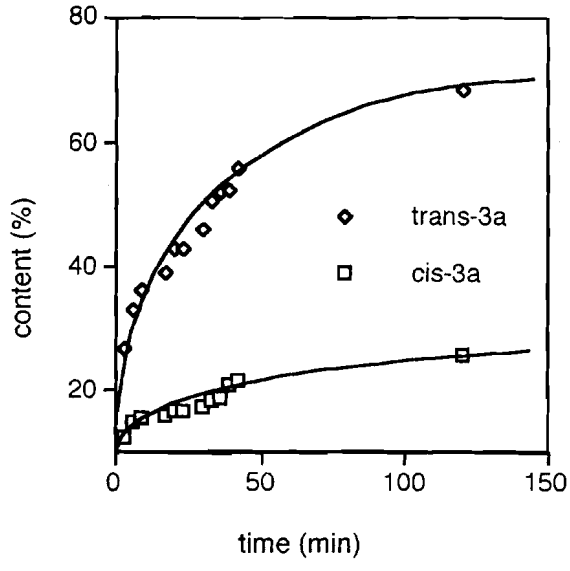

Figure 5. Change in the product distribution (*trans*-**3a** and *cis*-**3a**) with time at -5 °C after addition of (η^1-C_3H_5)$SnBu_3$ (0.019 M) to **2a** (0.012 M) in $CDCl_3$ (0.5 mL).

The reaction of (cyclopent-2-enyl)tributyltin and (2-butenyl)tributyltin was also monitored by observing the decay of **2a**. **4a** and **5a** were formed much more slowly than that of **3a**, and 2 h was not enough for the complete conversion of **2a** even at room temperature. The molar ratio at 3 min after the addition of the tin reagent (1.5 equiv) to **2a** in $CDCl_3$ at 25 °C was 0.71:0.15:0.14 for **2a**:*trans*-**4a**:*cis*-**4a**. This trans/cis isomer ratio did not change appreciably when **2a** was allowed to react with the tin reagent (1.8 equiv) for 3 h in CH_2Cl_2 and then chromatographed to afford **4a** in a 90 % yield. Since the formation of **4a** and **5a** accompanied isomerization at the same time, the formation rates could not be estimated independently.

4.2.4 **Isomerization Behavior.**

As noted above, *trans*-**3a** and *trans*-**3b** formed preferentially were gradually isomerized to *cis*-**3a** and *cis*-**3b**, respectively, until the equilibrium states (both $K_{eq} = 2.3$ for **3a** and **3b**) were reached, as shown in Figure 6. This isomerization process in $CDCl_3$ at 25 °C followed the first-order rate law. The rate constants k_3 for the isomerization from the trans isomer to the cis isomer were determined as 7.1×10^{-4} s^{-1} for **3a** and 4.4×10^{-4} s^{-1} for **3b**.

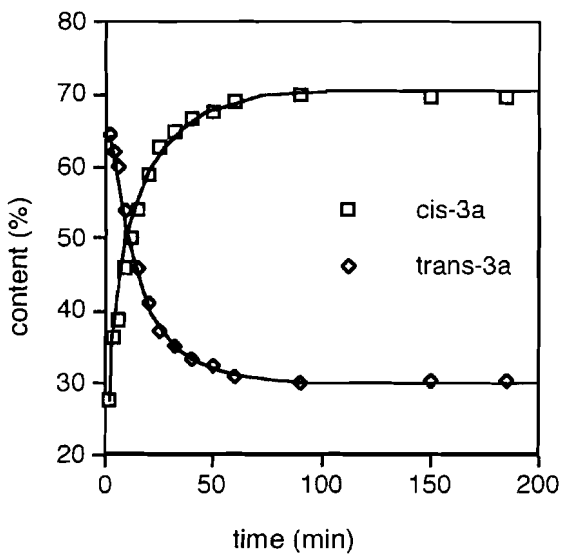

Figure 6. Change in the product distribution (*trans*-**3a** and *cis*-**3a**) with time at 25 °C after addition of $(\eta^1\text{-}C_3H_5)SnBu_3$ (0.019 M) to **2a** (0.013 M) in $CDCl_3$ (0.5 mL).

Ligand rotation in the (π-allyl)palladium(II) complexes has been well-documented. There are two types of π-allyl ligand rotation; one is accompanied by exchange between syn and anti positions, and the other causes exchange between two syn positions and between two anti positions. Syn-anti exchange is frequently observed for the π-allyl ligand of palladium(II) complexes with phosphine ligands.[11,13] It takes place mostly via the η^3-η^1

isomerization mechanism; (i) η^3-to-η^1 allyl coordination change, (ii) rotation around a C-C single bond in the (η^1-allyl)Pd intermediate, and (iii) η^1-to-η^3 allyl coordination change. On the other hand, syn-syn–anti-anti exchange is generally observed for (π-allyl)palladium(II) complexes with bidentate nitrogen base ligands.[9,14] This exchange is caused by a mechanism involving (i) dissociation of one of the Pd-N bonds, followed by (ii) rotation around the remaining Pd-N bond and (iii) remaking of the Pd-N bond as shown in Scheme 2. This difference in the ligand rotation mechanism between amine complexes and phosphine complexes is explained by the fact that the dissociation energy for Pd-N bonds is smaller than that for Pd-P bonds having π-back bonding.

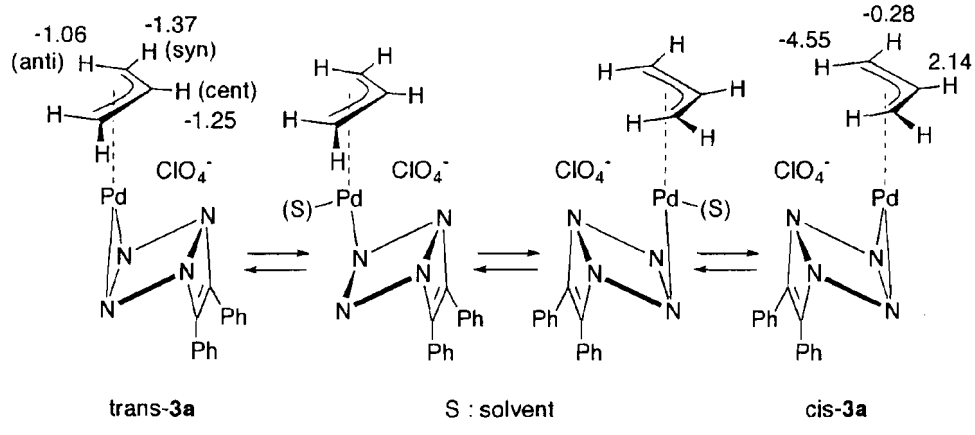

Scheme 2

4.2.4.1 **Syn-syn/anti-anti Exchange**

The isomerization mechanism between *trans*-**3a** and *cis*-**3a** was studied by the phase-sensitive 2D NOESY experiment in tetrachloroethane-d_2 at 80 °C.[9,13,14] The cross-peaks due to chemical exchange between signals at –1.06 ppm ($H_{anti(trans)}$ in Figure 7) and –4.55 ppm ($H_{anti(cis)}$ in Figure 7), between signals at –1.37 ppm ($H_{syn(trans)}$ in Figure 7) and –0.28 ppm ($H_{syn(cis)}$ in Figure 7),

and between signals at –1.25 ($H_{cent(trans)}$ in Figure 7) and 2.14 ppm ($H_{cent(cis)}$ in Figure 7) are observed. These negative cross-peaks are indicative of syn-syn–anti-anti exchange. There are no visible cross peaks between $H_{anti(trans)}$ and $H_{syn(cis)}$ and between $H_{anti(cis)}$ and $H_{syn(trans)}$ that should arise from the syn-anti chemical exchange, whereas correlations between the intramolecular syn and anti π-allyl terminal methylene protons ($H_{syn(cis)}$-$H_{anti(cis)}$ and $H_{syn(trans)}$-$H_{anti(trans)}$) are indicated as positive cross-peaks.

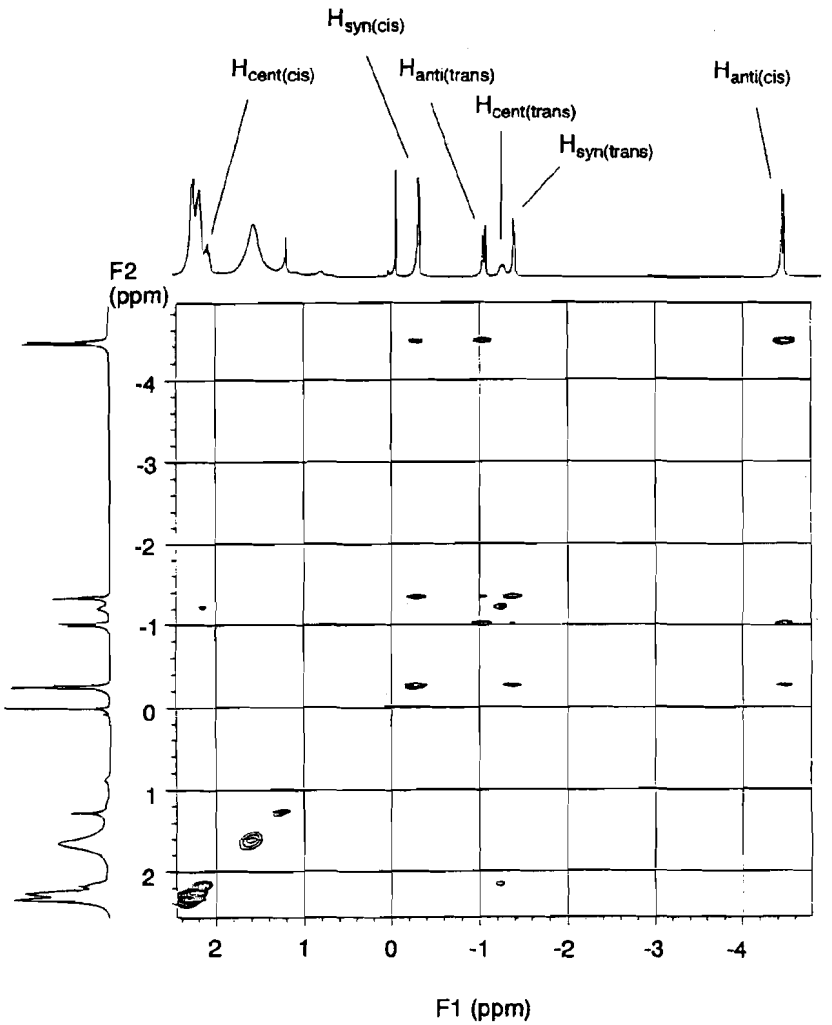

Figure 7. The 400-MHz phase-sensitive NOESY spectrum of **3a** in tetrachloroethane-d_2 at 80 °C. The correlations between $H_{anti(cis)}$ and $H_{anti(trans)}$, between $H_{syn(cis)}$ and $H_{syn(trans)}$, and between $H_{cent(cis)}$ and $H_{cent(trans)}$ are observed as negative cross peaks. Cross peaks between $H_{anti(cis)}$ and $H_{syn(cis)}$ and between $H_{anti(trans)}$ and $H_{syn(trans)}$ are positive and all the diagonal peaks are negative.

Ligand rotation is detectable if either the (chelating ligand)-Pd or the (π-allyl)-Pd part is nonsymmetric with respect to the plane bisecting the bite angle of the chelating ligand. In the cases of syn-syn–anti-anti exchange, NMR signals due to the two halves of the symmetric ligand show different chemical shifts at low temperatures, and they coalesce when the temperature is raised. Thus, line shape analysis and spin saturation transfer technique in the dynamic NMR experiments have generally been used for the determination of activation parameters in the ligand rotation.[15] This is partly because ligand rotation is so fast that each isomer cannot be observed separately by NMR at ambient temperature. Furthermore, it is difficult to obtain one rotational isomer as a pure form.

The activation energy for the ligand rotation of **3a** is so large that it can be measured by the concentration change of two rotational isomers with time at ambient temperature. It should be pointed out that two rotational isomers of (π-allyl)Pd complexes are identical if the auxiliary chelating ligand is symmetric with respect to both the plane bisecting the bite angle (L-Pd-L) and the Pd coordination plane, as in the case of 2,2'-bipyridine. This is so even if the π-allyl ligand is unsymmetrically substituted. Although both the (chelating ligand)-Pd and the (π-allyl)-Pd parts are symmetric with respect to the plane bisecting the bite angle of the chelating ligand, two rotational isomers of **3a** (cis and trans) can be differentiated due to the unique stereochemical feature of N^{21},N^{22}-bridged porphyrins. It is of great significance that 3/7 *trans*-**3a**/*cis*-**3a** equilibrium mixture in solution is converted into cis-only crystals, owing to the effect of crystal packing. Kinetics of the cis-to-trans isomerization could be measured by NMR when the cis isomer was dissolved in $CDCl_3$. An Eyring plot based on the rate constants measured at six different temperatures in the

range 278-308 K gave a straight line as sees in Figure 8. On the based of this plot, $\Delta H^{\ddagger}$ and $\Delta S^{\ddagger}$ values were obtained as 87.7 kJ mol^{-1} and –11.7 J K^{-1} mol^{-1}, respectively, and then the $\Delta G^{\ddagger}$ value of **3a** for this isomerization was calculated as 91.2 kJ mol^{-1} at 298 K.

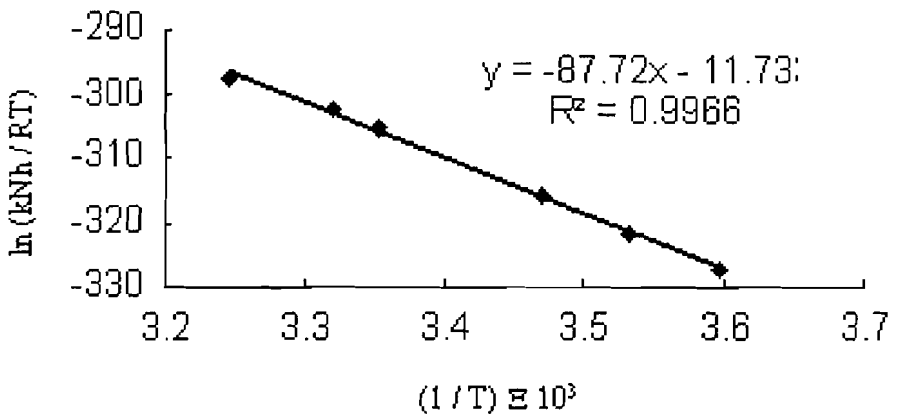

Figure 8. An Eyring plot based on the kinetic measurements of the isomerization between *cis*- and *trans*-**3a**.

In the case of syn-syn–anti-anti exchange in the cationic (η^3-trans-2-butenyl)Pd^{II} complexes of phenanthroline the $\Delta G^{\ddagger}_{298}$ value (58.2 kJ mol^{-1}) is obtained on the basis of an Eyring plot ($\Delta H^{\ddagger}$ = 55.0 kJ mol^{-1}; $\Delta S^{\ddagger}$ = –10.6 J K^{-1} mol^{-1}).[15] The syn-syn–anti-anti exchange in the cationic η^3-(2-methylallyl)Pd^{II} complex with unsymmetrical 2-pyridyl-*N*-benzylimine ligand was investigated by using NMR line shape analysis to give an activation energy E_a = 72 kJ mol^{-1}.[9] It has been pointed out that the activation energy for the syn-syn–anti-anti exchange of the (π-allyl)Pd^{II} complex with neutral pyridinylimidazolyl ligand ($\Delta G^{\ddagger}_{298}$ = 51.8 kJ mol^{-1} in CD_3CN) is smaller than that of the (π-allyl)Pd^{II} complex with monoanionic pyridinylimidazolate ligand ($\Delta G^{\ddagger}_{298}$ = 69.2 kJ mol^{-1} in CD_3CN).[16] The stronger Pd-N bonding in the latter explains the greater activation energy, because syn-syn–anti-anti exchange

requires dissociation of a Pd-N bond. Thus, the remarkably large activation energy $\Delta G^{\ddagger}$ of **3a** may be indicative of the strong Pd-N bonding. Alternatively, it can be explained in terms of steric hindrance of the porphyrin ligand in the rotation around the Pd-N bond followed by the dissociation of one Pd-N bond.

Table 4 shows the effect of solvent and temperature on the equilibrium states between trans and cis isomers of **3a**, **4a** and **5a**. These complexes were allowed to stand in solution until equilibrium was reached. In the case of **3a** and **4a**, the equilibrium constants (K_{eq}) greatly depend on solvent and of course on temperature. They were 2.3 and 0.89 in $CDCl_3$ and 3.0 and 2.4 in d_6-DMSO at room temperature, and 1.9 and 1.7 in d_6-DMSO at 80 °C.

Table 4. The Equilibrium States between *trans* and *cis* Conformational Isomers.

Compound		Solvent	Temp. (°C)	Molar ratio (%) trans	cis	K_{eq}
(3a)		$CDCl_3$	25	30	70	2.3
		d_6-DMSO	25	25	75	3.0
		d_6-DMSO	80	34	66	1.9
(4a)		$CDCl_3$	25	53	47	0.89
		d_6-DMSO	25	29	71	2.4
		d_6-DMSO	80	37	63	1.7
(5a)	*trans*-butenyl	$CDCl_3$	25	7	61	1.8[a]
	cis-butenyl			29	3	
(5a)	*trans*-butenyl	d_6-DMSO	80	9	87	7.3[a]
	cis-butenyl			3	1	

[a] equilibrium constant between sum of trans isomers (trans(trans)+trans(cis)) and cis isomers (cis(trans)+cis(cis))

Preference of cis over trans isomers in the case of **3a** may be explained by the greater repulsion between the porphyrin ligand and the π-allyl ligand in the trans form than in the cis form. The structures of cis-**3a'** and trans-**3a'** as depicted in Figure 4 show that the central carbon of the π-allyl group of trans-**3a** comes closer to the porphyrin plane than the terminal carbons, because square-planer coordination consists of porphyrin nitrogens and π-allyl terminal carbons. The relative stability of cis and trans isomers is governed mainly by steric repulsion between the π-allyl ligand and the porphyrin ligand.[17] The $-CH_2CH_2-$ part in the η^3-cyclopentenyl ligand of **4a** makes a greater steric constraint in the cis isomer than in the trans isomer, while the central methine of the π-allyl group induces steric repulsion in the trans isomer more than in the cis isomer. The combined steric effect results in the shift of the trans/cis ratio from 30/70 in the complex **3a** to 53/47 in the complex **4a**. The syn methyl substituent in the (η^3-*trans*-2-butenyl)Pd complex **5a** causes steric constraint in the trans isomer but not in the cis isomer, while the anti methyl substituent in the (η^3-*cis*-2-butenyl)Pd complex causes steric constraint in the cis isomer but not in the trans isomer. The observed trans/cis ratio of **5a** in $CDCl_3$ at room temperature is 7/61 in the (η^3-*trans*-2-butenyl)Pd complex and 29/3 in the (η^3-*cis*-2-butenyl)Pd complex, which is consistent with the above interpretation on the basis of steric repulsion.

4.2.4.2 **Syn-anti Exchange**

Figure 9 shows change of the isomer distribution of **5a** when a d_6-DMSO solution of **5a** was allowed to stand at 25 °C for 45 min and then at 60 °C for 90 min. The trans(cis) isomer decreased as the cis(trans) isomer increased, and the cis(cis) isomer decreased as the trans(trans) isomer increased. This change

in the ratio of the four components is explained in terms of the isomerization via a (η^1-allyl)Pd intermediate (See Scheme 3). In this case η^3-η^1 type isomerization is considered to be promoted at 60 °C. This η^3-η^1 type isomerization rate of **5a** could be estimated by using the decrease in sum of the trans(cis) and cis(cis) isomers and the increase in sum of the cis(trans) and trans(trans) isomers. Then the first-order rate constant k_5 for the *cis*-butenyl/*trans*-butenyl isomerization of **5a** via η^3-η^1 type mechanism at 60 °C was determined as 1.6×10^{-3} s^{-1} (K_{eq} = 24). The ratio of cis/trans ligand rotational isomers of the (η^3-*trans*-2-butenyl)Pd complex changes from 65/6 to 87/9 during this temperature change. The corresponding cis/trans ratio of the (η^3-*cis*-2-butenyl)Pd complexes changes from 4/25 to 1/3. These are syn-syn–anti-anti exchange processes. The interconversion between the *trans*-2-butenyl ligand and the *cis*-2-butenyl ligand is a syn-anti exchange process and the ratio changed from (65 + 6)/(4 + 25) to (87 + 9)/(1 + 3). Therefore, the (η^3-*trans*-2-butenyl)Pd complex is much more stable than the (η^3-*cis*-2-butenyl)Pd complex (Scheme 4). The observed ratio at 25 °C retains the cis/trans composition of the starting (2-butenyl)tributyltin, and an equilibrium state in the (η^3-2-butenyl)Pd porphyrin was not reached due to the very slow syn-anti exchange rate at 25 °C.

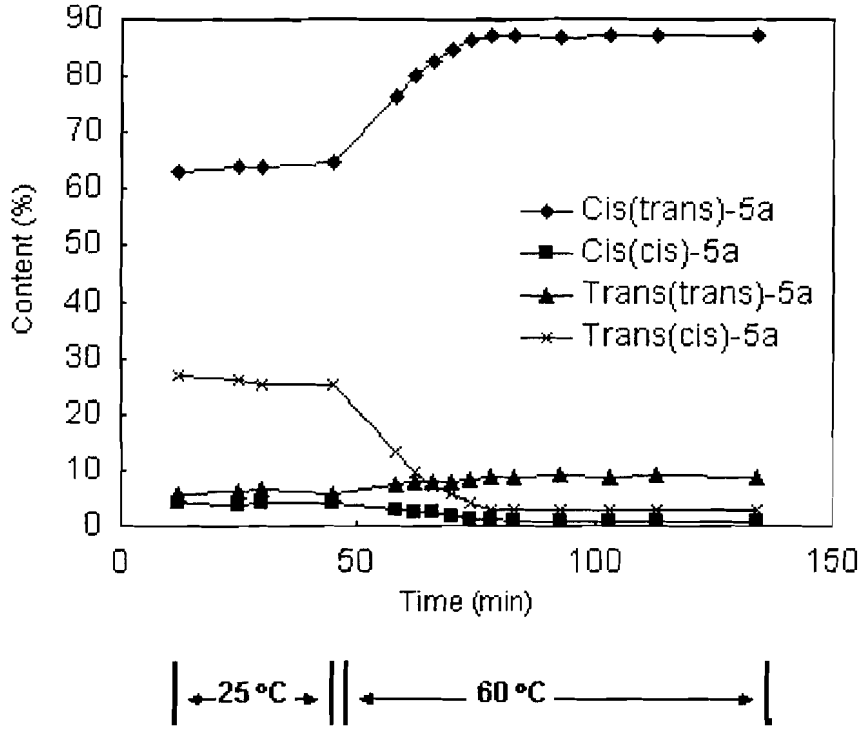

Figure 9. Change in the isomer ratio of butenyl complex **5a** with temperature in d_6-DMSO.

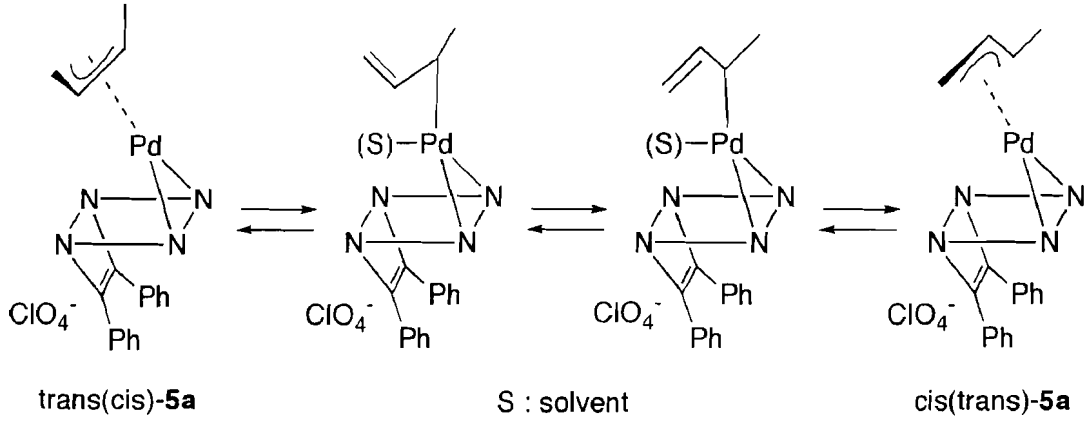

Scheme 3

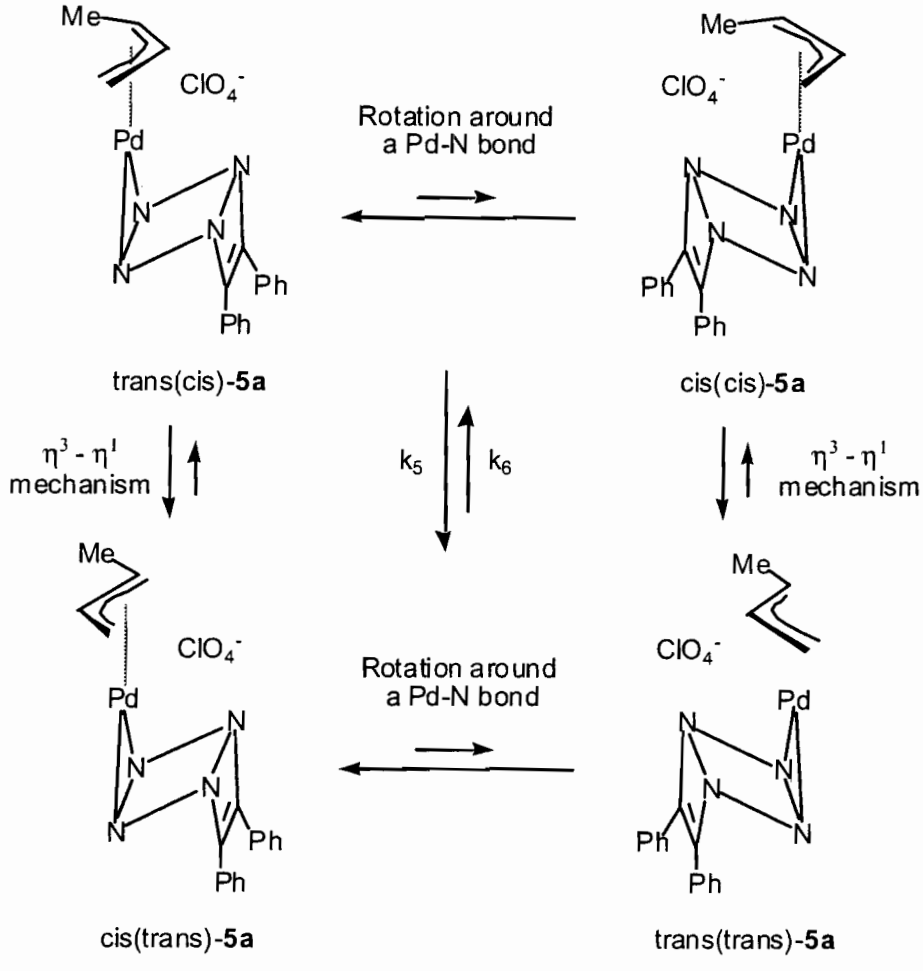

Scheme 4

The cross-peaks due to syn-syn–anti-anti exchange of **3a** in the phase-sensitive 2D NOESY experiment was observed in tetrachloroethane-d_2 at 80 °C, while it was not detected at room temperature. Since the cross-peaks due to the syn-anti exchange of **3a** could not be detected even in DMSO at 80 °C, the syn-syn–anti-anti exchange is estimated to be much faster than

syn-anti exchange under the same conditions. Heating to 140 °C caused decomposition of **3a**. Also in $CDCl_3$ at room temperature, η^3-η^1 type isomerization of **5a** is slower than syn-syn–anti-anti isomerization. This fact agrees with the result reported for the (π-2-butenyl)Pd^{II} complex with the 1,10-phenanthroline ligand in tetrachloroethane-d_2, in which the rate constant for η^3-η^1 type isomerization ($k_{298} = 2.8 \times 10^{-3}$ s^{-1}) is much smaller than that for syn-syn–anti-anti isomerization (k_{298} = 396 s^{-1}).[15] A much slower syn-syn–anti-anti isomerization of porphyrin Pd complexes as compared to that of 1,10-phenanthroline complexes can be ascribed to the steric hindrance of the porphyrin ligand in the rotation around the Pd-N bond, because it does not seem that the Pd to porphyrin nitrogen bonding is stronger than the Pd to 1,10-phenanthroline nitrogen bonding. η^3-η^1 type isomerization does not involve dissociation of a Pd-N bond and would not be greatly affected by the steric hindrance of the porphyrin ligand. Therefore, the rate constant for this type isomerization is diagnostic of the trans effect of porphyrin nitrogens. That is, strong Pd-N bonding should lead to fast η^3-η^1 type isomerization. Since the η^3-η^1 type isomerization of **5a** is not faster than that for the phenanthroline complex, the Pd-N bonding of **5a** does not seem to be much stronger than that of phenanthroline. This is consistent with the structural feature of **3a** that the Pd-N bondings are bent by 21.8° and 23.7° from the pyrrole ring planes.

4.3 Experimental Section

General Considerations. (Dichloro)palladium(II) complexes of N^{21},N^{22}-etheno-bridged porphyrins **1a-c** were synthesized according to the previously reported procedures.[6] Solvents were purified prior to use by

conventional methods. $CDCl_3$ was passed through basic Al_2O_3 before use. (Cyclopent-2-enyl)tributyltin was a gift from Dr. H. Miyake (Kobe University). (2-Butenyl)tributyltin was synthesized by the Grignard reaction of tributyltin chloride with 1-chloro-2-butene. Other chemicals were of reagent grade. Wakogel C-300 silica gel (Wako Junyaku) was used for column chromatography. ^1H NMR was recorded on JEOL EX-270 and AL-300 spectrometer. Chemical shifts were referenced with respect to $(CH_3)_4Si$ (0 ppm) as an internal standard. The UV-visible spectra were measured on a Shimadzu UV-3100B instrument. Elemental analyses of C, H, and N were made with a Yanaco MT-5 and Perkin-Elmer 2400 CHN corder. FAB mass spectra were measured in an *m*-nitrobenzyl alcohol matrix with a JEOL-JNS 600 instrument, and ESI-MS spectra were measured with a Mariner PE Biosystems spectrometer. X-ray crystallographic measurement was done on Rigaku AFC-5 automated four-circle diffractometer.

The compounds prepared here are perchlorates that involve the risk of an explosion and must be handled with extreme caution.

*General Procedure of Synthesis of π-(Allyl)palladium(II) Porphyrins (**3a-5a**).* Allyltributyltin derivatives (0.025 mmol) were added to a solution of **2a** (0.014 mmol) in dichloromethane (2 mL). After the mixtures were stirred for 3 h, the products were purified by column chromatography on silica gel with dichloromethane–acetone (7/1) as an eluent. Recrystallization from dichloromethane–hexane gave the mixtures of trans and cis isomers of π-(allyl)palladium(II) porphyrins..

The TPP free base form, N^{21},N^{22}-PhC=CPh-TPP, was prepared by vigorously mixing a CH_2Cl_2 solution of a monoprotonated form, N^{21},N^{22}-(PhC=CPh-TPP)$HClO_4$, with a 10% KOH solution.[18] Then the free base was allowed to react with $[Pd(C_3H_5)Cl]_2$ (1.1 equiv) in benzene at room

temperature overnight to give [(1,2-diphenyletheno-N^{21},N^{22})-*meso*-tetraphenylporphyrinato-N^{23},N^{24}](η^3-allyl)palladium(II) chloride **(3a')** in a 90% isolated yield, after evaporation of benzene and precipitation using CH_2Cl_2 and hexane.

(N^{21},N^{22}-PhC=CPh-TPP)(η^3-allyl)Pd(ClO_4) (**3a**). ^{1}H NMR (300 MHz, $CDCl_3$): δ 9.14, 8.87, 8.73, 8.22 (d × 4, 2H × 4, β-Py H of *trans*-**3a**), 9.11, 8.80, 8.75, 8.18 (d × 4, 2H × 4, β-Py H of *cis*-**3a**), 8.44-7.31 (m, Ph meso-H of *trans*-**3a** and *cis*-**3a**), 6.26 (t, bridge Ph p-H of *trans*-**3a** and *cis*-**3a**), 5.82 (br, bridge Ph m-H of *trans*-**3a** and *cis*-**3a**). See Table 1 for the allyl protons. Anal. Calcd for $C_{61}H_{43}N_4O_4ClPd$: C, 70.59; H, 4.18; N, 5.40 %. Found: C, 70.39; H, 3.98; N, 5.35 %. UV-vis (CH_2Cl_2; λ_{max}, nm (log ε)): 668.5 (4.15), 625.0 (4.23), 572.0 (4.09), 468.0 (5.15), 409.5 (4.95). FAB MS (*m/z*): found 937, theory 937 for $C_{61}H_{43}N_4Pd$ ($(M - ClO_4)^+$) (an observed isotopic pattern agrees with that simulated for $C_{61}H_{43}N_4Pd$).

(N^{21},N^{22}-PhC=CPh-TPP)(η^3-cyclopentenyl)Pd(ClO_4) (**4a**). ^{1}H NMR (300 MHz, $CDCl_3$): δ 9.16, 9.10, 8.83, 8.82, 8.72, 8.71, 8.20, 8.10 (d × 8, 2H × 8, β-Py H of *trans*-**4a** and *cis*-**4a**), 8.39-7.28 (m, Ph meso-H of *trans*-**4a** and *cis*-**4a**), 6.20 (t × 2, bridge-Ph p-H of *trans*-**4a** and *cis*-**4a**), 5.79 (br, bridge-Ph m-H of *trans*-**4a** and *cis*-**4a**). see Table 1 for the cyclopentenyl protons. Anal. Calcd for $C_{63}H_{45}N_4O_4ClPd{\cdot}2H_2O$: C, 68.79; H, 4.49; N, 5.09 %. Found: C, 68.70; H, 4.19; N, 5.04 %. UV-vis (CH_2Cl_2; λ_{max}, nm (log ε): 671.0 (4.45), 624.5 (4.51), 565.0 (4.43), 466.0 (5.42), 414.0 (5.32). FAB MS (*m/z*): found 963, theory 963 for ($C_{63}H_{45}N_4Pd$, $M - ClO_4)^+$). (an observed isotopic pattern agrees with that simulated for $C_{63}H_{45}N_4Pd$).

(N^{21},N^{22}-PhC=CPh-TPP)(η^3-butenyl)Pd(ClO_4) (**5a**). ^{1}H NMR (300 MHz, $CDCl_3$): δ 9.12-7.20 (β-Py H and Ph meso-H of four isomers were not assigned by overlap of signals), 6.20 (t × 2, bridge-Ph p-H of *trans*-**5a** and

cis-**5a**), 5.80 (br, bridge-Ph m-H of *trans*-**5a** and *cis*-**5a**). see Table 1 for the butenyl protons. Anal. Calcd for $C_{62}H_{47}N_4O_4ClPd \cdot H_2O$: C, 69.47; H, 4.61; N, 5.23 %. Found: C, 69.24; H, 4.60; N, 5.19 %. UV-vis (CH_2Cl_2; λ_{max}, nm (log ε)): 673.0 (4.23), 629.0 (4.28), 573.5 (4.11), 469.5 (5.15), 414.0 (5.05). ESI MS (*m/z*): found 951.2757, theory: 951.2694 for $C_{62}H_{45}N_4Pd$, ($(M\text{-}ClO_4)^+$).

Physicochemical Measurements. The rate constants for the formation of (π-allyl)Pd porphyrins **3a,b** and their trans-cis isomerization were determined by NMR experiments. (Allyl)$SnBu_3$ (9×10^{-6} mol) was added to a 0.5 mL $CDCl_3$ solution of **2a,b** (5-6 μmol) in a NMR tube, just after which the sample tube was transferred to a thermostated NMR spectrometer at 25 °C or 5 °C. The changes in concentrations of the components in the solution were estimated on the bases of ^1H NMR integrations with time. For the determination of the thermodynamic parameters for cis-to-trans isomerization of **3a**, 5 μmol of *cis*-**3a** was dissolved in 0.5 mL of $CDCl_3$ in a NMR tube, and the change in the isomer ratio was monitored with time at six different temperatures (5, 10, 15, 25, 28, and 35 °C). The observed rate constants were used for the Eyring plot that is included in the Supporting Informations. The η^3-η^1 type isomerization of **5a** was detected using d_6-DMSO solution (0.5 mL) of 3.8 μmol of the mixture of four isomers. The sample tube was kept at 25 °C for 45 min and then heated to 60 °C. NMR measurements were repeated four times at 25 °C and 11 times at 60 °C to make sure that isomer distribution reaches constant value.

The 400 MHz phase-sensitive 2D NOESY spectrum of **3a** was measured using a mixing time of 0.3 s in tetrachloroethane-d_2 at 80 °C.

A crystal of **3a**' obtained by recrystallization from CH_2Cl_2-hexane was mounted on an X-ray diffractometer, and measurements were done using graphite-monochromated Mo Kα radiation. The unit cell parameters were obtained from least-squares refinements of 8 reflections ($20.3 < 2\theta < 26.2°$).

The intensities of 3 representative reflections which were measured after every 150 reflections showed 0.85% increase over the course of data collection. The data were corrected for Lorentz and polarization effects and absorption based on azimuthal scans. The refined cell parameters and relevant crystal data are summarized in Table 2. The structure was solved by direct methods and refined by full-matrix least-squares method (Texsan[19]) on an SGI R-5000 workstation. All non-hydrogen atoms were refined anisotropically. Hydrogen atoms were included at standard positions (C-H = 0.95 Å) but not refined. Neutral atom scattering factors were taken from Cromer and Waber.[20] Anomalous dispersion effects were included in F_c; the values for $\Delta f'$ and $\Delta f''$ were those of Cromer.[21] The atomic coordinates with B(eq), U values, bond distances, bond angles, torsional angles, and least-squares planes are deposited as the Supporting Information.

4.4 References and Notes

1. (a) Müller, D.; Umbricht, G; Weber, B.; Pfaltz, A. *Helv. Chim. Acta* **1991**, *74,* 232. (b) Togni, A. *Tetrahedron: Asymmetry* **1991**, *2,* 683. (c) Pfaltz, A. *Acc. Chem. Res.* **1993**, *26,* 339. (d) Kubota, H.; Nakajima, M.; Koga, K. *Tetrahedron Lett.* **1993**, *34,* 8135. (e) Togni, A.; Venanzi, L. M. *Angew. Chem., Int. Ed. Engl.* **1994**, *17,* 497. (f) Tanner, D.; Andersson, P. G.; Harden, A.; Somfai, P. *Tetrahedron Lett.* **1994**, *35,* 4631. (g) Gamez, P.; Dunjic, B.; Fache, F.; Lemaire, M. *J. Chem. Soc., Chem. Commun.* **1994**, 1417. (h) Bolm, C.; Kaufmann, D.; Zehnder, M; Neuburger, M. *Tetrahedron Lett.* **1996**, *37,* 3985. (i) Oslob, J. D.; Åkermark, B.; Helquist, P.; Norrby, P. O. *Organometallics* **1997**, *16,* 3015.

2. (a) Johnson, L. K.; Mecking, S.; Brookhart, M. *J. Am. Chem. Soc.* **1996**, *118,* 267. (b) Rix, F. C.; Brookhart, M.; White, P. S. *J. Am. Chem. Soc.* **1996**, *118,* 2436. (c) Rix, F. C.; Brookhart, M.; White, P. S. *J. Am. Chem. Soc.* **1996**, *118,* 4746. (d) Brookhart, M.; Wagner, M. I. *J. Am. Chem. Soc.* **1996**, *118,* 7219. (e) LaPointe, A. M.; Rix, F. C.; Brookhart, M. *J. Am. Chem. Soc.* **1997**, *119,* 906. (f) Delis, J. G. P.; Aubel, P. G.; Vrieze, K.; van Leeuwen, P. W. N. M.; Veldman, N.; Spek, A. L.; van Neer, F. J. R. *Organometallics* **1997**, *16,* 2948. (g) Mecking, S.; Johnson, L. K.; Wang, L.; Brookhart, M. *J. Am. Chem. Soc.* **1998**, *120,* 888.

3. (a) Fuhrhop, J.-H. In *Porphyrins and Metalloporphyrins*; Smith, K. M., Ed.; Elsevier: Amsterdam, 1975; p 594. (b) Mauzerall, D. In *The Porphyrins*; Dolphin, D., Ed.; Academic: New York, 1979; Vol. 5, p 29. (c) Kalyanasundaram, K. *Photochemistry of Polyoyridine and Porphyrin Complexes*; Academic Press: London, **1992**. (d) Wasielewski, M. R. Chem. Rev. 1992, 92, 435.

4. (a) Guilard, R.; Tabard, A.; van Caemelbecke, E.; Kadish, K. M. *The Porphyrin Handbook*; Kadish, K. M., Smith, K. M., and Guilard, R., Ed.; Academic Press: New York, 2000; Vol. 3, pp 295. (b) Clarke, D. A.; Dolphin, D.; Grigg, R.; Johnson, A. W.; Pinnock, H. A. *J. Chem. Soc. (C)* **1968**, 881. (c) Ogoshi, H.; Setsune, J.; Omura, T.; Yoshida, Z.-I.. *J. Am. Chem. Soc.* **1975**, *97*, 6461.

5. Callot, H. J.; Fischer, J.; Weiss, R. *J. Am. Chem. Soc.*, **1982**, *104*, 1272.

6. (a) Takao, Y.; Takeda, T.; Watanabe, J.; Setsune, J. *Organometallics* **1999**, *18,* 2936. (b) Takao, Y.; Takeda, T.; Watanabe, J.; Setsune, J. *Organometallics* **2003**, *22,* 233.

7. Abbreviations. TPP = 5,10,15,20-tetraphenylporphyrin dianion; OEP = 2,3,7,8,12,13,17,18-octaethylporphyrin dianion.

8. (a) Smith, A. E. *Acta Crystallogr.* **1965**, *18,* 331. (b) Albinati, A.; Rüegger, H. *Organometallics* **1990**, *9,* 1826. (c) Annibale, G.; Cattalini, L.; Bertolosi, V.; Ferretti, V.; Gestone, G.; Tobe, M. L. *J. Chem. Soc., Dalton Trans.* **1989**, 1265. (d) Murrall, N. W.; Welch, A. J. *J. Organomet. Chem.* **1986**, *301,* 109.
9. Albinati, A.; Kunz, R. W.; Ammann, C. J.; Pregosin, P. S. *Organometallics* **1991**, *10*, 1800.
10. Satake, A.; Koshino, H.; Nakata, T. *Organometallics* **1999**, *18,* 5108.
11. (a) Barbaro, P.; Pregosin, P. S.; Saltmann, R.; Albinati, A.; Kunz, R. W. *Organometallics* **1995**, *14,* 5160. (b) Ramdeehul, S.; Barloy, L.; Osborn, J. A.; De Cian, A.; Fischer, J. *Organometallics* **1996**, *15,* 5442.
12. (a) Crociani, B.; Bertani, R.; Boschi, T.; Bandoli, G.; *J. Chem. Soc., Dalton Trans.* **1982**, 1715. (b) Togni, A.; Rihs, G.; Pregosin, P. S.; Ammann, C.; *Helv. Chim. Acta* **1990**, *73,* 723. (c) Miki, K.; Tanaka, N.; Kasai, N.; *J. Organomet. Chem.* **1981**, *208,* 407. (d) Ukhin. L. Y.; Dolgopolova, N.A.; Kuz'mina, L, G.; Struchkov, Y. T.; *J. Organomet. Chem.* **1981**, *210,* 263. (e) Facchin, G.; Bertani, R.; Calligaris, M.; Nardin, G.; Mari, M. *J. Chem. Soc., Dalton Trans.* **1987**, 1381.
13. (a) Breutel, C.; Pregosin, P. S.; Salzmann, R.; Togni, A. *J. Am. Chem. Soc.* **1994**, *116,* 4067. (b) Herrmann, J.; Pregosin, P. S.; Salzmann, R.; Albinati, A. *Organometallics* **1995**, *14,* 3311. (c) Fernández-Galán, R.; Jalón, F. A.; Manzano, B. R.; Rodríguez-de la Fuente, J.; Vrahami, M.; Jedlicka, B.; Weissensteiner, W.; Jogl, G. *Organometallics* **1997**, *16,* 3758.
14. (a) Gogoll, A.; Örnebro, J.; Grennberg, H.; Bäckvall, J.-E. *J. Am. Chem. Soc.* **1994**, *116,* 3631. (b) Crociani, B.; Antonaroli, S.; Paci, M.; DiBianca, F.; Canovese, L. *Organometallics* **1997**, *16,* 384. (c) Gogoll, A.; Grennberg, H.; Axén, A. *Organometallics* **1997**, *16,* 1167.
15. Hansson, S.; Norrby, P-O.; Sjögren, M. P. T.; Åkermark, B.; Cucciolito, M.

E.; Giordano, F.; Vitagliano, A. *Organometallics* **1993**, *12*, 4940.

16. Satake, A.; Koshino, H.; Nakata, T. *Abstracts of the 46th Symposium on Organometallic Chemistry, Japan*; Osaka, September **1999**; p112

17 a) Consiglio, G; Waymouth, R. M. Chem. Rev. **1989**, *89*, 257. (b) Kurosawa, H.; Ogoshi, S.; Kawasaki, Y.; Murai, S.; Miyoshi, M.; Ikeda, I. *J. Am. Chem. Soc.* **1990**, *112,* 2813. (c) Vitagliano, A.; Åkermark, B.; Hansson, S. *Organometallics* **1991**, *10*, 2592.

18 a) Takao, Y.; Takeda, T.; Miyashita, K.; Setsune, J. *Chem. Lett.* **1996**, 761. (b) Takao, Y.; Takeda, T.; Setsune, J. *Bull. Chem. Soc. Jpn.* **1998**, *71,* 1327.

19 *Texsan-Texray Structure Analysis Package*; Molecular Structure Corp.: The Woodlands, TX, 1985.

20. Cromer, D. T.; Waber, J. T.; *International Tables for X-ray Crystallography*; The Kynoch Press: Birmingham, England, 1974; Vol. IV, Table 2.2A.

21. Cromer, D. T.; Waber, J. T.; *International Tables for X-ray Crystallography*; The Kynoch Press: Birmingham, England, 1974; Vol. IV, Table 2.3.1.

Chapter 5

Properties and Reactions of μ-(Dihydroxo)dipalladium(II) Bis-porphyrin Complexes

5.1 Introduction

Since palladium(II) porphyrin is a coordinatively saturated metal complex, it is not useful for organometallic reactions that require coordination sites for organic substrates. By using N^{21},N^{22}-etheno-bridged porphyrin as a bidentate ligand, we have been investigating on the chemistry of organopalladium porphyrin complexes. As described in Chapter 2, single-crystal X-ray analysis of the Pd_2Cl_4 complex of N^{21},N^{22}-etheno-bridged porphyrin, N^{21},N^{22}-(EtC=CEt)(TPP)$(PdCl_2)_2$, showed a folded μ-(dichloro)dipalladium(II) structure. One Pd atom is coordinated by two adjacent imine nitrogens of the porphyrin and placed out of the porphyrin 4N mean plane by 1.32 Å. The other Pd is placed at a distance of 3.78 Å from the porphyrin 4N mean plane and comes close to the porphyrin ring with a dihedral angle (∠B) of 139.8° between two square planes of the Pd coordination as shown in Figure. 1. There are very few reports on the X-ray structure of μ-(dichloro)dipalladium(II) complexes with a bidentate nitrogen base ligand.[1,2] While both planar and folded Pd_2Cl_2 core are known, the *endo-type* conformation of the terminal $PdCl_2$ with respect to the porphyrin ligand is of interest.

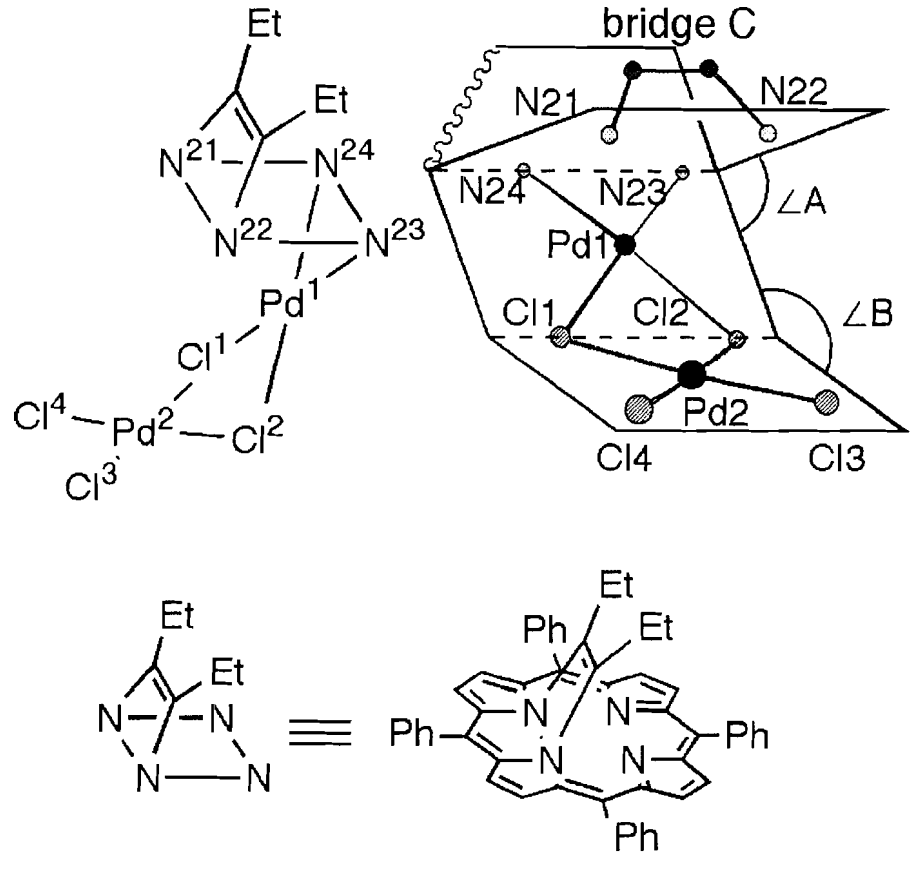

Figure 1. Dinuclear complex of N^{21},N^{22}-etheno-bridged porphyrin including two $PdCl_2$ (left); diagram of two square planes of Pd coordination and the porphyrin 4N mean plane (right).

Chapter 4 described that (π-allyl)palladium(II) complexes with N^{21},N^{22}-etheno-bridged porphyrins are formed by the reaction of bis(aqua)Pd^{II} porphyrin with allyltributyltin or by the reaction of N^{21},N^{22}-etheno-bridged TPP free base and μ-(dichloro)bis(π-allylpalladium(II)) as shown in Scheme 1. This unique porphyrin ligand covers one side of the square plane of Pd coordination and exerts great influence on the apparent rotation of the π-allyl

ligand relative to the porphyrin ligand. Furthermore, this porphyrin ligand has the advantage of the ring current effect that causes great low-frequency shift of the NMR signals due to the Pd-bound organic groups.

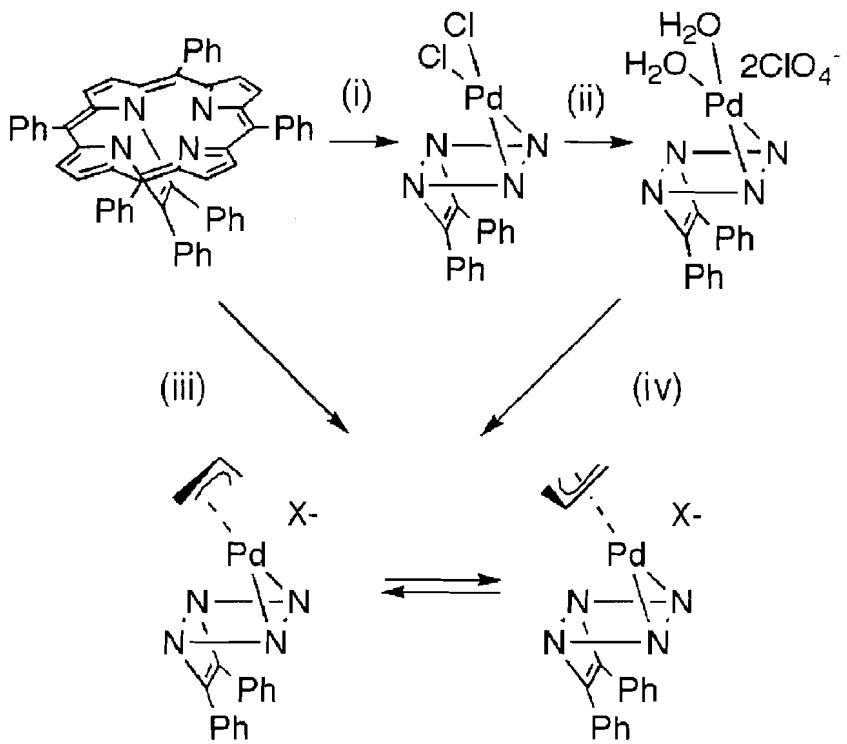

(i) $PdCl_2(MeCN)_2$ / NaCl aq. (ii) $2AgClO_4$
(iii) $[(C_3H_5)PdCl]_2$ (iv) $(n\text{-}Bu)_3Sn(C_3H_5)$

Scheme 1. Synthesis of (π-Allyl)palladium(II) complexes with N^{21},N^{22}-etheno-bridged porphyrins.

Palladium complexes with weakly coordinating anions have been known as unique Lewis acid catalysts for organic transformations.[3] The

coexistence of both basic ligand and acidic metal site is one of the most important features that lead to effective activation of substrates. In this sense, the μ-(dihydroxo) and μ-(dialkoxo)dipalladium(II) complexes have been attracting much interest and their use for the substitution, carbonylation and Mannich-type reactions is known.[3-6] Thus, it is interesting to see how the unique coordination mode of N^{21},N^{22}-etheno-bridged porphyrin would influence the structure and reaction of μ-(dihydroxo)dipalladium(II) core.

In this Chapter is described the synthesis of μ-dihydroxo-bridged complex of dimeric palladium(II) porphyrin as a mixture of two isomers. Their isomerization behavior is detected by NMR and their reactions with active methylene compounds to afford new organopalladium(II) porphyrins are shown here.

5.2 Results and Discussion

5.2.1 **Synthesis of μ-(dihydroxo)dipalladium(II) Complex of N^{21},N^{22}-(Diphenyletheno)-bridged TPP.**

A two phase mixture of CH_2Cl_2 solution of bis(aqua)[(1,2-diphenyletheno-N^{21},N^{22})-meso-tetraphenylporphyrinato-N^{23},N^{24}]palladium(II) bis(perchlorate), (N^{21},N^{22}-(PhC=CPh)(TPP)Pd$(H_2O)_2(ClO_4)_2$) (**1**), and 0.2% aqueous NaOH solution (1.0 equiv) was vigorously stirred for 2h at room temperature. After work-up, recrystallization from CH_2Cl_2 and hexane afforded (hydroxo)Pd(II) complex (**2**) in 92% yield. The complex **2** was also obtained by the addition of triethylamine (1.2 equiv) to CH_2Cl_2 solution of **1**. The ^{1}H NMR spectrum of **2** in $CDCl_3$ showed two singlets at -12.57 and -15.44 ppm with an integral ratio of 42:58. Since these signals disappeared by

adding D_2O, they were assigned to OH protons. The unusually low frequency chemical shifts may be caused by ring current effect from two porphyrins. These data are indicative of a mixture of two isomers (**2a** and **2b**) of μ-(dihydroxo)dipalladium(II) bisporphyrin (Scheme 2). The μ-(dihydroxo) and μ-(dialkoxo)dipalladium complexes reported so far are classified into two structural types, one of which includes a non-planar Pd_2O_2 core[3,5,7,8] and the other includes a planar Pd_2O_2 core.[2,8-10] Because of the requirement for parallel orientation of two porphyrin rings in order to avoid steric hindrance, one isomer with a planar $Pd_2(OH)_2$ core should have an off-set head-to-tail arrangement of two porphyrin rings and the other isomer with a folded $Pd_2(OH)_2$ core should have a superimposed head-to-head arrangement of two porphyrin rings as illustrated for **2a** and **2b**, respectively, in Scheme 2. The isomer distribution of **2** was changed during $CDCl_3$ solution of isolated **2** was allowed to stand at 25 °C for 230 min and then 50 °C for 15 min. ^{1}H NMR spectra showed that one isomer is gradually converted into the other isomer as shown in Figure 2. Since ^{1}H NMR spectrum of **2** in d_6-DMSO showed only one OH-signal at -9.43 ppm, interconversion between **2a** and **2b** would be promoted in DMSO owing to its good coordinating nature. The dinuclear structure is supported by the ESI-MS peak at m/e = 914.2066 which is in good agreement with a theory for $[N^{21},N^{22}$-(PhC=CPh)(TPP)Pd(OH)$]_2^{+2}$ (914.2178) as shown in Figure 3.

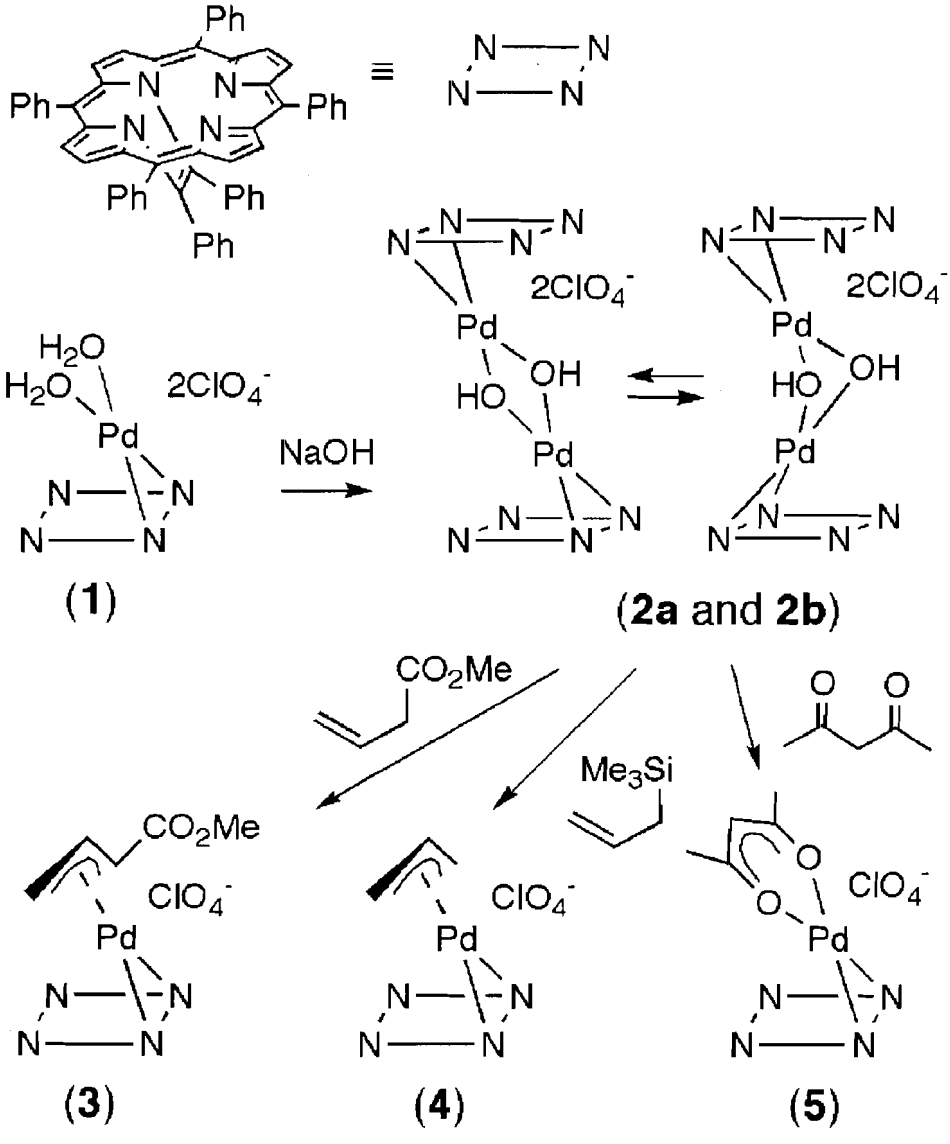

Scheme 2. Reaction of **2** with active methylene compounds.

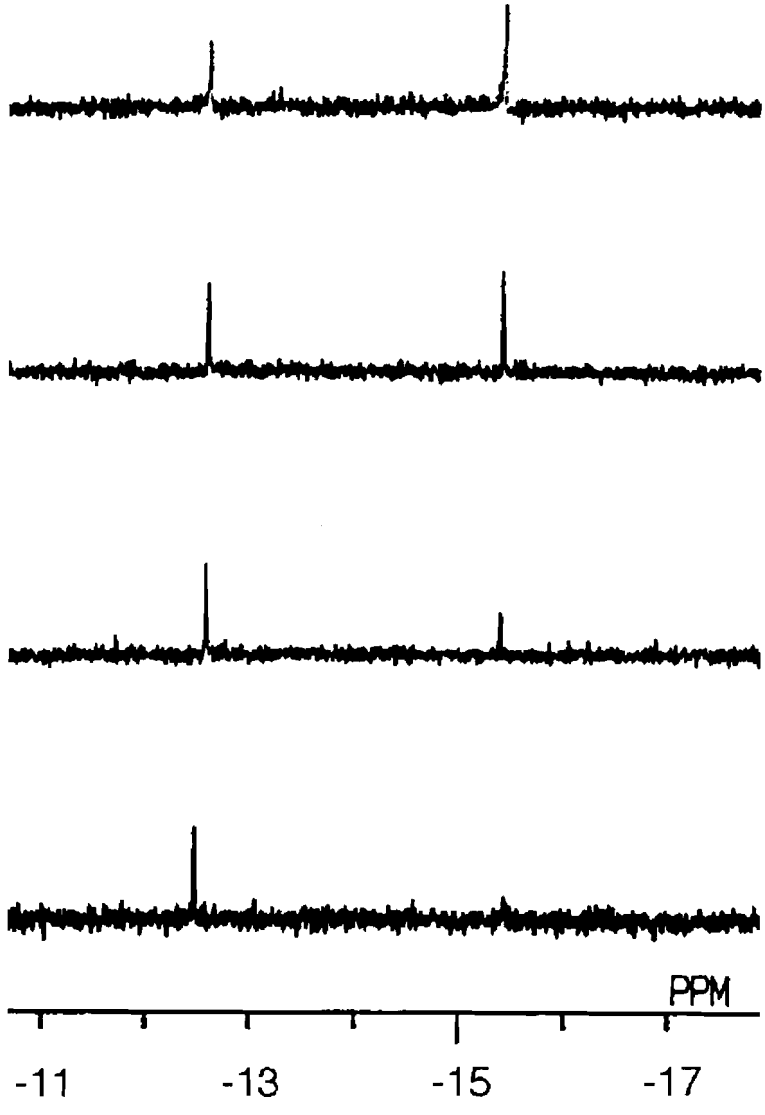

Figure.2. Low frequency region of ^{1}H NMR spectra (270 MHz in $CDCl_3$) of a mixture of **2a** and **2b**, 10 min (top), 40 min (2nd), 190 min (3rd) after dissolving of **2** at 25 °C, and 15 min after standing for 230 min at 25 °C followed by heating to 50 °C.

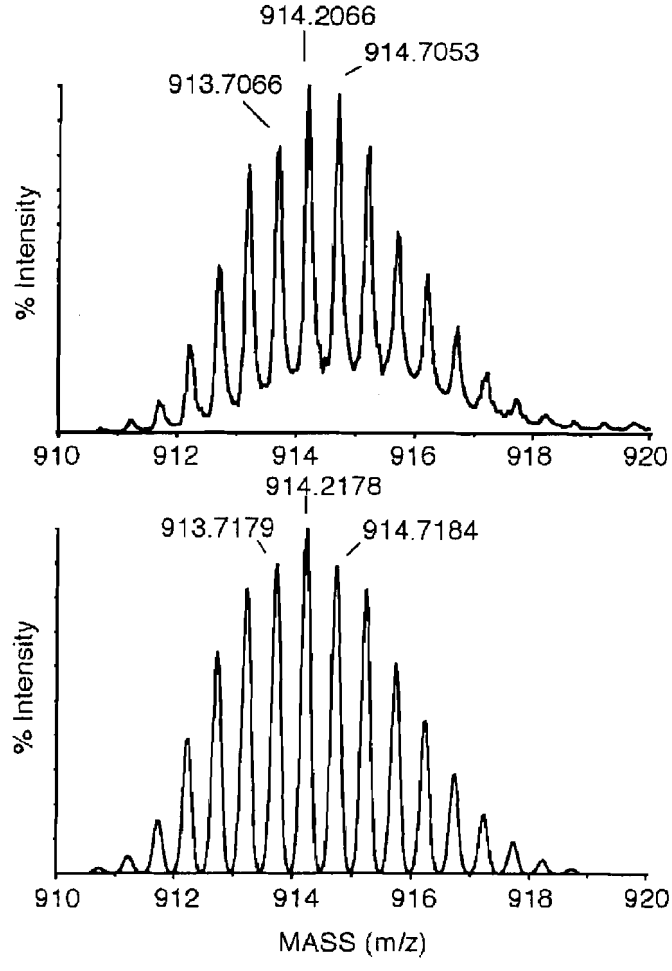

Figure. 3. ESI-MASS spectrum of **2** (top) and simulation for $[\mathbf{2} - 2(ClO_4^-)]^{2+}$ (bottom).

5.2.2 **Reaction with Active Methyrene Compounds.**

It is expected that the OH ligand should act as a base when the $Pd_2(OH)_2$ core of **2** is cleaved by addition of compounds with a coordinating power. Refluxing $CHCl_3$ solution of **2** and methyl 3-butenoate (10 molar equiv) for 4h afforded an (organo)Pd complex (**3**) in 76% isolated yield after recrystallization from CH_2Cl_2 and hexane. The ^1H NMR spectrum of **3** showed two doublets at –3.59 and -4.45 ppm with coupling constants of 11.0 and 12.6 Hz, respectively. These signals are quite similar to the doublet due

to the H_{anti} protons in the π-(allyl) ligand of the cis form of π-(allyl)Pd complex of N^{21},N^{22}-(diphenyletheno)-bridged TPP (**4**) (-4.55 ppm, J_{anti} = 11.9 Hz). Furthermore, chemical shifts of the $H_{central}$ and H_{syn} protons in the π-(allyl) ligand of **3** and cis-**4** are also quite similar as summarized in Table 1. Therefore, **3** is a cis isomer of π-(1-*syn*-methoxycarbonylallyl)Pd complex as shown in Scheme 2. There are four possible isomers for π-(1-substituted allyl)Pd complexes of N^{21},N^{22}-bridged porphyrin as shown in Scheme 3. Steric hindrance between the porphyrin ligand and the substituent at the terminal carbon of the π-(allyl) ligand resulted in the formation of only one isomer where 1-substituent is at the *syn* position of the *cis* isomer. While methyl 3-butenoate was deprotonated by the hydroxo ligand to generate 1-substituted allyl anion, allyltrimethylsilane underwent OH^- attack at silicon to liberate allyl anion. Thus, the reaction of **2** with allyltrimethylsilane gave 77% yield of **4** as a mixture of cis and trans isomers in a ratio of 7:3. The reaction of **2** with acetylacetone proceeded rapidly to give (acetylacetonato)Pd^{II} porphyrin complex (**5**) in 76% yield. The chemical shift of the methine proton of the acetylacetonato ligand at 3.04 ppm is not consistent with the porphyrin ring current effect expected for the presence of Pd-CH bonding.

Table 1. ^{1}H NMR Data of **3** and **4** in $CDCl_3$ [a]

Compd	R	allyl-H_{anti}	allyl-H_{syn}	allyl-H_{cent}
3	CO_2Me	–3.59 (11.0)	–0.19 (7.1)	2.73
		–4.45 (12.6)		
cis-**4**	H	–4.45 (11.9)	–0.28 (6.9)	2.14
trans-**4**	H	–1.06 (10.9)	–1.37 (5.9)	–1.25

[a] Chemical shifts (δ-value) with coupling constant (Hz) in the parentheses.

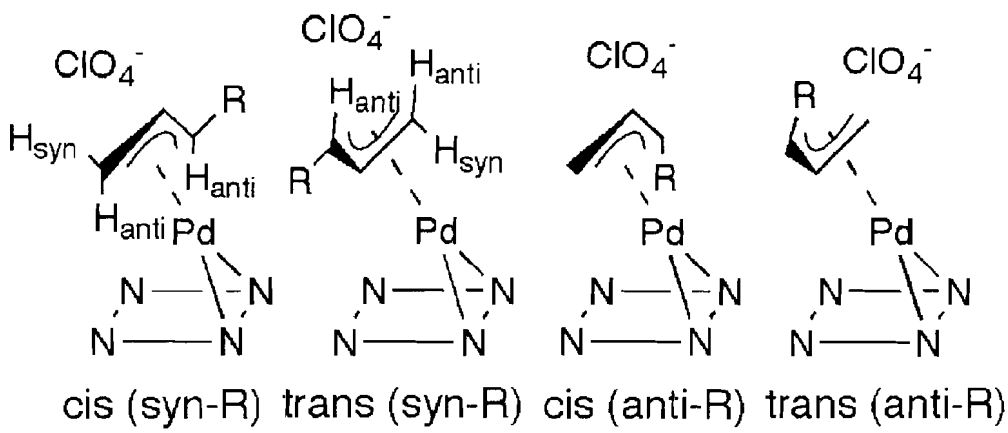

Scheme 3. Isomers for π-(1-substituted allyl)Pd complexes of N^{21},N^{22}-bridged porphyrin

Preparation of π-(allyl)Pd complexes using β,γ-unsaturated carbonyl compounds is well known.[11] However, palladium(II) complexes with bidentate nitrogen base ligand are not so reactive towards olefinic compounds. In fact, both (dichloro)Pd^{II} porphyrin and dicationic bis(aqua)Pd^{II} porphyrin **1** did not react with methyl 3-butenoate under the same conditions as those for **2**. It is true that the complex **1** readily reacts with allyltrimethylsilane at room temperature, but the product complex **4** decomposed with time probably due to the action of byproduct, trimethylsilyl perchlorate.

The μ-(dihydroxo)dipalladium(II) complex of N^{21},N^{22}-bridged porphyrin described here can provide both acidic site and basic site at the same time to promote formation of π-(allyl)Pd complexes under neutral conditions.

5.3 Experimental Section

General. Solvents were purified prior to use by conventional methods. Other chemicals were of reagent grade. $CDCl_3$ was passed through basic Al_2O_3 before use. ^1H NMR spectra were recorded on JEOL EX-270 and AL-300 spectrometer. Chemical shifts were referenced with respect to $(CH_3)_4Si$ (0 ppm) as an internal standard. ESI-MS spectrawere measured with a PE Biosystems Mariner spectrometer. Elemental analysis C, H, and N were made with a Yanaco MT-5 CHN corder. The UV-visible spectra were measured on a Shimadzu UV-3100B instrument.

Preparation of μ-(dihydroxo)dipalladium(II) complex of N^{21},N^{22}-(diphenyletheno)-bridged TPP. 0.72 mL of NaOH aqueous solution (0.05 mol L^{-1}) was added to dichloromethane solution (8mL) of the dicationic bis(aqua)palladium(II) complex of N^{21},N^{22}-(diphenyletheno)-bridged TPP **1** (40 mg). The mixture was stirred vigorously at room temperature for 2 h. Then the product was extracted with dichloromethane, dried over Na_2SO_4, and evaporated to dryness. Recrystallization from dichloromethane – hexane gave a mixture of two isomers of μ-(dihydroxo)dipalladium(II) complex of N^{21},N^{22}-(diphenyletheno)-bridged TPP **2**.

2: Yield 92 %; ^1H NMR (δ, $CDCl_3$): (**2a**) 9.43, 8.27, 8.05, 7.43, (d × 4, 4H × 4, pyrrole-β-H); 8.6-7.0 (m, 40H, *meso*-phenyl-H); 5.92 (t, 4H, bridge phenyl-*p*-H); 5.42 (broad, 8H, bridge phenyl-*m*-H); -12.57 (s ,2H, OH); (**2b**) 9.08, 8.45, 7.76, 7.55, (d × 4, 4H × 4, pyrrole-β-H); 8.3-6.8 (m, 40H, *meso*-phenyl-H); 5.90 (t, 4H, bridge phenyl-*p*-H); 5.42 (broad, 8H, bridge phenyl-*m*-H); -15.44 (s, 2H, OH); UV/Vis (CH_2Cl_2): λ_{max}(log ε) 666 (4.51), 641 (4.49), 467 (5.35), 409 (5.26) nm; MS (ESI in MeOH): m/z 914.2066 (calcd for $[C_{116}H_{78}N_8O_2Pd_2]^{+2}$ (M - $2ClO_4$)/2: 914.2178). Anal. Calcd for

$C_{58}H_{39}N_4O_5ClPd \cdot H_2O$: C, 67.51; H, 4.01; N, 5.43 %. Found: C, 67.50; H, 3.99; N, 5.46 %.

Reaction of μ-(dihydroxo)dipalladium(II)bis(N^{21},N^{22}-diphenylethen-TPP) with active methylene compounds. Active methylene compounds (0.15 mmol of methyl 3-butenoate for **3**, allyltrimethylsilane for **4**, and acetylacetone for **5**) were added to solution of μ-(dihydroxo)dipalladium(II)bisporphyrin bisperchlorate **2** (0.015 mmol) in chloroform (5 mL). After the mixtures were refluxed for 4 h, the products were reprecipitated with *n*-hexane.

3: Yield 76 %; ^{1}H NMR (δ, $CDCl_3$): 9.21, 9.08, 8.88, 8.86, 8.82, 8.80, 8.23, 8.19 (d × 8, 1H × 8, pyrrole-β-H); 8.4-7.1 (m, 20H, *meso*-phenyl-H); 6.22 (t, 2H, bridge phenyl-*p*-H); 5.80 (broad, 4H, bridge phenyl-*m*-H); 2.93 (s, 3H, OCH_3); 2.73 (m, 1H, allyl central CH); -0.19 (d, J_{syn} = 7.1 Hz, 1H allyl terminal CH); -3.59 (d, J_{anti} = 11.0 Hz, 1H allyl terminal CH); -4.45 (d, J_{anti} = 12.6 Hz, 1H allyl terminal CH); UV/Vis (CH_2Cl_2): λ_{max}(log ε) 666 (4.21), 634 (4.14), 581 (3.94), 469 (5.11), 407 (4.89) nm; MS (ESI in MeCN): m/z 995.54 (calcd for $[C_{63}H_{45}N_4O_2Pd]^+$ (M - ClO_4): 995.25). Anal. Calcd for $C_{63}H_{45}N_4O_6ClPd \cdot 2H_2O$: C, 66.85; H, 4.36; N, 4.95 %. Found: C, 67.16; H, 4.45; N, 5.08 %.

4: Yield 77 %; Data were exhibited in previous report.[12]

5: Yield 76 %; ^{1}H NMR (δ, $CDCl_3$): 9.09, 8.85, 8.67, 8.24 (d × 4, 2H × 4, pyrrole-β-H); 8.4-7.3 (m, 20H, *meso*-phenyl-H); 6.25 (t, 2H, bridge phenyl-*p*-H); 5.82 (broad, 4H, bridge phenyl-*m*-H); 3.04 (s, 1H, CH); 0.04 (s, 6H, CH_3); UV/Vis (CH_2Cl_2): λ_{max}(log ε) 670 (3.97), 475 (4.76), 407 (4.58) nm; MS (ESI in MeCN): m/z 995.57 (calcd for $[C_{63}H_{45}N_4O_2Pd]^+$ (M - ClO_4): 995.25). Anal. Calcd for $C_{63}H_{45}N_4O_6ClPd \cdot H_2O$: C, 67.93; H, 4.25; N, 5.03 %. Found: C, 67.66; H, 4.55; N, 5.32 %.

Monitor of isomerization of 2. 3 mg of **2** was dissolved in 0.5 mL of $CDCl_3$ in a NMR tube and ^1H NMR spectra were taken from time to time. The sample tube was kept at 25 °C for 230 min and then heated to 50 °C during NMR measurements. The change in concentrations of each isomer in the solution was estimated on the basis of the ^1H NMR integrations of the signals corresponding to OH protons at –12.57 and –15.44 ppm with time.

5.4 References

1. (a) M. Calter, T. K. Hollis, L. E.. Overman, J. Ziller and G. G. Zipp, *J. Org. Chem.*, **62**, 1449 (1997). (b) B. Bock, H. Noth and U. Wietelmann, *Z. Naturforsch., Teil B*, **56**, 659 (2001).
2. M. Akita, T. Miyaji, N. Muroga, C. Mock-Knoblauch, W. Adam, S. Hikichi and Y. Moro-oka, *Inorg. Chem.*, **39**, 2096 (2000).
3. C. Pisano, G. Consiglio, A. Sironi and M. Moret, *J. Chem. Soc., Chem. Commun.*, **1991**, 421.
4. G. Mann, C. Incarvito, A. L. Rheingold and J. F. Hartwig, *J. Am. Chem. Soc.*, **121**, 3224 (1999).
5. V. V. Grushin and H. Alper, *Organometallics,* **12**, 1890 (1993).
6. (a) E. Hagiwara, A. Fuji and M. Sodeoka, *J. Am. Chem. Soc.,* **120**, 2474 (1998). (b) A. Fuji, E. Hagiwara and M. Sodeoka, *J. Am. Chem. Soc.,* **121**, 5450 (1999).
7. (a) A. R. Siedle and L. H. Pignolet, *Inorg. Chem.*, **21**, 3090 (1982). (b) V. Dura-Vila, D. M. P. Mingos, R. Vilar, A. J. P. White and D. J. Williams, *Chem. Commun.*, **2000**, 1525.
8. S. Kannan, A. J. James and P. R. Sharpa, *Polyhedron*, **19**, 155 (2000).

9. (a) G. López, J. Ruiz, G. García, C. Vicente, J. Casabó, E. Molins and C. Miravitlles, *Inorg. Chem.*, **30**, 2605 (1991). (b) G. Pieri, M. Paasquali, P. Leoni and U. Englert, *J. Organomet. Chem.*, **491**, 27 (1995).

10.(a) R.-D. Schnebeck, E. Freisinger and B. Lippert, *Eur. J. Inorg. Chem.*, **2000**, 1193. (b) A. J. Atkins, A. J. Blake and M. Schroder, *J. Chem. Soc., Chem. Commun.*, **1993**, 353.

11. J. Tsuji and S. Imamura, *Bull. Chem. Soc. Jpn.*, **40**, 197, (1967).

12. (a) Y. Takao, T. Takeda, J. Watanabe and J. Setsune, *Organometallics,* **18**, 2936 (1999). (b) Y. Takao, T. Takeda, J. Watanabe and J. Setsune, *Organometallics,* **22**, 233 (2003).

Chapter 6

Insertion of Isonitrile into the Pd-C Bond of Palladium(II) Complexes of N^{21},N^{22}-Bridged Porphyrins

6.1 Introduction

One of the most attractive examples of late transition metal catalysis are olefin polymerization by nickel(II) and palladium(II) complexes with a bulky diimine ligand.[1] Brookhart, Sen, and Nozaki et al have recently reported the alternating copolymerizations of carbon monoxide with α-olefins catalyzed by cationic palladium(II) complexes of chiral bidentate ligands, affording completely alternating copolymers with head-to-tail regioselectivity and isotacticity.[2,3] The studies regarding the reactions of organopalladium(II) complexes of bidentate nitrogen base ligands with carbon monoxide or isonitrile are of importance as a basis of their application to organic synthesis and polymer synthesis.[4] Only late transition metal complex is known for the polymerization catalyst of isonitrile which is isoelectronic with carbon monoxide and stabilizes organometallic complexes well.[5] Recently, living polymerization reactions of isonitriles catalyzed by the late transition metal complexes, such as (η^3-allyl)nickel complex and organopalladium complex were found.[6] But further development of the novel living polymerization using isonitrile as one of the components is desired in view of its limited usage at present, although some fine polymerization of isonitrile have been studied.[7]

The investigation on palladium(II) complexes of N^{21},N^{22}-bridged porphyrins seems to provide some information regarding mechanistic aspects

of Pd catalysis. We have described synthesis and isomerization behavior of (η^3-allyl)palladium(II) porphyrins as the first organopalladium(II) complexes of bidentate porphyrin ligands.[8] Reactions of (methyl)palladium and (η^3-allyl)palladium complexes of N^{21},N^{22}-bridged porphyrin ligand with isonitriles are described here.

6.2 Results and Discussion

6.2.1 **Reaction of Methylpalladium(II) Complex of N^{21},N^{22}-Bridged Porphyrin with Isonitriles.**

Isonitriles inserted into Pd-C bond of (methyl)palladium(II) complex containing N^{21},N^{22}-bridged porphyrin ligand to form (methylimino)palladium(II) complexes. The neutral (organo)palladium(II) complex, chloro[(1,2-di-phenyletheno-N^{21},N^{22})-meso-tetraphenylporphyrinato-N^{23},N^{24}](methyl)palladium (II), Pd(Me)Cl(N^{21},N^{22}-PhC=CPh-TPP) (**1**) reacted with isonitriles, *tert*-butyl isonitrile (BIC), 2,6-dimethylphenyl isonitrile (DIC), and tosylmethyl isonitrile (TIC). The reaction of **1** with BIC was monitored by ^{1}H NMR spectroscopy in $CDCl_3$ solution as shown in Figure 1. Immediately more than 2-fold molar amount of BIC was added to **1**, the ^{1}H NMR signal of the methyl group of **1** at –4.13 ppm disappeared, and a new singlet signal (–4.43 ppm) appeared. A singlet at 0.32 ppm observed is assigned to the coordinated BIC protons because it is shifted to lower frequency region than the signal of free BIC at 1.90 ppm. Further, as the intensity of this second signal decreased, the third singlet signal grew at higher frequency (–2.58 ppm). Thus, it was suggested that at first BIC coordinated to Pd via displacement of the chloro ligand with shift of the methyl signal to lower frequency. Then the methyl group migrated to the imino carbon

of the precoordinated BIC which caused the methyl signal to shift to by 1.55 ppm higher frequency. Thus, the overall change is the insertion of one BIC into Pd – carbon bond of (methyl)palladium complex and formation of (methylimino)palladium complex with porphyrin ligand.[11] Two singlet signals at 0.37 and 0.11 ppm assigned to *tert*-butyl protons in the final product exhibited the coordination of the another BIC to Pd as shown in Scheme 1.

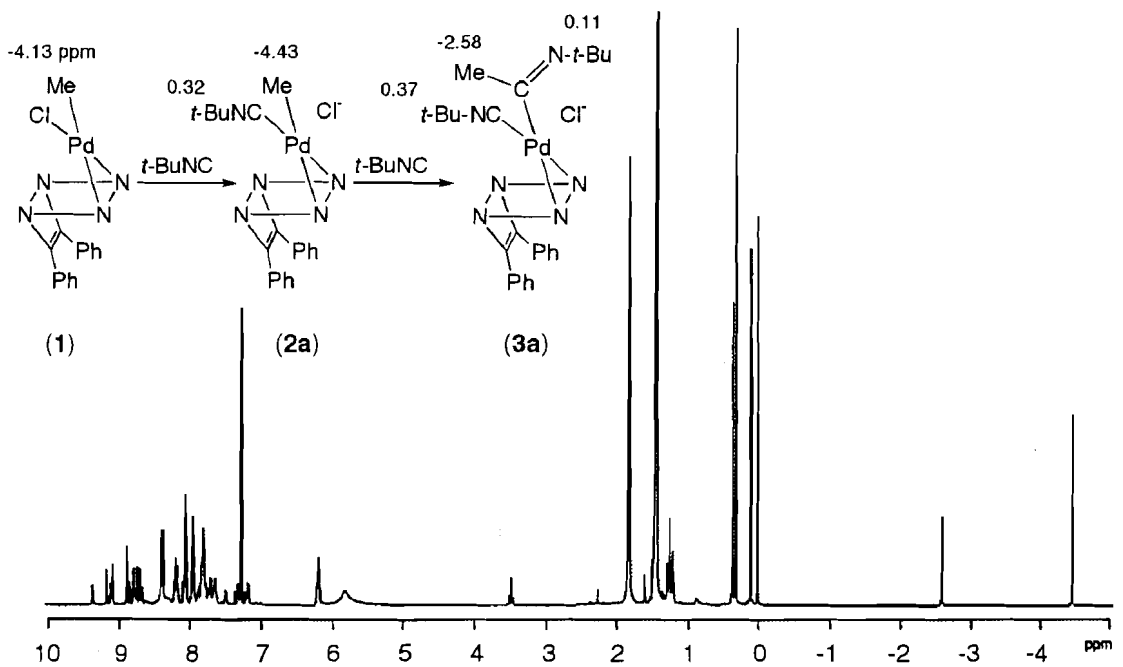

Figure 1. Insertion reaction of *tert*-butyl isonitrile into **1**, and ^{1}H NMR spectrum on the formation process of **3a** in $CDCl_3$.

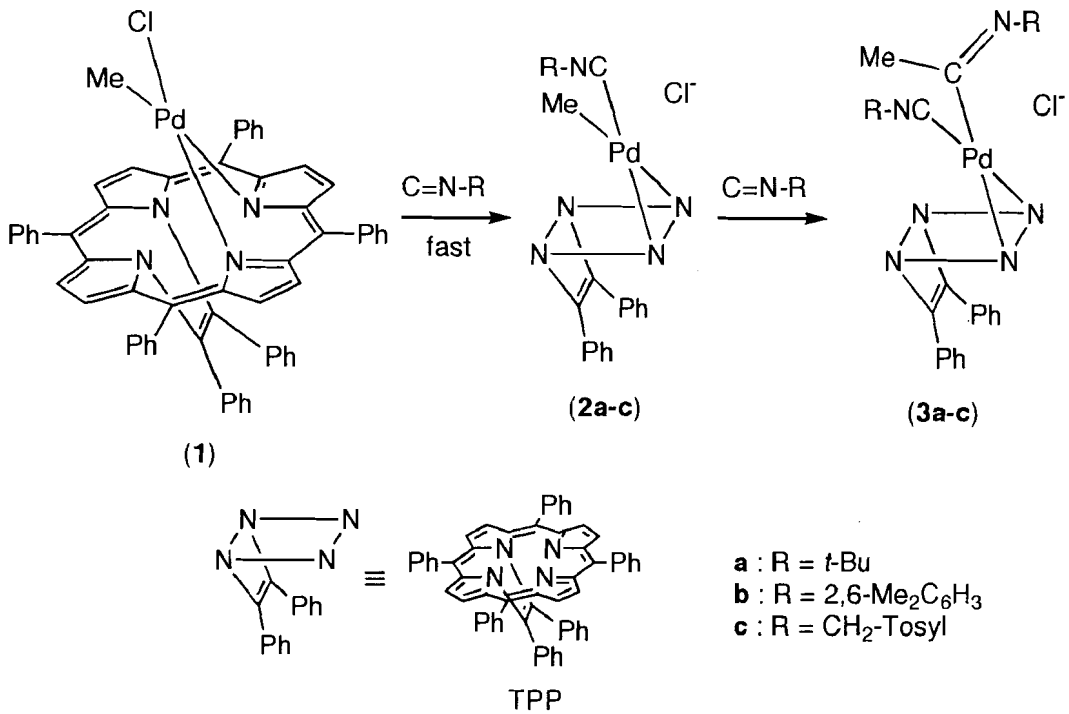

Scheme 1

6.2.2 **Reaction of (η^3-Allyl)palladium(II) Complex of N^{21},N^{22}-Bridged Porphyrin with Isonitriles.**

(η^3-allyl)palladium(II) complexes of N^{21},N^{22}-bridged porphyrin, N^{21},N^{22}-(PhC=CPh)(TPP)Pd(R)X (R = η^3-allyl, X = Cl (**4**); R = η^3-allyl, X = ClO_4 (**5**); R = η^3-butenyl, X = ClO_4 (**6**)) were allowed to react with isonitriles (4 – 9.5 equiv.) as shown in Scheme 2. Figure 2 shows ^{1}H NMR spectrum after the addition of 9.5 equivalents of *t*-BuNC to **4** in $CDCl_3$. With decreasing of intensity of the signals due to η^3-allyl protons of *cis*-**5** at –4.52, –0.25, and 2.08 ppm and *trans*-**5** at –1.13, –1.13, and –1.40 ppm in CD_3CN, five signals assigned to one set of allyl protons increased. The signals due to the methylene protons appeared at –2.32 and –2.91 ppm. These chemical shifts are at by 1.5 - 2 ppm higher frequency than the Pd-Me signal of **2a**. This chemical shift

difference is in the range expected for the substitution by a vinyl group. The vinyl protons at 3.19, 3.48, and 2.92 ppm show typical coupling constants with J_{anti} = 16.5 Hz, and J_{syn} = 9.9 Hz and their chemical shifts are shifted to by ca. 2 ppm lower frequency regions compared with ordinary vinyl proton chemical shifts. Furthermore, one *t*-butyl singlet appeared at 0.29 ppm that is very similar to the chemical shift at 0.25 ppm of the *t*-BuNC ligand of **2a**. These NMR features are consistent with coordination of *t*-BuNC with concomitant change of the η^3-allyl ligand to η^1-allyl ligand. This spectral change is reversible and the proportion of the starting (η^3-allyl)Pd complex **5** was increased by diluting solution containing N^{21},N^{22}-(PhC=CPh)(TPP)Pd^{II}(η^1-allyl)(*t*-BuNC)ClO_4 (**8a**). The equilibrium state could be shifted in favor of **8a** by increasing the amount of *t*-BuNC. However, too much concentration of isonitrile resulted in the dissociation of the porphyrin ligand.

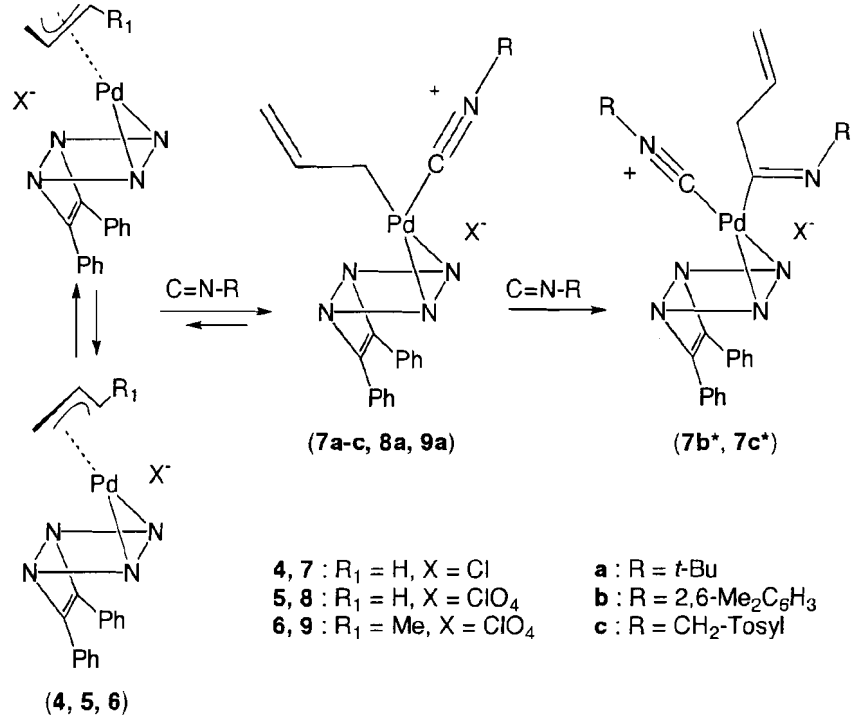

Scheme 2

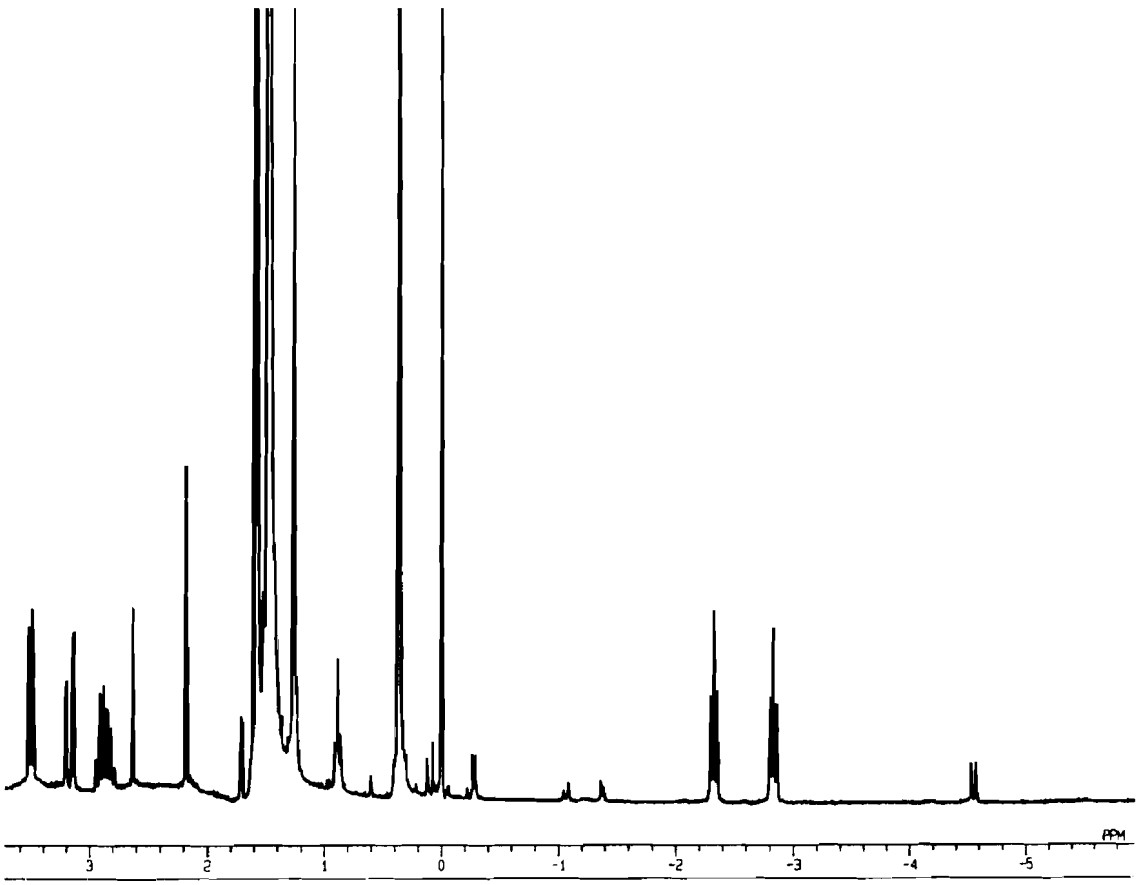

Figure 2. ^{1}H NMR spectrum on the formation process of **8a** in $CDCl_3$.

^{1}H NMR spectroscopy showed the formation of similar products in the reaction of 2,6-dimethylphenyl isonitrile (DIC), and tosylmethyl isonitrile (TIC) with **4** and **5**. The chemical shifts for the organic ligands of the complexes formed in the reaction of isonitriles with (methyl)palladium(II) complex **2** and (η^3-allyl)palladium(II) complexes **4** - **6** are summarized in Table 1. All the $Pd^{II}(\eta^1$-allyl)(CNR) complexes **7** - **9** show two methylene signals at the chemical shift region between –2 and –3 ppm. In the case of the reaction of DIC and TIC with (η^3-allyl)palladium(II) complex **4**, the second products (**7b*** and **7c***) were observed. Since the signals due to the methylene protons of **7b*** and **7c***

were shifted to by 0.7 – 2.7 ppm higher frequency region than **7b** and **7c**, it was considered that the second isonitrile inserted between Pd and η^1-allyl ligand to generate complexes similar to **3b** and **3c**.[12] This is supported by the similarity of the chemical shift of *ortho*-dimethyl substituent of the DIC ligand between **7b*** and **3b**.

Some factors that influence on this coordination reaction were examined, including organic ligand and counter anion in the starting complexes, isonitriles, Pd/RNC molar ratio, and solvent. Table 2 shows the % conversion to Pd^{II}(C(=NR)alkyl)(RNC) complexes **3** and **7*** and to Pd^{II}(alkyl)(RNC) complexes **7** - **9** at the time of 3 min and 80 min after addition of isonitriles to **1**, **4**, **5** and **6**. The reactions of 4-fold molar amount of DIC and TIC with **1** in CD_3CN at 25 °C proceeded much faster than that of BIC, and afforded 85 % conversion to **3b** and 95 % conversion to **3c** in 3 min. The migration of the Pd-bound alkyl group to the coordinated isonitrile is the rate determining step and is enhanced by R groups on the isonitrile having electron-withdrawing properties, such as a tosylmethyl group, and reduced by an electron-donating R group, such as *tert*-butyl.[4c] In the reaction of (η^3-allyl)palladium complex with DIC and TIC under the same condition, the initially formed complexes **7b** and **7c** were gradually converted to **7b*** and **7c***, respectively. While much amount of BIC (9.5 equiv) naturally drives the equilibrium in favor of **7a** in the reaction of **4** in CD_3CN, the rapidly formed **7a** decreased from 94% to 30% with time in $CDCl_3$. In the reaction of **5**, the initially formed **8a** is relatively stable in both solvents. The coordination of BIC to **4** in DMSO was slow and afforded 49 % conversion to **7a** in 80 min. Thus, good coordinating solvents such as CD_3CN and DMSO retard the reaction with isonitriles but enhance the stability of the product.

Table 1. ^{1}H NMR Chemical Shifts (δ) for **3a-c, 7a-c** in CD_3CN.

comp.	Me (s, 3H)	β-Pyrrole (d × 8, 1H × 8, J =4.4–5.5Hz)	others
2a	–4.47	9.12, 9.05, 8.82 × 2,	0.25
		8.70, 8.68, 8.45, 8.13	(s, 9H, *t*-Bu)
3a	–2.60	9.31, 9.05, 8.92, 8.84,	0.06, 0.28 (s × 2,
		8.79, 8.54, 8.44, 8.12	9H × 2, *t*-Bu)
2b	–4.25	9.20, 9.17, 8.85, 8.84,	0.96
		8.67, 8.45,	(s, 6H, Me_2)
3b	–1.67	9.47, 9.01, 8.93, 8.75,	1.12
		8.55, 8.53, 8.16, 8.12	(s, 6H × 2, Me_2)
2c	–4.65	9.44, 9.17, 9.09, 8.97,	overlapped
		8.85, 8.79, 8.68, 8.65	
3c	–2.50	9.35, 9.05, 8.96, 8.82,	overlapped
		8.75, 8.72, 8.58, 8.14	

	allyl			
	terminal CH (d, 1H)	central CH (m, 1H)	CH_2 (dd × 2, 1H × 2)	others
7a	3.19 (J_{anti}=16.5Hz)	2.92	–2.32 (*J*=7.7Hz)	0.29 (s, 9H, *t*-Bu)
	3.48 (J_{syn}=9.9Hz)		–2.91 (*J*=7.7Hz)	9.07, 8.76, 8.74, 8.20, 8.18
				8.17, 8.12, 8.01 (β-pyrrole)
7b	3.21 (J_{anti}=15.4Hz)	3.04	–1.99 (*J*=7.7Hz)	1.01 (s, 6H, Me_2)
	3.50 (J_{syn}=9.9Hz)		–2.70 (*J*=7.7Hz)	
7b*	3.44 (J_{anti}=17.0Hz)	3.80	–0.67 (*J*=6.9, 16.2Hz)	1.13 (s, 6H × 2, Me_2)
	4.07 (J_{syn}=10.4Hz)		–1.99 (*J*=6.9, 16.2Hz)	
7c	4.35 (J_{anti}=16.5Hz)	4.21	–2.34 (*J*=7.7Hz)	overlapped
	4.51 (J_{syn}=9.9Hz)		–3.04 (*J*=7.7Hz)	
7c*	3.5 - 4.0	3.5 - 4.0	0.39 (*J*=8.2, 18.4Hz)	overlapped
			–2.14 (*J*=8.2, 17.6Hz)	
8a	3.19 (J_{anti}=16.5Hz)	2.93	–2.32 (*J*=7.4Hz)	
	3.49 (J_{syn}=9.9Hz)		–2.90 (*J*=7.7Hz)	9.10, 9.08, 8.91, 8.82, 8.76
				8.68, 8.20, 8.17 (β-pyrrole)
cis-	4.10 (dq)	2.87 (dt)	–2.57 (*J*=8.0Hz)	0.29 (s, 9H, *t*-Bu)
9a	(*J*=10.4Hz)	(*J*=9.3Hz)	–2.99 (*J*=8.5Hz)	–0.48 (d, 3H, Me)
				(*J*=7.1Hz)
trans-	3.62 (dq)	2.57 (dt)	–2.29 (*J*=7.7Hz)	0.29 (s, 9H, *t*-Bu)
9a	(*J*=6.6, 14.8Hz)	(*J*=6.9, 13.7Hz)	–2.87 (*J*=8.0Hz)	0.62 (d, 3H, Me)
				(*J*=6.6Hz)

Table 2. Formation of **3a-c**, **7a-c**, **8a** and **9a** after Addition of Isonitriles to **1**, **4**, **5** and **6**.

comp.	R_1	X	R	R-NC (eq.)	Solv.	content (%) 3min	80m
3a	-	Cl	*t*-Bu	4.0	CD_3CN	13	98
3b	-	Cl	2,6-$Me_2C_6H_3$	4.0	CD_3CN	85	100
3c	-	Cl	CH_2-Tosyl	4.0	CD_3CN	95	100
7a	H	Cl	*t*-Bu	4.0	CD_3CN	35	55
7b	H	Cl	2,6-$Me_2C_6H_3$	4.0	CD_3CN	37 (7*)	33 (28*)
7c	H	Cl	CH_2-Tosyl	4.0	CD_3CN	46 (36*)	63*
7a	H	Cl	*t*-Bu	9.5	CD_3CN	66	83
7a	H	Cl	*t*-Bu	9.5	$CDCl_3$	94	30
7a	H	Cl	*t*-Bu	9.5	DMSO	22	49
8a	H	ClO_4	*t*-Bu	4.0	CD_3CN	88	83
8a	H	ClO_4	*t*-Bu	9.5	$CDCl_3$	62	56
9a	Me	ClO_4	*t*-Bu	4.0	CD_3CN	15(cis) 22(trans)	21(cis) 29(trans)

ESI-MS spectrum of **7a** showed a molecular ion at m/e = 1019.3050 which is in good agreement with a theory for $[N^{21},N^{22}$-(PhC=CPh)(TPP)Pd($CH_2CH=CH_2$)(*t*-BuNC)]$^+$ (1019.3274). Observed peaks at m/e = 1103.3260 and 552.1739 correspond to the insertion product $[N^{21},N^{22}$-(PhC=CPh)(TPP)Pd(C(=N-*t*-Bu)$CH_2CH=CH_2$)(*t*-BuNC)]$^+$ (1103.4010; 552.2041 for monoprotonated dication). The fragment ions at m/e = 396.1513 and 313.0831 are in agreement with [Pd(η^1-allyl)(*t*-BuNC)$_3$]$^+$ (396.1633) and

$[Pd(\eta^3\text{-allyl})(t\text{-BuNC})_2]^+$ (313.0896). Then the insertion of isonitriles into organopalladium complexes with porphyrin ligand appears to be worth further consideration.

6.3 Experimental Section

General. Solvents were purified prior to use by conventional methods. $CDCl_3$ was passed through basic Al_2O_3 before use. All chemicals were of reagent grade. (η^3-Allyl)palladium porphyrin perchlorate **5** and (η^3-butenyl)palladium porphyrin complex perchlorate **6** were prepared by the method described. ^1H NMR was recorded on JEOL EX-270 and AL-300 spectrometer. Chemical shifts were referenced with respect to $(CH_3)_4Si$ (0 ppm) as an internal standard. ESI-MS spectra were measured with a Mariner PE Biosystems spectrometer.

Preparation of chloro(methyl)palladium(II) complex of N^{21},N^{22}-diphenyletheno-bridged TPP (1). To 0.1 g of N^{21},N^{22}- diphenyletheno-bridged TPP free base was added a benzene solution (0.03 cm^3) of chloro(methyl)palladium complex with cycrooctadiene, Pd(Me)Cl(COD), (1.1 equiv). The mixture was stirred at room temperature for 24 h, then solvent was evaporated. Reprecipitation of green solid from dichloromethane – hexane gave 44 % yield of **1**.

Preparation of chloro(η^3-allyl)palladium(II) complex of N^{21},N^{22}-diphenyletheno-bridged TPP (4). To 0.09 g of N^{21},N^{22}-diphenyletheno-bridged TPP free base was added a benzene solution (0.024 cm^3) of allylpalladium chloride dimmer, $[Pd(C_3H_5)Cl]_2$, (1.1 equiv). The mixture was stirred at room temperature for 24 h, then solvent was evaporated. Reprecipitation of green

solid from dichloromethane – hexane gave 90 % yield of **3**.

Reaction of organopalladium(II) complexes of N^{21},N^{22}-diphenyletheno-bridged TPP with isonitriles. To a $CDCl_3$ solution (1.5 cm^3) of **1**(0.016 mmol) was added *tert*-butyl isonitrile (4 equiv) at 25 °C, and the progress of reaction was monitored by ^1H NMR in 24 h. After the reaction drying in vacuo and washing with n-hexane afforded 55 % yield of **3**. The reactions of **4** – **6** with isonitriles (4 – 9.5 equiv) were also monitored by ^1H NMR.

2a: ^1H NMR (δ, CD_3CN): 9.12, 9.05, 8.82 × 2, 8.70, 8.68, 8.45, 8.13 (d × 8, 1H × 8, pyrrole-β-H); 8.5-7.2 (m, 20H, *meso*-phenyl-H); 6.21 (t, 2H, bridge phenyl-*p*-H); 5.82 (broad, 4H, bridge phenyl-*m*-H); -4.47 (s, 3H, Me); 0.25 (s, 9H, *t*-Bu).

3a: ^1H NMR (δ, CD_3CN): 9.31, 9.05, 8.92, 8.84, 8.79, 8.54, 8.44, 8.12 (d × 8, 1H × 8, pyrrole-β-H); 8.4-7.3 (m, 20H, *meso*-phenyl-H); 6.21 (t, 2H, bridge phenyl-*p*-H); 5.84 (broad, 4H, bridge phenyl-*m*-H); –2.60 (s, 3H, Me); 0.06, 0.28 (s, 9H × 2, *t*-Bu).

2b: ^1H NMR (δ, CD_3CN): 9.20, 9.17, 8.85, 8.84, 8.67, 8.45 (d × 6, 1H × 6, pyrrole-β-H, Others are overlapped); 8.3-6.7 (m, 20H, *meso*-phenyl-H); 6.16 (t, 2H, bridge phenyl-*p*-H); 5.81 (broad, 4H, bridge phenyl-*m*-H); –4.25 (s, 3H, Me); 0.96 (s, 6H, Me_2).

3b: ^1H NMR (δ, CD_3CN): 9.47, 9.01, 8.93, 8.75, 8.55, 8.53, 8.16, 8.12 (d × 8, 1H × 8, pyrrole-β-H); 8.5-6.8 (m, 20H, *meso*-phenyl-H); 6.19 (t, 2H, bridge phenyl-*p*-H); 5.84 (broad, 4H, bridge phenyl-*m*-H); –1.67 (s, 3H, Me); 1.12 × 2 (s, 6H × 2, Me_2).

2c: ^1H NMR (δ, CD_3CN): 9.44, 9.17, 9.09, 8.97, 8.85, 8.79, 8.68, 8.65 (d × 8, 1H × 8, pyrrole-β-H); 8.4-6.8 (m, 20H, *meso*-phenyl-H); 6.20 (t, 2H, bridge phenyl-*p*-H); 5.84 (broad, 4H, bridge phenyl-*m*-H); –4.65 (s, 3H, Me); others are overlapped.

3c: ^{1}H NMR (δ, CD_3CN): 9.35, 9.05, 8.96, 8.82, 8.75, 8.72, 8.58, 8.14 (d × 8, 1H × 8, pyrrole-*β*-H); 8.5-6.8 (m, 20H, *meso*-phenyl-H); 6.22 (t, 2H, bridge phenyl-*p*-H); 5.84 (broad, 4H, bridge phenyl-*m*-H); –2.50 (s, 3H, Me); others are overlapped.

7a: ^{1}H NMR (δ, CD_3CN): 9.07, 8.76, 8.74, 8.20, 8.18, 8.17, 8.12, 8.01 (d × 8, 1H × 8, pyrrole-*β*-H); 8.4-7.2 (m, 20H, *meso*-phenyl-H); 6.21 (t, 2H, bridge phenyl-*p*-H); 5.85 (broad, 4H, bridge phenyl-*m*-H); 3.19 (d, 1H, allyl anti-CH); 3.48 (d, 1H, allyl syn-CH); 2.92 (m, 1H, allyl central CH); –2.32, –2.91 (dd × 2, 1H × 2, CH_2); 0.29, (s, 9H, *t*-Bu); MS (ESI in MeCN): m/z 1019.3050 (calcd for $[C_{66}H_{52}N_5Pd]^+$ (M – Cl): 1019.3274).

7b: ^{1}H NMR (δ, CD_3CN): 9.1-8.1 (8H, pyrrole-*β*-H); 8.2-6.7 (m, 20H, *meso*-phenyl-H); 6.23 (t, 2H, bridge phenyl-*p*-H); 5.85 (broad, 4H, bridge phenyl-*m*-H); 3.21 (d, 1H, allyl anti-CH); 3.50 (d, 1H, allyl syn-CH); 3.04 (m, 1H, allyl central CH); –1.99, –2.70 (dd × 2, 1H × 2, CH_2); 1.01, (s, 6H, Me_2).

7b*: ^{1}H NMR (δ, CD_3CN): 9.0-8.1 (8H, pyrrole-*β*-H); 8.2-6.7 (m, 20H, *meso*-phenyl-H); 6.25 (t, 2H, bridge phenyl-*p*-H); 5.85 (broad, 4H, bridge phenyl-*m*-H); 3.44 (d, 1H, allyl anti-CH); 4.07 (d, 1H, allyl syn-CH); 3.80 (m, 1H, allyl central CH); –0.67, –1.99 (dd × 2, 1H × 2, CH_2); 1.13, (s, 6H × 2, Me_2); MS (ESI in MeCN): m/z 1199.1 (calcd for $[C_{79}H_{61}N_6Pd]^+$ (M – Cl): 1199.5).

7c: ^{1}H NMR (δ, CD_3CN): 9.2-8.2 (8H, pyrrole-*β*-H); 8.6-6.9 (m, 20H, *meso*-phenyl-H); 6.19 (t, 2H, bridge phenyl-*p*-H); 5.83 (broad, 4H, bridge phenyl-*m*-H); 4.35 (d, 1H, allyl anti-CH); 4.51 (d, 1H, allyl syn-CH); 4.21 (m, 1H, allyl central CH); –2.34, –3.04 (dd × 2, 1H × 2, CH_2); Others are overlapped.

7c*: ^{1}H NMR (δ, CD_3CN): 9.1-8.2 (8H, pyrrole-*β*-H); 8.6-6.9 (m, 20H, *meso*-phenyl-H); 6.22 (t, 2H, bridge phenyl-*p*-H); 5.85 (broad, 4H, bridge

phenyl-*m*-H); 3.5-4.0 (allyl CH); 0.39, –2.14 (dd × 2, 1H × 2, CH_2); Others are overlapped. MS (ESI in MeCN): m/z 1327.2 (calcd for $[C_{66}H_{52}N_5Pd]^+$ (M – Cl): 1327.5).

8a: ^{1}H NMR (δ, CD_3CN): 9.10, 9.08, 8.91, 8.82, 8.76, 8.68, 8.20, 8.17 (d × 8, 1H × 8, pyrrole-*β*-H); 8.5-7.2 (m, 20H, *meso*-phenyl-H); 6.21 (t, 2H, bridge phenyl-*p*-H); 5.84 (broad, 4H, bridge phenyl-*m*-H); 3.19 (d, 1H, allyl anti-CH); 3.49 (d, 1H, allyl syn-CH); 2.93 (m, 1H, allyl central CH); -2.32, -2.90 (dd × 2, 1H × 2, CH_2); 0.29, (s, 9H, *t*-Bu).

9a: ^{1}H NMR (δ, CD_3CN): 9.1-8.2 (8H, pyrrole-*β*-H of *cis*-**9a** and *trans*-**9a**); 8.4-7.2 (m, 20H, *meso*-phenyl-H of *cis*-**9a** and *trans*-**9a**); 6.20 (t, 2H, bridge phenyl-*p*-H of *cis*-**9a** and *trans*-**9a**); 5.83 (broad, 4H, bridge phenyl-*m*-H of *cis*-**9a** and *trans*-**9a**); 4.10 (dq, 1H, allyl terminal CH of *cis*-**9a**); 3.62 (dq, 1H, allyl terminal CH of *trans*-**9a**); 2.87 (dt, 1H, allyl central CH of *cis*-**9a**); 2.57 (dt, 1H, allyl central CH of *trans*-**9a**); –2.57, –2.99 (dd × 2, 1H × 2, CH_2 of *cis*-**9a**); –2.29, –2.87 (dd × 2, 1H × 2, CH_2 of *trans*-**9a**); –0.48 (d, 3H, CH_3 of *cis*-**9a**); 0.62 (d, 3H, CH_3 of *trans*-**9a**); 0.29, (s, 9H, *t*-Bu of *cis*-**9a** and *trans*-**9a**).

6.4 References

1. (a) Mecking, S.; Johnson, L. K.; Wang, L.; Brookhart, M. *J. Am. Chem. Soc.* **1998**, *120*, 888. (b) Tempel, D. J.; Johnson, L. K.; Huff, R. L.; White, P. S.; Brookhart, M. *J. Am. Chem. Soc.* **2000**, *122*, 6686.
2. (a) Brookhart, M.; Wagner, M. I.; Balavoine, G. G. A.; Haddou, H. A. *J. Am. Chem. Soc.* **1994**, *116*, 3641. (b) Jiag, Z.; Sen, A. *J. Am. Chem. Soc.* **1995**, *117*, 4455.
3. (a) Nozaki, K.; Sato, N.; Tonomura, Y.; Yasutomi, M.; Takaya, H.; Hiyama.

T.; Matsubara, T.; Koga, N. *J. Am. Chem. Soc.* **1997**, *119*, 12779. (b) Nozaki, K.; Hiyama, T. *J. Synth. Org. Chem. Jpn.*, **1998**, *56*, 645.

4. (a) Markies, B. A.; Kruis, D.; Rietveld, M. H. P.; Verkerk, K. A. N.; Boersma, J.; Kooijman, H.; Lakin, M. T.; Spek, A. L.; van Koten, G. *J. Am. Chem. Soc.* **1995**, *117*, 5263. (b) Groen, J. H.; Elsevier, C. J.; Vrieze, K.; Smeets, W. J. J.; Spek, A. L. *Organometallics*, **1996**, *15*, 3445. (c) Delis, J. G. P.; Aubel, P.G.; Vrieze, K.; van Leeuwen, P. W. N. M.; Veldman, N.; Spek, A. L.; van Neer, F. J. R. *Organometallics*, **1997**, *16*, 2948.
5. Otsuka, S.; Nakamura, A.; Yoshida, T. *J. Am. Chem. Soc.* **1969**, *91*, 5932.
6. (a) Deming, T. .; Novak, B. M. *J. Am. Chem. Soc.* **1993**, *115*, 9101. (b) Ito, Y.; Murakami, M. *J. Am. Chem. Soc.* **1990**, *112*, 6446.
7. Ito, Y.; Mitake, T.; Hatano, S.; Shima, R.; Ohara, T.; Suginome, M. *J. Am. Chem. Soc.* **1998**, *120*, 11880
8. (a) Y. Takao, T. Takeda, J. Watanabe and J. Setsune, *Organometallics,* **18**, 2936 (1999). (b) Y. Takao, T. Takeda, J. Watanabe and J. Setsune, *Organometallics,* **22**, 233 (2003).

Conclusions

This dissertation dealt with synthesis and reactions of palladium(II) complexes coordinated by N^{21},N^{22}-etheno-bridged porphyrin ligands. The results and findings are summarized as follows.

Chapter 2 describes synthesis and structure of Pd(II) complexes with *N*,*N*'-etheno-bridged porphyrins. The reaction of N^{21},N^{22}-etheno-bridged porphyrins with $PdCl_2$ preferentially afforded dinuclear complexes which can be converted to mononuclear complexes by ligand exchange. The X-ray structure showed di-μ-chlorodipalladium(II) complex coordinated by the porphyrin as the terminal ligand with the distal Pd(2) coming close to the porphyrin ring. The etheno substitution makes the pyrrole rings to cant, and two pyrrole rings are favorably situated for the coordination to the Pd atom. After all, the present Pd complexes are not demetallated and N-dealkylated at all in solution.

Chapter 3 describes preparation and spectroscopic characteristics of Pd(II) complexes of N^{21},N^{22}-bridged porphyrin with pyridine and ethylenediamine. Square planar mixed-ligand Pd(II) complexes with N^{21},N^{22}-bridged porphyrin and ethylenediamine were prepared. Since the N^{21},N^{22}-bridged porphyrin ligand strongly coordinates to Pd, the porphyrin ligand dissociates much more sluggishly than 2,2'-bipyridine. The N^{21},N^{22}-bridged porphyrin ligand influences the dynamic behavior of the coexisting ligand in the same coordination sphere. Ligation of chloride to form square pyramidal Pd(II) structure was indicated by UV-Vis and ^{1}H NMR.

Chapter 4 describes synthesis of (π-allyl)palladium(II) complexes with *N*, *N*'-bridged porphyrins. Bis(aqua)Pd^{II} complexes of N^{21},N^{22}-etheno-bridged porphyrins reacted with allyltins, resulting in the formation of (π-allyl)palladium(II) derivatives with N^{21},N^{22}-bridged porphyrin ligands. The

substituent at the allyl moiety exerted influence on the equilibrium state of two product isomers with different orientations of π-allyl ligands relative to the porphyrin ligand. The rate for syn-syn–anti-anti isomerization of the π-allyl ligand of Pd(II) porphyrin is remarkably slower than those for (π-allyl)Pd^{II} complexes with ordinary nitrogen base ligands. The porphyrin ring current effect greatly helps differentiating two isomers and thus elucidating isomerization behaviors. The present study shows the great possibilities of N^{21},N^{22}-bridged porphyrin as a ligand stereochemically controlling the reactivity of organo ligands by covering one side of the square plane of Pd coordination.

Chapter 5 describes preparation of μ-(dihydroxo)dipalladium(II) bis-porphyrin complex and its reaction with active methylene compounds. μ-(Dihydroxo)dipalladium(II) bisporphyrin complex was obtained by the reaction of dicationic bis(aqua)Pd^{II} complex of N^{21},N^{22}-bridged porphyrin with NaOH or triethylamine. It is a mixture of two isomers and can provide both acidic site and basic site at the same time. It caused deprotonation from active methylene compounds to give organopalladium(II) porphyrin complexes under neutral conditions.

Chapter 6 describes insertion of isonitriles into Pd(II) complexes of *N*,*N*'-etheno-bridged porphyrins. The insertion of 2,6-dimethylphenyl isonitrile and tosylmethyl isonitrile to (methyl)Palladium(II) porphyrin are faster than that of *t*-butyl isonitrile. In the reaction of (π-allyl)Palladium porphyrin, coordination of *t*-butyl isonitrile to Pd(II) in concurrence with change of the η^3-allyl ligand to η^1-allyl ligand is reversible, while 2,6-dimethylphenyl isonitrile and tosylmethyl isonitrile insert between Pd and η^1-allyl ligand.

List of Publications

"Synthesis of binuclear palladium(II) complexes of bidentate N(21),N(22)-bridged porphyrins." Y. Takao, T. Takeda, K. Miyashita, and J. Setsune, Chemmstry Letters, 761-762, 1996

"Synthesis and structure of palladium(II) complexes with N(21),N(22)-bridged porphyrin ligands." Y. Takao, T. Takeda, K. Miyashita, and J. Setsune, Bulletin Chemical Society of Japan, 71, 1327-1335, 1998

"Coordination of amines to palladium(II) complexes of N^{21},N^{22}-bridged porphyrins." Y. Takao, T. Takeda, and J. Setsune, Bulletin Chemical Society of Japan, in press

"Apparent π-allyl rotation in the π-(allyl)palladium(II) complexes of N^{21},N^{22}-bridged porphyrins." Y. Takao, T. Takeda, J. Watanabe, and J. Setsune, Organometallics, 18, 2936-2938, 1999

"Isomerization behavior in the π-(allyl)palladium(II) complexes with N^{21},N^{22}-bridged porphyrin ligands." Y. Takao, T. Takeda, J. Watanabe, and J. Setsune, Organometallics, 22, 233-241, 2003

"Properties and reactions of μ-(dihydroxo)dipalladium(II) bis-porphyrin complexes. Y. Takao, T. Takeda, S. Tanikawa, and J. Setsune, Journal of Porphyrins and Phthalocyanines, in press

"Insertion of isonitrile into the Pd-C bond of Pd complexes of N^{21},N^{22}-bridged porphyrins." J. Setsune, T. Yamauchi, S. Tanikawa, Y. Takao, and T. Takeda, to be submitted

Acknowledgements

The author would like to express her thanks to Professor Jun-ichiro Setsune of the Faculty of Science, Kobe University, for his continuous guidance and suggestions throughout this work.

The author also makes grateful acknowledgement to Dr. T. Takeda, Director of the Osaka Municipal Technical Research Institute, for his encouragement and help.

The author is deeply grateful to Dr. M. Hashimoto, Kobe University, for his help in X-ray analysis and to Ms. M. Nishinaka for microanalysis. The author is also grateful to Prof. H. Miyake for the gift of an allyltin reagent.

The author would like to acknowledge Dr. M. Sawada, Mr. H. Yamada, and Mrs. F. Fukuda, MAC, ISIR, Osaka University, for FAB MS analysis and elemental analysis.

The author expresses her gratitude to Dr. K. Koyama, Chief of the Techno Chemistry Department, for his support, and to all of the other members of the department for their experimental help.

Thanks are given to Dr. J. Watanabe, Ms. S. Tanikawa, Mr. T. Yamanouchi, and to other members of Laboratory of Organometallic Chemistry for their cooperation and kind help.

Finally, the author wishes to express her gratitude to her parents for their understanding and warm-hearted encouragement and to her husband and family for their helpful support.